

Coastal protection in the Mekong Delta

Wave load and overtopping of sea dikes
as function of their location in the cross-section,
for different foreshore geometries

Silke Tas



Cover photo: Fishing hut in Rach Gia Bay, Kien Giang province, Vietnam.

Coastal protection in the Mekong Delta

Wave load and overtopping of sea dikes
as function of their location in the cross-section,
for different foreshore geometries

by

Silke Tas

to obtain the degree of Master of Science
in Hydraulic Engineering
with a specialisation in Coastal Engineering

at Delft University of Technology,
in collaboration with the University of Danang, Vietnam,
on an Erasmus Mundus Mobility with Asia (EMMA) scholarship,

to be defended publicly on Friday 25 November 2016 at 14:00.

Student number:	4169905	
Project duration:	November, 2015 – November, 2016	
Thesis committee:	Prof. dr. ir. M.J.F. Stive,	TU Delft, supervisor
	Prof. dr. Nguyen The Hung,	University of Danang
	Dr. ir. M. Zijlema,	TU Delft
	Ir. H.J. Verhagen,	TU Delft
	Dr. ir. J.S.M. van Thiel de Vries,	Boskalis, Ecoshape
	Ir. M. Tonneijck,	Royal HaskoningDHV

An electronic version of this thesis is available at <http://repository.tudelft.nl/>.

Preface

This MSc thesis is the conclusion not only of this graduation project, but also of the years leading up to this point. During this project, I have been able to apply a lot of knowledge, knowledge that was once mainly classroom or textbook theory, to a topical issue: coastal protection of mangrove coasts. In this subject, I have been able to combine my passion for coastal engineering with my interest in numerical modelling and my belief in the Building with Nature-approach. On top of that, I have been given the unique opportunity to live and work in Vietnam for a couple of months, which has enabled me to see the Mekong Delta with my own eyes, but also to begin to understand the Vietnamese culture, and the way they approach the problem.

I believe that this is also the strength of my project. I have approached the problem from a technical point of view, following a scientific approach, but I did not stop there. I have tried to follow all the steps that have to be followed in practice, from problem definition, through scenario development, numerical modelling, cost-benefit analysis to implementation. However, thanks to my stay in Vietnam, I have been able to combine and compare the Dutch and Vietnamese approaches, with the ultimate goal of an approach that combines the strengths of both, and most importantly, is therefore not only feasible but also acceptable to all stakeholders.

However, there is also another important lesson I have learned. In the end, decision making is always a political process, and the technically preferred solution is not always the politically practicable solution. Nevertheless, I believe that it is important to conduct independent and unbiased scientific research, in order to provide an objective argument in the decision-making process and to improve the quality of the decision.

But the part of which I am maybe most proud, is the numerical modelling. After months of weird model results (including the discovery after two months that the installation of SWASH on my laptop was corrupt), I have finally managed to unravel some of the mysteries and identify the causes of the divergent model behaviour. I hope that this improved knowledge can contribute to the full understanding and numerical implementation of wave transformation on gentle slopes.

I would like to thank prof. dr. ir. Marcel Stive, for helping me through this thesis ride, and introducing me to Vietnam. I would also like to thank prof. dr. Nguyen The Hung and his staff of the division of Water Resources Engineering at the University of Danang for the warm welcome and most smooth cooperation, and the Erasmus Mundus programme for making this dream come true. Further, I would like to thank dr. ir. Marcel Zijlema, for his help with the numerical modelling, ir. Henk Jan Verhagen for sharing his worldwide experience in coastal protection with me, dr. ir. Jaap van Thiel de Vries for keeping me creative and realistic, and Michel Tonneijck for relating my abstract work to reality. Also, I would like to thank dr. Stefan Groenewold and the rest of the GIZ team in Ho Chi Minh City for welcoming me in their office and sharing their experience in the field with me. Finally, I could never have finished this without the endless love of my parents and Guus.

Silke Tas
Delft, October 2016

Abstract

Coastal protection in the Mekong Delta is of paramount importance. The low-lying coastal area has always been vulnerable to flooding by extreme events, but the coastal erosion and consequent land losses have increased to alarming magnitude in the most recent years. This MSc thesis aims to provide insight in the optimal protection strategy for each situation, through investigating the wave load and overtopping of sea dikes, as function of the location of the dike in the cross-section, for different foreshore geometries.

The Mekong Delta coast can be classified into three categories, based on the erosion rate: a stable coastline, an accreting coastline and an eroding coastline. For each category, several coastal protection scenarios have been developed. In case of a stable coastline, a simple coastal protection strategy consisting of a sea dike in combination with its foreshore will be most appropriate. The same strategy can be applied to an accreting shoreline, however optimising details may increase the benefits. In the last category, the foreshore erodes. The first strategy is to accept the erosion, and simply place the dike more inland, this is called managed retreat. The second strategy uses the mangrove forest on the foreshore to slow down the erosion. The third strategy stops the erosion by nourishing the foreshore, restoring the sediment balance, and the fourth strategy fights the erosion by constructing a structure that can withstand the erosion and extreme wave loads.

In order to be able to numerically model each scenario, boundary conditions are required. Since the Mekong Delta is an extremely varied region, one set of boundary conditions cannot represent the entire Delta, therefore a range of boundary conditions has been set up. Three bathymetric profiles and four vegetation settings have been defined. Further, as the Dutch and Vietnamese approach with respect to the choice of lifetime and return period differs significantly, also 12 combinations of return period and lifetime will be modelled.

The numerical models used for this project are SWAN and SWASH. SWAN will translate the offshore boundary conditions into nearshore conditions, and SWASH will use these conditions as input in order to calculate the wave transformation up to the shoreline. During the project, it was discovered that wave transformation on these extremely gentle slopes (in the order of 1:1000) has never been researched, and in combination with the total lack of measurements, the numerical models could not be validated. However, by comparing the model results to theory, and analysing each single source term in the energy balance, some improvements have been made to the model. Thus, sufficient confidence in the model was built up to model the design storm conditions in the Mekong Delta for each scenario.

For each situation, all scenarios have been evaluated with a cost-benefit analysis in order to determine the optimal strategy. When the coastline is stable, the cost-benefit analysis showed that there is a direct reduction in net costs as the dike is placed further inland. Further, the additional costs for designing a dike with a longer lifetime or a dike that can withstand a longer return period, are significantly smaller than both the additional benefits and the initial costs. Finally, the construction costs can be reduced significantly by allowing a limited amount of overtopping.

In case of accretion, the best coastal protection strategy proved to be a dike with a long lifetime, in combination with alternative use of the foreshore, for example for extensive aquaculture. In case of erosion, managed retreat turned out to be the optimal strategy, however in practice there are often limitations imposed on the distance the dike can be retreated. Mangrove reforestation could only be applied in case of erosion that was limited both in duration and in strength. The other two strategies (nourishment and strong structures) appeared to be extremely expensive, and can therefore only be justified in case the value of the hinterland is high, which is not yet the case in the Mekong Delta. However, the Delta is rapidly developing, therefore it is recommended in the case of erosion to design for a short lifetime and re-evaluate the situation in the near future.

Contents

Preface	iii
Abstract	v
Table of contents	ix
List of symbols	xi
List of Figures	xiii
List of Tables	xv
1 Introduction	1
1.1 Problem description	1
1.2 Decision support tool	2
1.3 Report outline	2
2 Approach	5
2.1 Introduction approach	5
2.2 Context: The Mekong Delta	7
2.2.1 The Mekong River	7
2.2.2 The Vietnamese Mekong Delta	8
2.2.3 Socio-economic background of the Mekong Delta	9
2.2.4 Sediment dynamics	9
2.2.5 Coastal protection in the Mekong Delta	10
2.2.6 Innovative coastal protection strategies in case of strong erosion	12
2.3 Scenarios	14
2.3.1 Accretion	14
2.3.2 Stable coastline	15
2.3.3 Erosion	15
2.4 Boundary conditions	16
2.4.1 Lifetime and return period	16
2.4.2 Bathymetry	17
2.4.3 Wave conditions	18
2.4.4 Water level	19
2.4.5 Vegetation	19
2.4.6 Cyclones	21
2.4.7 Limitations of the model input	21
2.5 Numerical modelling	23
2.5.1 Model requirements	23
2.5.2 Model description	23
2.5.3 Model set-up	24
2.6 Evaluation framework	26
2.6.1 Cost-benefit analysis	26
3 Results	31
3.1 Analysis model performance	31
3.1.1 From linear wave theory to the Mekong Delta	31
3.1.2 Variance density spectrum analysis	39
3.1.3 Extremely gentle slopes	48
3.1.4 Wave transformation inside mangrove forests	54

3.2	Analysis model results	56
3.2.1	General wave transformation	56
3.2.2	Effect of bathymetry on wave transformation	58
3.2.3	Effect of lifetime and return period on wave transformation	60
3.2.4	Effect of vegetation on wave transformation	61
3.2.5	Conclusion	63
4	Discussion	65
4.1	Individual analysis components cost-benefit analysis	65
4.1.1	Construction and maintenance costs of sea dikes	65
4.1.2	Mangrove reforestation and maintenance costs	66
4.1.3	Ecosystem services	67
4.1.4	Reduced flooding risk	67
4.1.5	Costs of land loss.	67
4.1.6	Costs and benefits of land conversion.	67
4.1.7	Overview individual cost and benefit components	68
4.2	Cost-benefit analysis for a stable coastline	70
4.2.1	Effect of bathymetry on costs and benefits	70
4.2.2	Effect of lifetime on costs and benefits	72
4.2.3	Effect of return period on costs and benefits	73
4.2.4	Effect of vegetation on costs and benefits.	74
4.2.5	Effect of allowable overtopping on costs and benefits	75
4.2.6	Designing for cyclones	75
4.2.7	Conclusion	76
4.3	Cost-benefit analysis in case of accretion.	77
4.3.1	Redesign after short lifetime	77
4.3.2	Alternative use foreshore.	77
4.3.3	Comparison.	77
4.3.4	Conclusion	78
4.4	Cost-benefit analysis in case of erosion.	79
4.4.1	Mangrove reforestation.	79
4.4.2	Managed retreat	79
4.4.3	Soft solution.	79
4.4.4	Hard solution	80
4.4.5	Conclusion	80
5	Conclusions and recommendations	81
5.1	Conclusions.	81
5.1.1	Numerical modelling of gently sloping mangrove coasts	81
5.1.2	Stable coastline.	82
5.1.3	Accretion	82
5.1.4	Erosion	82
5.2	Limitations	83
5.3	Recommendations	83
	Bibliography	85
A	Appendix: Boundary conditions	91
A.1	Wave conditions	91
A.1.1	Available data.	91
A.1.2	Design wave characteristics	95
A.2	Water level	96
A.2.1	Tides	96
A.2.2	Wind set-up	96
A.2.3	Other components storm surge	97
A.2.4	Relative sea level rise	98
A.2.5	Design water level	98

B Appendix: Input files SWAN and SWASH	99
B.1 Input file SWAN	100
B.2 Input file SWASH	101
C Appendix: Evaluation framework	103
C.1 Construction and maintenance	103
C.1.1 From hydraulic conditions to dike dimensions	103
C.1.2 Construction and maintenance costs of dikes.	106
C.1.3 Mangrove reforestation.	109
C.1.4 Hard solutions	109
C.1.5 Soft solutions	110
C.2 Value of land	111
C.2.1 Flooding risk	111
C.2.2 Ecosystem services	111
C.2.3 Land loss	112
C.2.4 Land conversion	112

List of symbols

Symbol	Definition	Unit
A	cross-sectional area	m^2
a	wave amplitude	m
B	yearly benefits	VND/y
C	costs	VND
c	wave celerity	m/s
c_g	wave group celerity	m/s
D	damage costs	VND
d	actual water level, including water level set-up, $d = h + \eta$	m
E	wave energy per unit surface area	J/m ²
F	fetch	m
\tilde{F}	dimensionless fetch	-
f	frequency	Hz
g	gravitational acceleration (9.81 m/s ²)	m/s ²
H	wave height	m
H_{max}	maximum individual wave height	m
H_s	significant wave height	m
\tilde{H}	dimensionless significant wave height	-
\tilde{H}_∞	dimensionless wave height for fully developed sea state in deep water	-
h	still water depth	m
h_D	dike height	m
\tilde{h}	dimensionless water depth	-
I	investments, construction costs	VND
k	wave number	m ⁻¹
L	wave length	m
M	yearly maintenance costs of the protection measure	VND/y
n	ratio of wave group celerity over individual wave celerity	-
P	uniform pressure	kPa
P_f	probability of failure	-
PV	present value	VND
q	overtopping discharge	m ³ /s/m
R_{cp}	freeboard	m
R_{up}	wave run-up	m
r'	real interest rate	-
S	settlement	m
s_0	wave steepness	-
T	wave period	s
\tilde{T}	dimensionless wave period	-
T_l	lifetime	y
T_p	peak wave period	s
T_r	return period	y
\tilde{T}_∞	dimensionless wave period for fully developed sea state in deep water	-

Symbol	Definition	Unit
t	time	s
U	wave energy flux per unit wave crest width	J/ms
u	wind speed	m/s
\tilde{u}	dimensionless wind speed	-
V	value of land with a certain land use	VND/m ²
w	width (distance perpendicular to the shoreline)	m
x	coordinate perpendicular to shoreline (in direction of wave propagation)	m
z_s	safety height increment	m
z_w	water level	m
α	slope	-
γ	breaker parameter	-
ζ	settlement influence factor	-
η	water level set-up, surface elevation	m
μ	Poisson's ratio of the soil (for saturated soil $\mu = 0.5$)	-
ξ_0	Iribarren breaker parameter	-
ρ_a	density of air (1.21 kg/m ³)	kg/m ³
ρ_w	density of water (1300 kg/m ³)	kg/m ³
τ_w	wind shear stress	Pa
ω	angular frequency	s ⁻¹

List of Figures

2.1	Flow chart of the adapted approach.	5
2.2	Map of the entire Mekong River basin	7
2.3	Map of the Mekong Delta in Vietnam	8
2.4	Mekong Delta shoreline evolution over the past century	10
2.5	Flow chart of the different situations and corresponding protection strategies	14
2.6	Flowchart visualising the range of situations covered in this approach.	16
2.7	Representative bathymetric profiles	18
2.8	Vertical schematisation of a mangrove tree in SWASH (Burger, 2005)	20
2.9	Costs and benefits of coastal protection strategies	26
3.1	Linear shoaling	33
3.2	Shoaling and wave breaking, nonlinear case	34
3.3	Wave transformation of a JONSWAP spectrum	35
3.4	Wave transformation of a JONSWAP spectrum on a slope of 1/800	35
3.5	Wave transformation of a JONSWAP spectrum on a slope of 1/1500	36
3.6	Wave transformation of a JONSWAP spectrum on a slope of 1/1500, with wind	37
3.7	Spectrum generated by SWAN used as SWASH input	38
3.8	Spectrum generated by SWAN enhanced and used as SWASH input	38
3.9	Evolution of the wave spectrum from offshore to nearshore	39
3.10	Evolution of the individual source terms of the energy balance	40
3.11	Evolution of the wave spectrum from offshore to nearshore, with wind	42
3.12	Evolution of the individual source terms of the energy balance, with wind	42
3.13	Evolution of the wave spectrum from offshore to nearshore, with wind and steep waves	43
3.14	Evolution of the individual source terms of the energy balance, with wind and steep waves	43
3.15	Evolution of the wave spectrum from offshore to nearshore, with steep waves	44
3.16	Evolution of the individual source terms of the energy balance, with steep waves	45
3.17	Evolution of the wave spectrum, with steep waves, including whitecapping.	46
3.18	Evolution of the individual source terms, with steep waves, including whitecapping.	46
3.19	Evolution of the wave spectrum, with steep waves, including wind and whitecapping.	47
3.20	Evolution of the individual source terms, with steep waves, incl. wind and whitecapping.	47
3.21	Location of breaking point for waves with different offshore steepness	49
3.22	Effect of constant and variable breaker parameter in SWAN.	50
3.23	Effect of various α and β values in BREAK command SWASH.	51
3.24	Comparison of the wave transformation of a regular wave and a JONSWAP spectrum	52
3.25	Wave transformation for full model set-up on a slope of 1/200.	53
3.26	Wave height reduction inside mangrove forests	54
3.27	Wave transformation as modelled by SWAN	56
3.28	Evolution of the wave spectrum, from offshore to nearshore	57
3.29	Evolution of the individual source terms of the energy balance	57
3.30	Wave transformation nearshore as modelled by SWASH and SWAN	58
3.31	Wave transformation nearshore for different bathymetries	59
3.32	Wave transformation nearshore for different lifetimes and return periods	60
3.33	Wave transformation nearshore for different vegetation densities on a steep bottom slope	61
3.34	Wave transformation nearshore for different vegetation densities on a mild bottom slope	62
4.1	Dike construction costs as function of dike height and maintenance costs as function of lifetime	66
4.2	Individual components of a cost-benefit analysis	68
4.3	Individual components of a cost-benefit analysis in separate graphs	69

4.4	Effect of bathymetry on costs and benefits	71
4.5	Effect of lifetime on costs and benefits	72
4.6	Effect of the return period on costs and benefits	73
4.7	Effect of vegetation on costs and benefits	74
4.8	Effect of overtopping on construction costs dike	75
4.9	Costs and benefits of designing with and without cyclones	76
4.10	Comparison costs and benefits of two dikes with a lifetime of 20 and 100 years	78
A.1	Design wave conditions, fitted to available data.	95
A.2	Water level set-up generated by wind friction	97
C.1	Standard dike cross-section according to Vietnamese design guidelines	107
C.2	Concrete breakwater along the west coast of Cà Mau	110

List of Tables

2.1	Failure probabilities for different combinations of lifetime and return period	17
2.2	Design wave conditions	19
2.3	Estimated design water levels	19
2.4	Overview of input parameters to model mangrove vegetation in SWASH	21
2.5	Summary estimated parameters cost-benefit analysis	29
A.1	Wind speed (in m/s) averaged over 10 minutes for different return periods	92
A.2	Coefficients for the Young and Verhagen formulae	93
A.3	Estimated wave height and wave period based on wind speed	93
A.4	Wave height and wave period for different return periods at Bach Ho	94
A.5	Extrapolated wave height and wave period for different return periods at Bach Ho	94
A.6	Design wave conditions	95
A.7	Estimated wind set-up	97
A.8	Estimated design water levels	98
C.1	Cost components and total dike construction costs for various dike heights.	108
C.2	Maintenance costs mangrove reforestation	109

Introduction

1.1. Problem description

Coastal protection in the Mekong Delta is of paramount importance. The coastal erosion and consequent land losses have increased to an alarming magnitude in the most recent years. The low-lying coastal area has always been very vulnerable to flooding by extreme events. However, in the future these events are expected to become more frequent and more intense due to climate change. Another important aspect related to climate change is the sea level rise. In combination with the high subsidence rates from which the Delta is currently suffering, the coastal zone will only become more exposed due to the high relative sea level rise.

It is within the context of coastal protection in the Mekong Delta that this MSc thesis is situated. More specifically, the wave load and overtopping of the dike will be investigated, as function of the location in the cross-section, for different foreshore geometries (with mangroves, without mangroves, different bottom slopes, mudflats, ...).

A very popular coastal protection measure along mangrove coasts nowadays is the restoration of mangrove belts, which can provide coastal protection as one of their ecosystem services. Thus, the design requirements for the coastal structure behind the mangrove forest may be reduced. However, due to the serious erosion problems, mangroves are still eroding at many places, which results in dike exposure and eventually dike failure. The huge erosion rates are (partly) caused by on the one hand a reduced sediment supply (damming of the Mekong river, sand mining) and on the other hand an increased sediment demand (increased accommodation space due to rising sea level and subsidence). Facing this erosion, other approaches also have to be analysed.

An alternative approach could be managed retreat, placing the dike more inland, abandoning the land in front of the dike, which can provide protection. Another alternative approach is nourishing the eroding coastlines. Nourishments are common practice along sandy coasts, but have never been applied to muddy coasts. Even though nourishing muddy shores can be very complex, it is a promising alternative that deserves further enquiry. Finally, at coasts where retreat is no option, a "super strong structure" could be the only alternative for nourishments. This structure should have such a strong foundation and toe protection that it can withstand the strong erosive forces and wave loading. However, it is unclear whether such a structure is even technically feasible on these soils, and if it is, it will come at extremely high costs. Therefore, a cost-benefit analysis will be required.

So, in order to determine the wave load and overtopping on the dike, several scenarios will be analysed. The main parameter in defining these scenarios will be the erosion rate. In the case the coastline is relatively stable, a relatively simple case of dike and foreshore (with or without mangroves and/or aquaculture) can be designed. In the case of accretion, this approach is still valid, but optimisation is possible. However, if there is erosion, the scenarios become more complex. If the erosion rate is limited, mangrove reforestation could be a possible scenario. Another possible solution could be to retreat, and place the dike further inland. The location of the new dike could be determined based on an estimate of the expected erosion over the lifetime of the dike.

However, if the erosion rate becomes too high, retreating is no longer an option, because either the dike would be exposed again in a relatively short period, or the amount of land that has to be abandoned

would become so large that in no way the benefits can compensate the costs. In such a scenario, the possibility of nourishments should be investigated. This will require a clear view of the sediment balance of the region, to enable an estimate of the required volumes of sediment. An alternative for that scenario is the construction of a super strong structure, which can withstand the extreme erosive forces, and the resulting wave loading.

The wave loading and overtopping of the sea dike in each scenario will be evaluated through numerical modelling. Each scenario will further be evaluated by means of a cost-benefit analysis. The costs of the coastal protection measures, as well as the additional costs related to land loss for example, are compared to the benefits, which consist mainly of reduced flooding risk thanks to the protection, but also ecosystem services provided by the coastal ecosystems such as mangroves.

1.2. Decision support tool

A coastal protection strategy is only successful if it is well imbedded in its environment, but also the inverse is true, a region such as the Mekong Delta can only develop if its border with the sea is well protected. During the development of the Mekong Delta Plan (Consortium Royal HaskoningDHV, WUR, Deltares, Rebel, 2013), this awareness has given rise to special attention for its coastal vulnerability. GIZ (Gesellschaft für Internationale Zusammenarbeit) has been involved in the coastal protection of the Mekong Delta through providing technical support. Together with the governments of Vietnam, Germany and Australia, the Integrated Coastal Management Programme has been developed, with the objectives of preparing the coastal area of the Mekong Delta for a changing environment and of laying the foundations for a sustainable growth of the region. GIZ is currently implementing this plan, which consists of 5 components, two of which are coastal protection and mangrove forestry.

During the implementation of this plan, the need has risen for strategy advice on the (future) dike trajectories, the level of protection and the type of coastal defence. The Netherlands Enterprise Agency (Rijksdienst voor Ondernemend Nederland, RVO), in collaboration with GIZ and Delft University of Technology has launched a project in order to develop a decision support tool (DST) to provide this strategic advice. The project will be carried out by Royal HaskoningDHV.

The decision support tool should establish a link with the Mekong Delta Plan, in order to guarantee a successful implementation. The advice will be (partly) based on a cost-benefit analysis, but should also take into account uncertainties due to climate change and socio-economic developments. Finally, it is strongly encouraged to look for possibilities to adopt the Building with Nature approach.

By participating in this project, great value is added to this MSc thesis. The purpose is to contribute on a technical level to the understanding of coastal protection in this region and to assist in determining the optimal dike trajectories, levels of protection and types of coastal defence. This is the reason why a generic approach is adopted in this thesis, as the objective is to provide knowledge and understanding, which can be applied to the entire Mekong Delta, but also even to other regions. The strength of this approach lies in the fact that the entire decision-making process is simulated, from identifying the characteristics of the coastal zone, through defining, modelling and comparing different scenarios, to making a decision based on a cost-benefit analysis.

As such, the thesis can contribute in two ways to the project: first, understanding of the link between the characteristics of a coastal zone and the optimal dike trajectory, level of protection and coastal defence type, and second, a method to determine the optimal dike trajectory for specific (complex) situations.

1.3. Report outline

The report is structured according to a typical research process: first the approach is outlined (chapter 2), then the results are presented (chapter 3), after which they are discussed (chapter 4) and finally the conclusions are drawn, together with recommendations for future research (chapter 5).

Chapter 2 starts with the introduction of the approach adopted for this project (section 2.1). The rest of the chapter introduces all knowledge required for each step of the approach. First, the context of the Mekong Delta is sketched and some more information on the current coastal protection of the region is given in section 2.2. Then, the scenarios are introduced that will be modelled and compared (section 2.3). In order to be able to model the scenarios, the boundary conditions for each scenario have to be defined. This is done in section 2.4 and appendix A. The numerical models are described in section 2.5, as well as their set-up. Moreover, an example of the input files of these models can be found in Appendix B. The chapter concludes with the set up of the evaluation framework in section 2.6

and appendix C, which will be based on a cost-benefit analysis.

In chapter 3, the model results will be presented. However, before the scenarios can be modelled, the validity of the model has to be verified. This will be done in section 3.1. Eventually, the outcomes of each situation that has been modelled are presented in section 3.2.

In chapter 4, the model results from the previous chapter will be evaluated and the different scenarios will be compared. In section 4.1, the individual components of the cost-benefit analysis are investigated, in order to assess their influence on the net costs. After this, the cost-benefit analysis is applied to a stable coastline (section 4.2), an accreting coastline (section 4.3) and an eroding coastline (section 4.4).

Finally, chapter 5 presents all conclusions that have been drawn from this research (section 5.1), as well as the limitations of the followed approach (section 5.2). The chapter concludes with recommendations for further research (section 5.3).

At the end of the report, a list of all references used in this report is given.

2

Approach

2.1. Introduction approach

The main purpose of this thesis is to find the optimal protection strategy for different situations. The first step towards this goal is to get familiar with the problem and possible solutions through a literature study. Based on this knowledge, the following approach was developed.

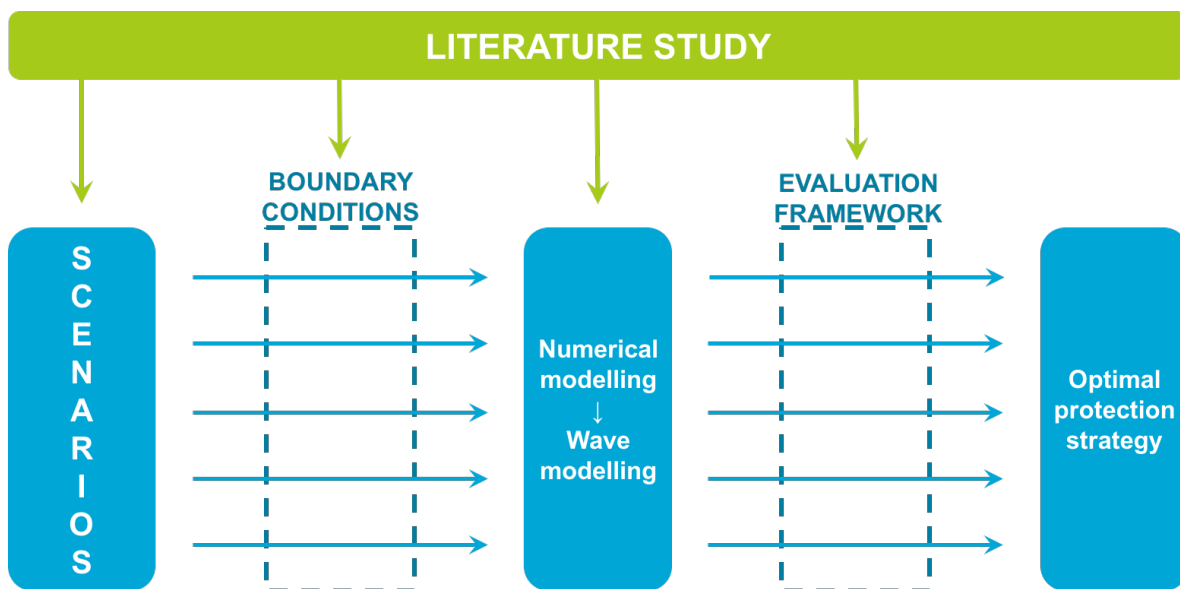


Figure 2.1: Flow chart of the adapted approach.

As can be observed in Figure 2.1, the literature study forms the common thread through the entire process. Based on the understanding of the problem, acquired through the literature study, different scenarios have been developed. However, these scenarios are not always suitable for each situation. The leading parameter in defining which scenarios are applicable in a certain situation, is the erosion rate. Based on this parameter, three situations can be defined: erosion, accretion and a stable coastline.

Following Figure 2.1, each scenario will be numerically modelled. This means that for each situation and scenario, corresponding boundary conditions have to be defined. These boundary conditions will be derived from literature. With these boundary conditions, a numerical model can be set up, in order to determine the hydraulic conditions and estimate the corresponding wave load and overtopping.

For each of the three situations, different scenarios will be investigated. In order to be able to make comparisons between those scenarios, an evaluation framework will be set up. The scenarios will be evaluated through a cost-benefit analysis. The outcome of these analyses will make it possible to determine the preferred protection strategy for each situation.

The different aspects of this approach will be laid out in detail in the next sections. In section 2.2 the Mekong River and its delta is introduced, as well as its coastal protection issues. Based on this knowledge, in section 2.3, the different scenarios will be developed. Once the scenarios have been defined, the corresponding boundary conditions will have to be determined. This will be done in section 2.4. Section 2.5 discusses the numerical models that will be used, and how these models will be set up. Finally, the evaluation framework will be set up in section 2.6.

2.2. Context: The Mekong Delta

2.2.1. The Mekong River

The Mekong River is one of the world's great rivers, with a length of 4800 km (Renaud and Kuenzer, 2012) and a basin area of 795 000 km² (Le Anh Tuan et al., 2007; Mekong River Commission (MRC), 2010). The river has a mean annual water discharge of 470 km³/year (Lu and Siew, 2005). In terms of biodiversity, the Mekong River even has the second richest river basin worldwide (World Wildlife Fund, 2004).

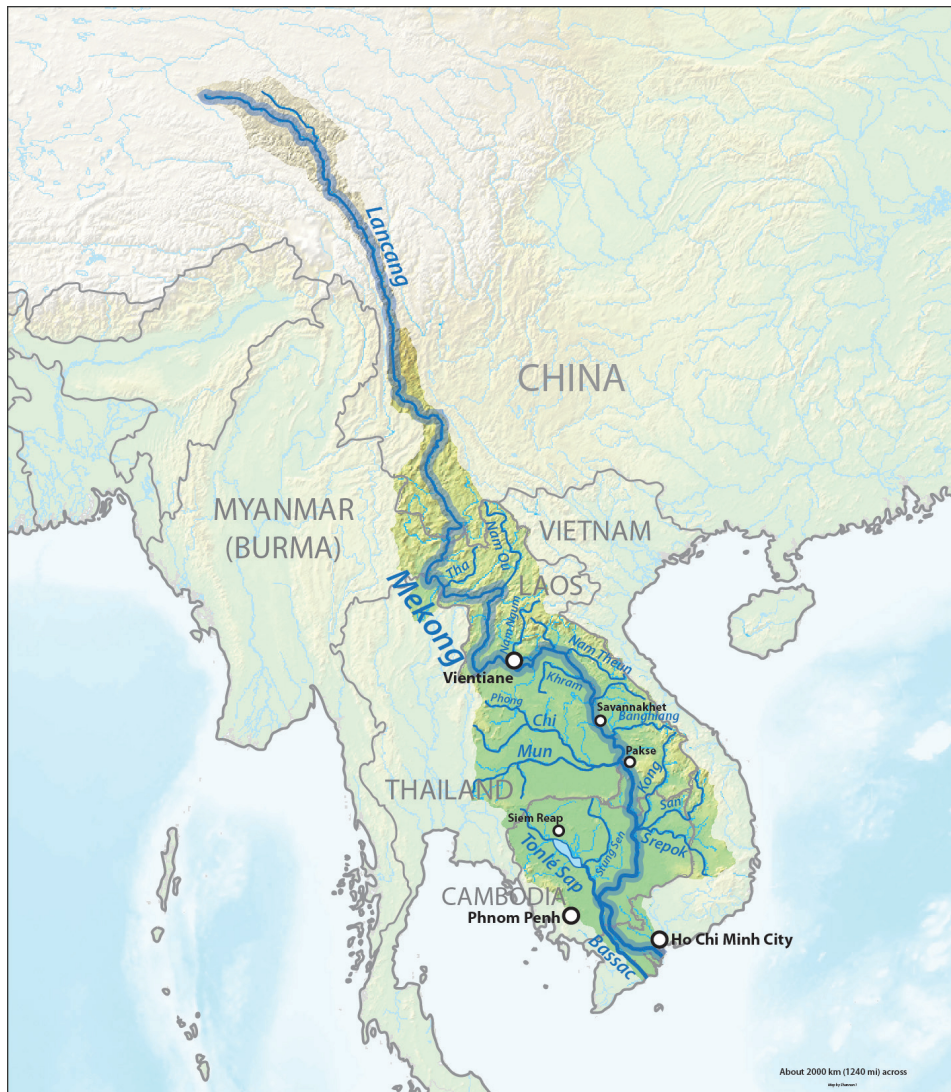


Figure 2.2: Map of the entire Mekong River basin (DEMIS Mapsserver, 2015).

The Mekong River flows through six countries: it springs on the Tibetan Plateau in China after which it flows through Myanmar, Laos, Thailand and Cambodia, eventually ending in Vietnam where it flows via the Mekong Delta into the East Sea (also known as the South China Sea).

The fact that the Mekong River flows through six countries complicates the management of its resources. Therefore, the four downstream countries (Laos, Thailand, Cambodia and Vietnam) established the Mekong River Commission (MRC) in 1995. The two upstream countries, China and Myanmar, became dialogue partners in 1996 (Mekong River Commission (MRC), 2010). Especially the generation of hydropower is subject of discussion, as the number of dams in the Mekong River basin increases year by year. In 2011, there were 64 dams in use, and another 233 under construction or in planning (Nowacki et al., 2015). Authorities in the Vietnamese Mekong Delta are worried about the impact of upstream measures on the Delta. Extensive cooperation will be key to sustainable management

of the basin in the future, as the impact of hydropower generation and climate change increases.

2.2.2. The Vietnamese Mekong Delta

The Mekong Delta is an area of floodplains surrounding the downstream part of the Mekong River, generally starting downstream of the city of Kratie in Cambodia. Although this area also contains part of Cambodia, in the rest of this report the Mekong Delta will only refer to the Vietnamese part of this region.

The Mekong Delta has a surface area of 39 000 km² (Renaud and Kuenzer, 2012) and is home to nearly 18 million people, which is about 22% of the entire Vietnamese population (Le Anh Tuan et al., 2007). The region forms a triangle at the southernmost point of Vietnam, bounded by the Cambodian border, Ho Chi Minh City, the East Sea and the Gulf of Thailand. In Cambodia, the Mekong River divides into two branches: Bassac (Hau River) and Mekong (Tien River), which are further split up into nine estuaries (see Figure 2.3). This explains why the Delta is sometimes called the “Nine dragons river delta” (Consortium Royal HaskoningDHV, WUR, Deltares, Rebel, 2013).

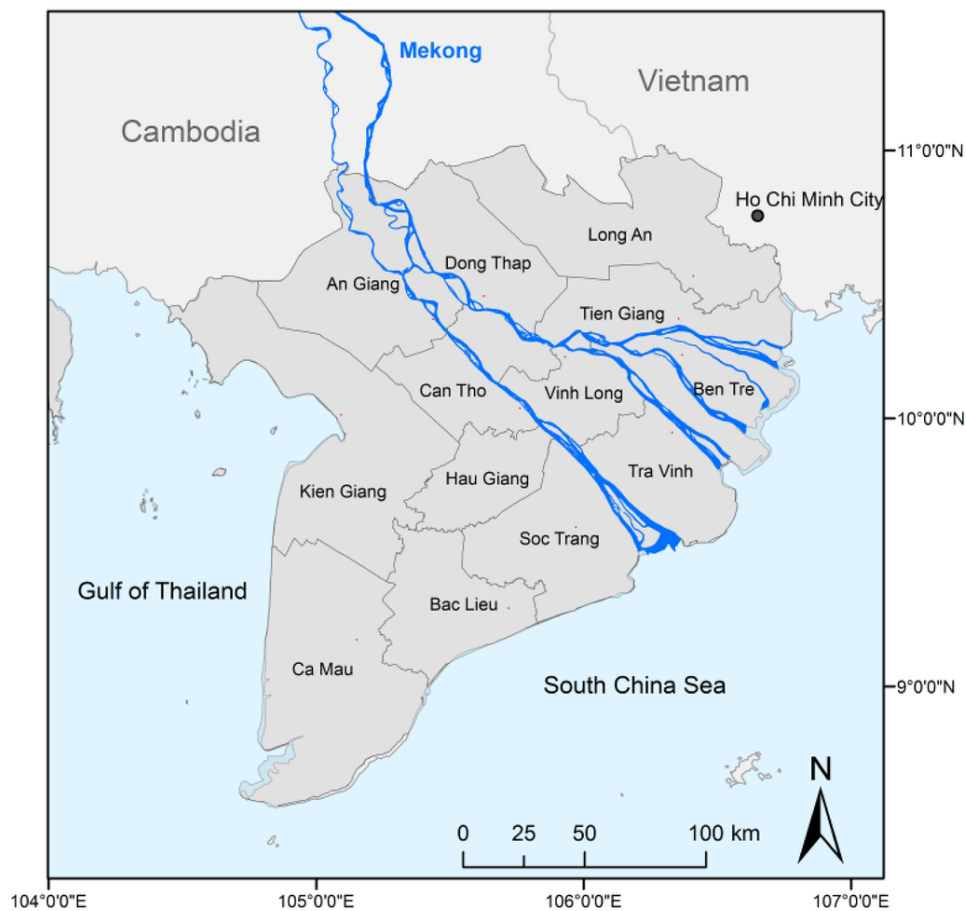


Figure 2.3: Map of the Mekong Delta in Vietnam. This map was drawn from Kuenzer et al. (2013) and shows the most downstream part of the Mekong River and the provinces of the Mekong Delta.

The Delta is very flat, the elevation varies between 0 and 4 m above mean sea level (MSL) with an average of 0.8 m above MSL (Consortium Royal HaskoningDHV, WUR, Deltares, Rebel, 2013). Over the last 300 years, an extensive network of canals has been constructed (Nguyen M Quang, 2000). Through this network the river also discharges into the Gulf of Thailand at the west coast of the Delta. The Delta has a tropical monsoon climate, with distinct wet and dry seasons. During the wet season, from July to December, a large part of the Delta is flooded due to both the high discharges of the Mekong River and local precipitation (Le Anh Tuan et al., 2007). Ojendal (2000) has calculated that the flood flows are about 25 to 30 times as large as the dry season flows. As a consequence, water shortage and salinity intrusion form serious threats during the dry season. The Mekong Delta is often

called the “rice bowl” of Vietnam due to its huge rice production. The Delta owes its fertile grounds to the yearly floods that deposit fertile sediments on fields and wetlands. This illustrates the complex relationship between the inhabitants of the Delta and the Mekong River: the river fertilises the delta, but it also causes flooding problems and salinity intrusion.

2.2.3. Socio-economic background of the Mekong Delta

Deltas are often densely populated areas, and the Mekong Delta, with its population of nearly 18 million people, is no exception. However, only a quarter of its population lives in urbanised regions, compared to the national average of a third (Consortium Royal HaskoningDHV, WUR, Deltares, Rebel, 2013). The delta region has a significant advantage over the rest of Vietnam thanks to its rich natural and human resources, allowing successful agriculture, such as rice cultivation, highly productive shrimp farms, fruit orchards and vegetable crops. 50% of all rice produced in Vietnam is cultivated in the Mekong Delta.

Yet, the advantage of the Delta also comes with disadvantages. The low-lying area is very vulnerable to flooding and salinity intrusion. The demands on the water resources, such as water quality and fresh water supply, have reached their limits due to intensified agriculture. Moreover, climate change and upstream developments (such as dams) further influence the water resources of the Delta (Consortium Royal HaskoningDHV, WUR, Deltares, Rebel, 2013). These disadvantages have resulted in the slower urbanisation and industrialisation in the delta region compared to the rest of Vietnam. Hence, the Mekong Delta Plan states that further development of the Mekong Delta depends to a large extent on the effectiveness of measures regulating the water resources system, such as flood protection, salinity control, water quality and fresh water supply (Consortium Royal HaskoningDHV, WUR, Deltares, Rebel, 2013). This illustrates the importance of this project in the context of coastal protection.

In 2008, Oxfam published a report focusing on poverty in relation to climate change in Vietnam (Oxfam, 2008). According to this report, the number of poor people had been reduced by 70% in 15 years. However, in 2004, 16 million people (which is 19% of the Vietnamese population) were still living under the poverty limit, and 28 million were living just above it. A large part of these poor men and women are living in the coastal areas, such as the Mekong Delta. They are especially vulnerable to (natural) disasters because they often live in fragile homes in exposed areas and they have fewer resources to recover. It is expected that climate change will only aggravate these issues. Climate scientists in Vietnam have monitored an increase in the number of disaster events, as well as an annual temperature rise of 0.1°C between 1993 and 2000 (Ministry of Natural Resources and Environment (MONRE), 2008). Even though the annual volume of rainfall has remained largely stable, the localised intensity and unpredictability of the rainfall has increased, leading to severe floods. On top of this, more droughts have been recorded in the Mekong Delta in recent years, which have tended to last longer. The number of typhoons has reduced in the last four decades, but they have become more intense, and they have tracked more southwards, which means that the Mekong Delta is now increasingly suffering the impact of typhoons.

2.2.4. Sediment dynamics

The delta of the Mekong River as it is known nowadays is the result of a process of progradation. Due to an enormous sediment load provided by the Mekong River, and a decelerating sea level rise, the delta has prograded over a distance of 250 km over the last 3000 à 5500 years (Xue et al., 2010, 2012). During this period, the delta environment has evolved from a “tide-dominated” to a “tide-and-wave-dominated” environment.

Anthony et al. (2015) have used satellite images to assess the current situation of the Mekong Delta. These images show that the Mekong Delta is now dominated by strong erosion. Maps indicating the erosion and accretion rates along the coastline of the Mekong Delta show that almost the entire coastline is eroding, except for some stretches close to the river mouths. In Figure 2.4, such a map is given. The map is made by GIZ and based on historical maps of the Delta.

Delta shoreline dynamics are very complex, and changes can be caused by many factors, such as changes in sediment supply, subsidence and changes in waves, currents and winds. Measurements show that the wave and wind conditions have not significantly changed over the most recent period, during which the delta progradation turned into erosion (Anthony et al., 2015).

The main cause seems to be a reduced sediment supply to the coast, which can be caused by dam retention of sediment upstream and mining activities both upstream and in the delta region. The pits

Shoreline changes from 1904 till 2015 in the Mekong Delta

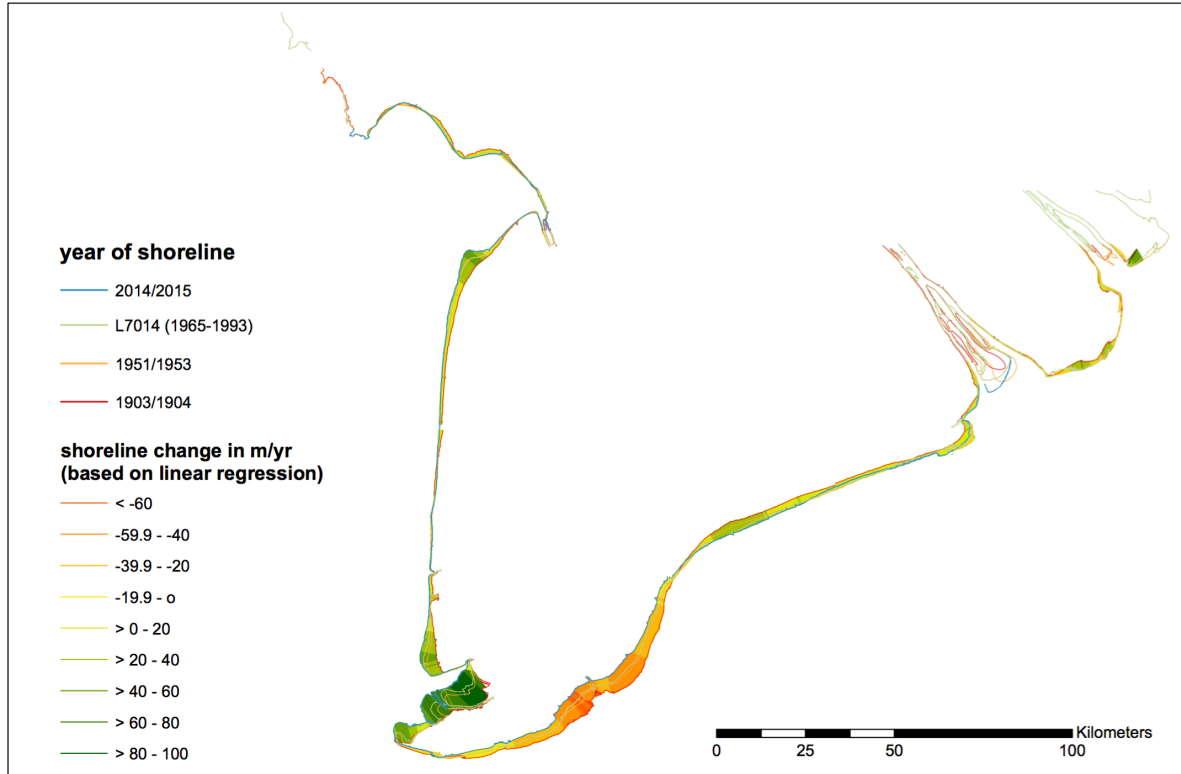


Figure 2.4: Map of the Mekong Delta representing the evolution of the shoreline over the last century (GIZ, 2015).

created by the sand mining serve as enormous sediment traps during the flood discharges. Another possible cause is the accelerated subsidence of the delta region. Deltas are prone to natural subsidence, related to draining and compaction of the deposited sediments. This subsidence is further accelerated by several human activities, such as extra soil loading due to cities, enhanced drainage, but most importantly the extraction of fluids (such as groundwater, oil, gas etc.).

Even if all the causes of the erosion can be identified, it remains unclear how much each factor contributes, since no overall sediment budget exists. The construction of hydropower dams is often considered the main cause of the coastal erosion, however, Figure 2.4 shows that in various locations erosion has been going on for more than a century, while the dams are only a recent evolution. This illustrates that the exact causes and processes are still poorly understood.

2.2.5. Coastal protection in the Mekong Delta

In the most simple coastal protection strategies, the system consists of a sea dike and foreshore. Different foreshore geometries are possible: bare mudflats, mangroves or even a combination of mangroves and aquaculture. There is a tremendous amount of literature on the role of mangroves in coastal protection, a brief overview is given below. However, at many locations along the Mekong Delta coastline, the mangrove forest has already disappeared. Therefore, it is also essential to investigate the effect of bare mudflats in wave attenuation. On the other hand, it is also possible to turn those bare mudflats again into mangrove forests through mangrove reforestation.

The role of mangroves in coastal protection

Mangroves are a group of trees and shrubs that grow along the coastline, between mean water level and high water level. According to NOAA (National Oceanic and Atmospheric Administration, 2008), there are about 80 species of mangrove trees. They are adapted to growing in the waterlogged mud along sheltered coasts where fine sediments can accumulate. Because of this harsh environment, mangrove trees have developed a complex root system, to be able to obtain oxygen directly from the air, and to withstand wave impacts.

It is crucial to recognise the organisation of a mangrove system when planting or restoring mangrove forests: planting monocrops guarantees failure (Othman, 1994). Verhagen and Tran Thi Loi (2012) have given an overview of mangrove species in Vietnam, with the conditions for their environment. In 2012 and 2013, three technical reports were published in the Natural Coastal Protection Series, investigating the role of ecosystems in coastal defence (Mcivor et al., 2012b,a, 2013). These reports focus on the three major aspects of protection provided by mangroves: wave reduction, storm surge reduction and soil surface elevation. Other reports also mention the ability of mangrove forests to reduce coastal erosion (Guannel et al., 2015; Gedan et al., 2011; Othman, 1994). These ecosystem services are investigated in more detail below.

An important note should be made: ecosystem services can only be provided by healthy ecosystems. Thus, healthy mangroves are a prerequisite for any form of coastal protection provided by the mangroves. According to Spalding et al. (2014), requirements for a healthy mangrove ecosystem include sufficient sediment supply, fresh water supply and connections with other ecosystems. On the other hand, the health of the mangroves can be jeopardised by pollution, subsidence or unsustainable use. A final requirement for a healthy mangrove ecosystem is a minimum width of the mangrove belt. Phan Khanh Linh et al. (2015) have researched the coastal mangrove squeeze in the Mekong Delta, and have proven the existence of a critical minimum width, with an average value of 140 m for the (south)eastern Mekong Delta coast.

Wave attenuation Waves entering the mangrove forest lose energy as they pass through the (dense) network of trunks, branches and especially aerial roots (Spalding et al., 2014). A multitude of studies has been performed into the subject of wave attenuation in mangroves, Mcivor et al. (2012b) give an overview of some of these studies. Even though the amount of wave attenuation found in those studies differs, the conclusion is unanimous: mangroves are able to attenuate wind and swell waves.

Most studies have focused on short waves. These waves are most affected by the mangrove forest. However, due to the shallow foreshore, short waves are already significantly attenuated before even reaching the mangrove forest. Phan Khanh Linh et al. (2015) have discovered that long waves are attenuated less effectively by the mangrove forest, which means that the hydrodynamics further into the forest are dominated by the tide and long waves. As a result, long wave reflection at the shoreline cannot be neglected.

Water level reduction There is some discussion as to whether mangrove forests can reduce water levels and protect coastal areas from storm surges. Verhagen and Tran Thi Loi (2012) clearly state that mangrove forests do not decrease the flood level. Nevertheless, in the same report they also conclude that the number of casualties behind mangrove belts was less, which implies that, indirectly, mangroves do offer protection against storm surges. Other authors do mention a flood level reduction in mangrove forests, for example Spalding et al. (2014) mention a reduction of storm surge depth by 5 - 50 cm per km. This small reduction rate is the main cause of discussion; for narrow mangrove belts the reduction is negligible, a mangrove belt of a couple of kilometres has become relatively rare. Nevertheless, even a small reduction in surge level can already have an impact on the extent of flooding.

Sea level rise response A sustainable protection strategy also includes future uncertainties, such as sea level rise for example. In the Mekong Delta, the relative sea level rise is rather large, as it is a combination of the eustatic sea level rise of ca. 3.4 mm/year (Beckley et al., 2007) and the subsidence of the delta up to 30 mm/year (Anthony et al., 2015). This means that the required dike height will increase throughout the lifetime of the dike.

Three solution strategies can be developed: construct a high dike from the start, allow dike heightening throughout the lifetime, or benefit from the mangrove's ability to increase the soil elevation. Hillen (2008) and Mai Van Cong et al. (2008) have compared the costs of the two first strategies, while Mcivor et al. (2013) have investigated the response of mangrove soil surface elevation to sea level rise.

Shallow foreshores

Mangrove coasts are characterised by a very wide, shallow coastal shelf. Even in the case that the mangrove belt has disappeared, this shallow foreshore can still significantly influence the waves approaching the coast. van Gent (2001) has analysed the evolution of wave height distributions and wave energy spectra between deep water and the toe of coastal structures, and has derived a generic wave

runup formula. His conclusions are also confirmed by Phan Khanh Linh et al. (2015), who showed through numerical modelling that the very gentle slopes of the foreshore cause a strong damping of the wave heights.

Integrated aquaculture

A main threat to the survival of mangrove forests is illegal deforestation by the local population. Coastal protection strategies should therefore also try to integrate as many other functions as possible to increase the quality of life. One integration strategy could be to integrate shrimp farming in the mangrove forests that also provide coastal protection. This type of strategy has been analysed in several studies, such as Binh et al. (1997); Fiselier (1990).

Such integrated aquaculture should be extensive, in order to maintain the protection services provided by the mangroves. Moreover, using low densities of mangrove inside the aquaculture ponds has shown to have a positive effect on the shrimp yields (Binh et al., 1997).

2.2.6. Innovative coastal protection strategies in case of strong erosion

In the case there is limited coastal erosion, simple protection strategies can still be applied, however additional measures should be taken to provide erosion protection. Mangrove forests have shown to provide some protection against erosion, mostly by slowing down the process (Spalding et al., 2014; Mcivor et al., 2013). Whereas mangroves can mitigate erosion, bare mudflats cannot, and therefore an adaptation strategy is required, for example by retreating and constructing the dike more land inward. When the erosion rate has become too high, the previous strategies will no longer be sufficient. The dike will eventually become exposed, because the mangrove forests and mudflats will erode and further retreat is no longer possible.

Two strategies are proposed to protect the coastal area in this case. Either the foreshore is nourished, such that the mudflats and mangroves will not completely erode (soft solution), or the erosion is accepted and the dike is designed such that it can withstand the design forces (hard solution). Hoi An Erosion Consortium (2015) has investigated the choice between hard and soft solutions, based on the Dutch experience. Comparing the costs of nourishments with costly revetments, it was concluded that hard structures cannot compete with soft solutions. However, these conclusions were based on a sandy shore. It is unknown how the two solution strategies relate on muddy shores, especially since nourishments have never been applied to coasts with fine sediment.

Soft solution strategy

The idea of nourishments is inspired by the experience with sandy coasts. As mentioned above, nourishments have never been applied to muddy shores. It is expected that this poses some additional difficulties. Some questions that arise when considering this strategy are: What are the required sediment properties? Where can the suited sediment be found? How can the sediment be collected, brought to the nourishment location and kept in place? How much sediment should be supplied? These questions will be discussed in the following paragraphs. It is important to realise the current practical shortcomings of this solution strategy, however, this will not be the focus of this thesis. For the rest of the project, it is therefore assumed that nourishments are possible.

The main purpose of nourishments is to restore, temporarily, the sediment balance by providing sediment. However, since mangrove forests provide so many ecosystem services, a secondary goal of nourishments is to bring back the mangrove belts, by restoring the abiotic conditions. Mangrove trees will also make the nourishment more successful on the long term by reinforcing the soil and keeping the sediment in place. Therefore, when investigating the required sediment properties for nourishments, the requirements imposed by mangroves should also be included. This means that not only the particle diameter and gradation are relevant, but also the amount of nutrients (Tolhurst and Chapman, 2005; Oxmann et al., 2010).

Once the requirements for the sediment have been set, the suited sediment has to be localised. The closer the borrow area to the nourishment site, the cheaper the transport. Therefore, the borrow area will be a location on the shelf, which is fed by the sediment coming from the rivers. However, one should pay attention not to just "pump the sediment around", if the borrow area is so close to the site that the sediment flows back too fast.

Nowacki et al. (2015) have investigated flow and sediment dynamics in the lowermost portion of the Mekong River. They measured a seaward sediment export during high flow and landward import during low flow. The sediment exported during high flow was mainly caused by fluvial advection, while

exchange flow and tidal processes were mainly responsible for the sediment import during low flow. This also resulted in coarser sediment during high flow than during low flow.

The main issue with respect to the transport of the sediment is the low settlement rate. This implies that the sediment will settle slowly in the hopper, resulting in either high overflow losses, or transport of high amounts of water. At the nourishment site, the slowly settling sediment risks to be transported off the site before it has had time to settle.

In mangrove reforestation projects, the sediment and seedlings also have to be protected to prevent flushing away with the tide. A lot of research has been performed in this field, designing dams and other protection structures. Harihar (2015) has developed a design consisting of bamboo-piled walls and drains, showing that the use of local, natural materials is very cost-effective. The little dams prevent the sediment from flowing away, while the drains speed up the settling process. A similar design will be required for nourishment projects.

It is useful to estimate the sediment balance of the coastal zone that needs protection, especially if the shoreline is currently experiencing high erosion. Nourishment does not take away the causes of erosion, and will have to be repeated at regular intervals. Therefore, it is also useful to have an insight in the causes of the erosion problems (see section 2.2.4). For example, by reducing the ground water extraction, the subsidence rate will decrease. Regular flushing of the dams upstream on the Mekong River would increase the sediment load arriving in the delta region.

The sediment discharge of the Mekong River was often estimated around 150 Mt/y: 160 Mt/y (Milliman and Syvitski, 1992; Einsele, 2000) and 144 ± 36 Mt/y (Ta Thi Kim Oanh et al., 2002). Including the effects of damming, a generally accepted sediment discharge lies around 100 Mt/y (Milliman and Farnsworth, 2011). However, these estimates do not account for deposition in the tidal zone of the river, since they are based on measurements slightly upstream. Nowacki et al. have calculated that the real sediment discharge to the delta will lie 60% lower (Nowacki et al., 2015).

Hard solution strategy

This super strong structure will have to withstand strong wave forces, but even more crucial, extreme erosion. Therefore, the revetment and toe protection are paramount. Wave action will create an enormous scour hole, so the scour protection should be large enough to keep the hole at a sufficiently large distance of the structure. Materials to be used for these solution (large rock or concrete) cannot be found close to the project location, so this will increase the price even more. On the other hand, labour is relatively inexpensive in Vietnam, so the costs of a labour-intensive design will be lower than in the Netherlands. An overview of bed and shore protections can be found in Schiereck and Verhagen (2012).

2.3. Scenarios

There are many different coastal protection strategies. Whether a strategy is appropriate for a certain situation is, to a great extent, determined by the erosion rate. One strategy could be suited for a relatively stable coast, while another strategy could provide sufficient protection in case of erosion. However, most of the strategies that are applied nowadays are not suited for high erosion rates. This large influence of the erosion rate on coastal protection strategies is the reason why erosion rate has been chosen to be the leading parameter in defining the different situations that will be investigated. Based on the erosion rate, three different situations are identified: accretion, a stable coastline (no erosion nor accretion) and erosion.

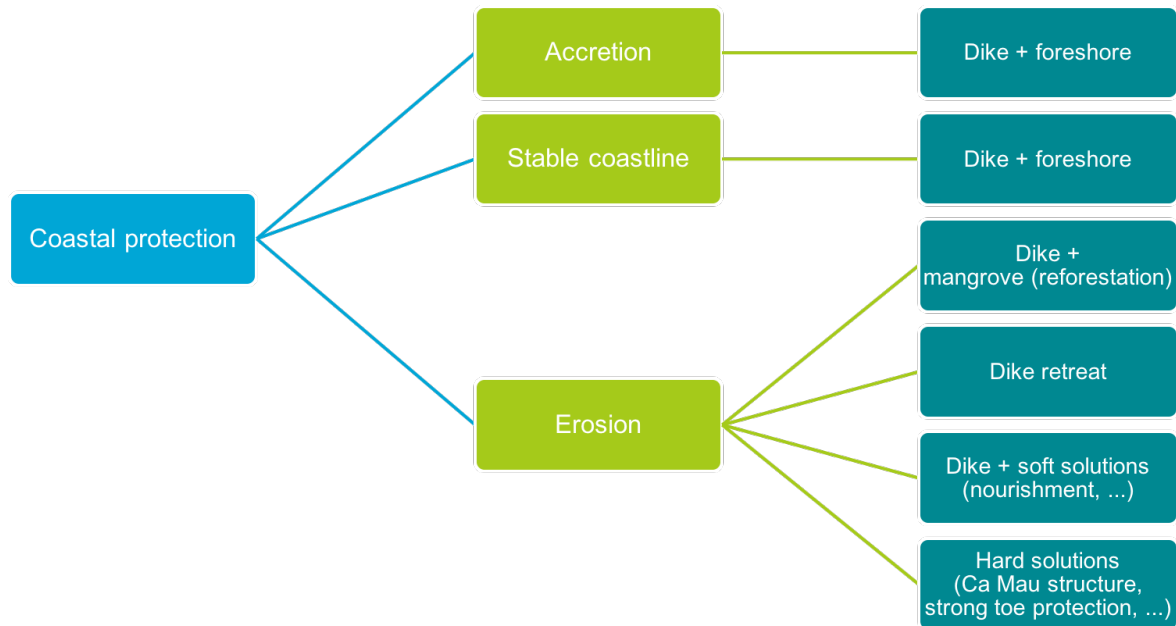


Figure 2.5: Flow chart of the different situations and corresponding protection strategies

Figure 2.5 visualises the different situations, and the corresponding protection strategies. Note that many other protection strategies are possible, however, in order to limit the modelling, only those scenarios that are expected to be most favourable in each situation are mentioned. For example, a super strong structure could also provide sufficient coastal protection in case of a stable coastline, however the cost-benefit analysis will prove that this is much more expensive than a simple dike + foreshore strategy, which can provide sufficient protection as well. Therefore, this is not a complete overview of all possible protection strategies, but a condensed overview of the strategies that are expected to be favourable in each situation.

In subsection 2.2.4, the current situation along the coasts of the Mekong Delta was summarised. Figure 2.4 contains a map of the shoreline changes along the Mekong Delta coast over the last century. Two conclusions can be drawn from this figure. First, there is a large range of erosion and accretion rates. This implies that different protection strategies will be needed, since it is impossible to design one protection strategy that is optimal everywhere. The second conclusion is that at some locations, the erosion rates are extremely high. At these locations, the current protection strategies will fail, showing the need for innovative and sustainable coastal protection strategies that can work in case of high erosion rates.

2.3.1. Accretion

From the point of view of coastal protection, accretion is actually a favourable situation, since the foreshore grows and therefore also the protective properties of the foreshore will increase over time. This is especially useful in case the boundary conditions (waves, storm surges) would also increase over time (relative sea level rise, and possible increase in storm intensity due to climate change). Another strategy would be to move forward at the same rate as the accretion. Especially when there is pressure on the available land surface, this is an attractive strategy. The location of the dike will again

be found through economic optimisation. It might also be useful to look into possible uses of the land in front of the dike, without damaging its coastal protection function.

2.3.2. Stable coastline

The most simple situation is the case in which there is hardly any erosion or accretion and the coastline can be considered stable. In this situation, a simple sea dike is probably the most appropriate protection strategy. The dimensions and location of the dike should be economically optimised, taking into account the damping properties of the foreshore.

2.3.3. Erosion

In the case of eroding coastlines, coastal protection becomes a more complex issue. Due to the erosion of the foreshore, the wave load on the dike increases over time, and eventually exceeds the design conditions. There are two types of strategies: either preventing the foreshore to erode, or accepting the erosion and adapting the coastal strategy to a certain amount of erosion. A combination of these strategies is also possible.

Mangrove forests are known to stabilise the foreshore (Mcivor et al., 2013) and can therefore contribute to the first type of protection strategy. However, in many locations where coastal erosion occurs, the mangrove forest has already (partly) disappeared, since it cannot withstand too high erosion rates. In those locations the dike has become completely exposed to the waves, often leading to failure. Mangrove rehabilitation projects can help to bring back the mangroves, and are therefore an integral part of this solution strategy. However, if the erosion rates are too high, mangrove reforestation cannot succeed, therefore this strategy is only viable for limited erosion.

Another protection scenario in the case of (limited) erosion is dike retreat. The erosion of the foreshore is accepted (or slowed down by additional measures, for example mangrove reforestation, but not completely halted), and the dike is placed more inland. This means that some land is sacrificed, but the design conditions at the dike are less severe, and therefore the dike can be designed less strong (especially the revetment and toe protection of a dike can be extremely expensive). A cost-benefit analysis will balance the costs of the land lost by retreating with the avoided costs of the sea dike design.

Eventually, the erosion rate will become so high, that the dike retreat strategy is no longer viable, because the distance over which the dike has to be retreated becomes so large that such land loss is no longer acceptable. In case of extreme erosion, therefore, new protection strategies need to be developed. Two innovative strategies will be investigated in this project: a soft solution strategy, including foreshore nourishments, and a hard solution strategy, including extremely strong structures.

Although foreshore nourishment is not a new strategy, it is innovative as it has only been applied to sandy foreshores so far. The purpose of this project is not to develop a nourishment technique for mangrove-mud coast, but, assuming it is possible to modify the foreshore geometry through nourishment, to investigate what would be the effect of different foreshore geometries on the wave load and overtopping of the sea dike.

The second strategy consists of super strong structures. This can be a sea dike with a super strong toe protection, which can withstand the design conditions, even if the foreshore has completely eroded and strong scour occurs in front of the dike. Another super strong structure could be some kind of breakwater, which is placed in front of the dike and replaces the damping function of the eroded foreshore.

2.4. Boundary conditions

In order to use a numerical model, boundary conditions are required. A generic approach is followed, which means that the boundary conditions should be chosen in such a way that they are representative for the entire Mekong Delta coast. However, this is a very varied region, so it is impossible to find one set of representative boundary conditions. Therefore, different sets of boundary conditions, representing a range of situations, will be defined. This is also visualised in Figure 2.6.

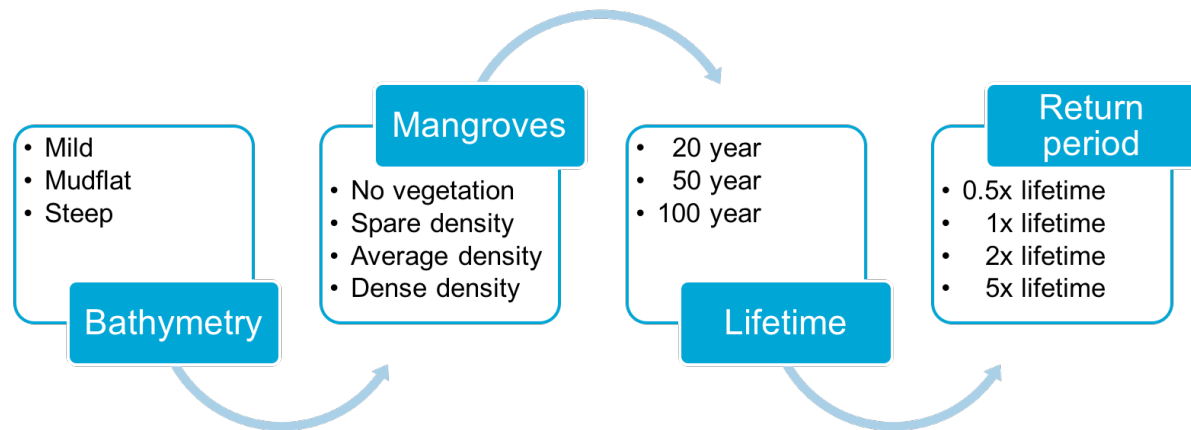


Figure 2.6: Flowchart visualising the range of situations covered in this approach.

This range of boundary conditions will be applied to each scenario that was developed in section 2.3 (see also Figure 2.5).

In the following sections, the lifetime and return period (subsection 2.4.1), bathymetry (subsection 2.4.2), wave conditions (subsection 2.4.3), water level (subsection 2.4.4) and vegetation (subsection 2.4.5) are given. A detailed computation of the wave conditions and water levels can be found in Appendix A

2.4.1. Lifetime and return period

Water level and wave conditions depend on the associated return period. Choosing a return period is not straightforward, since the combination of return period and lifetime determine the failure probability through Equation 2.1.

$$P_f = 1 - (1 - 1/T_r)^{T_l} \quad (2.1)$$

Where

P_f	probability of failure	[-]
T_r	return period	[y]
T_l	lifetime	[y]

The current practice in Vietnam is to choose a return period which is smaller than the lifetime, or at most equal to the lifetime (Tran Quang Hoai et al., 2012). However, this is not a sustainable approach, since this means that the probability of failure is extremely high. In other words, the probability that the dike will experience conditions heavier than the conditions it was designed for during its lifetime is very high. It is therefore very difficult to guarantee a certain level of safety.¹

On the other hand, in the Netherlands the return periods are extremely high (up to 10 000 years, Mai Van Cong (2010)). This implies that the design requirements for the coastal protection are very high, and

¹A possible explanation for this approach can be found in the origin of the finances. In case of heavy damage due to storm, repair costs are provided from separate funding, whereas for initial construction costs often the local authorities, with restricted financial means, are responsible.

the dikes are very expensive. There are two reasons why this is not necessarily the most appropriate approach for Vietnam. First of all, the land protected by the dike, the hinterland, needs to justify the investments. It makes no sense to build an enormous sea dike to protect some agricultural land. The protection level must be in proportion with the protected value. Another reason why it would not be wise to apply such high return periods, is the lack of data. Due to this lack of data, the uncertainty in the conditions corresponding to longer return periods becomes quite high, so an even higher investment would be required to guarantee this high level of safety (if it is even possible to guarantee such a high level of safety which such large uncertainties).

Also the choice of the lifetime is not straightforward. Due to rapid developments in the Mekong Delta, it might be wiser to choose a short lifetime. On the other hand, if such large investments are made, a longer lifetime would seem more worthwhile.

The Vietnamese design guidelines distinguish between five different classes, depending on the value of the hinterland. The lifetimes corresponding to these classes are 30 years, 50 years and 100 years, while the return periods vary between 10 and 150 years (Tran Quang Hoai et al., 2012).

For this project, three different lifetimes will be compared: 20 years, 50 years and 100 years. Since lifetime, return period and failure probability are related, the return period will be expressed as function of the lifetime. In order to compare the Dutch and Vietnamese approach to defining the return period, a range of return periods will be used. The smallest return period considered will be equal to half of the lifetime. The other three return periods will be once, twice and five times the lifetime. This means that the return periods for a lifetime of 20 years are respectively 10, 20, 40 and 100 years; for a lifetime of 50 years respectively 25, 50, 100 and 250 years; and for a lifetime of 100 years respectively 50, 100, 200 and 500 years. An overview of the failure probability for each combination of lifetime and return period, computed with Equation 2.1, is given in Table 2.1.

Return period [y]	$0.5T_l$	T_l	$2T_l$	$5T_l$
Lifetime [y]				
20	87.84	64.15	39.73	18.21
50	87.01	63.58	39.50	18.16
100	86.74	63.40	39.42	18.14

Table 2.1: Failure probabilities (in %) for different combinations of lifetime and return period

2.4.2. Bathymetry

The bathymetric profiles that will be used in this generic modelling approach are based on the results of two measurement campaigns in the province of Ca Mau carried out in 2013 by Albers and Stolzenwald (2014) in cooperation with the Southern Institute of Water Resources Research (SIWRR, in Ho Chi Minh City) and should be representative for the entire Mekong Delta.

Since it is impossible to determine one single bathymetric profile that is representative for the entire coastline, three profiles will be defined: a mildly sloping profile (representative for the east coast of the Mekong Delta), a profile with a steeper bottom slope (representative for the west coast), and a profile with a mudflat (representative for the area around the tip of Cà Mau). Note that the notions of mild and steep are relative, since mangrove coasts in general have very gentle foreshores and a very wide coastal shelf. These three profiles cover a large part of the situations that are encountered along the coast of the Mekong Delta.

The three profiles are visualised in Figure 2.7. The mildly sloping profile has a bottom slope of 1:1500, the more steep profile has a bottom slope of 1:800 (note that these bottom slopes are extremely gentle). The mudflat is 2 km wide and lies at 1 m below MSL, seaward of the mudflat the bottom slope is also 1:800. The x-axis points perpendicularly towards the coastline and the origin is located at MSL shoreline. The z-axis is positive upwards and has its origin at MSL. This coordinate system will be used for the rest of this report, except if stated otherwise.

The steep profile and the profile with mudflats more or less need the same cross-shore space, therefore it will be useful to investigate what the effect of the mudflat on the wave transformation will be, even without the presence of mangroves. Furthermore, also the tidal levels are indicated in Figure 2.7 (HW, MSL and LW). For more information on tidal levels, see subsection A.2.1.

In reality, the bottom slope inside mangrove forests is often steeper than the bottom slope of the fore-

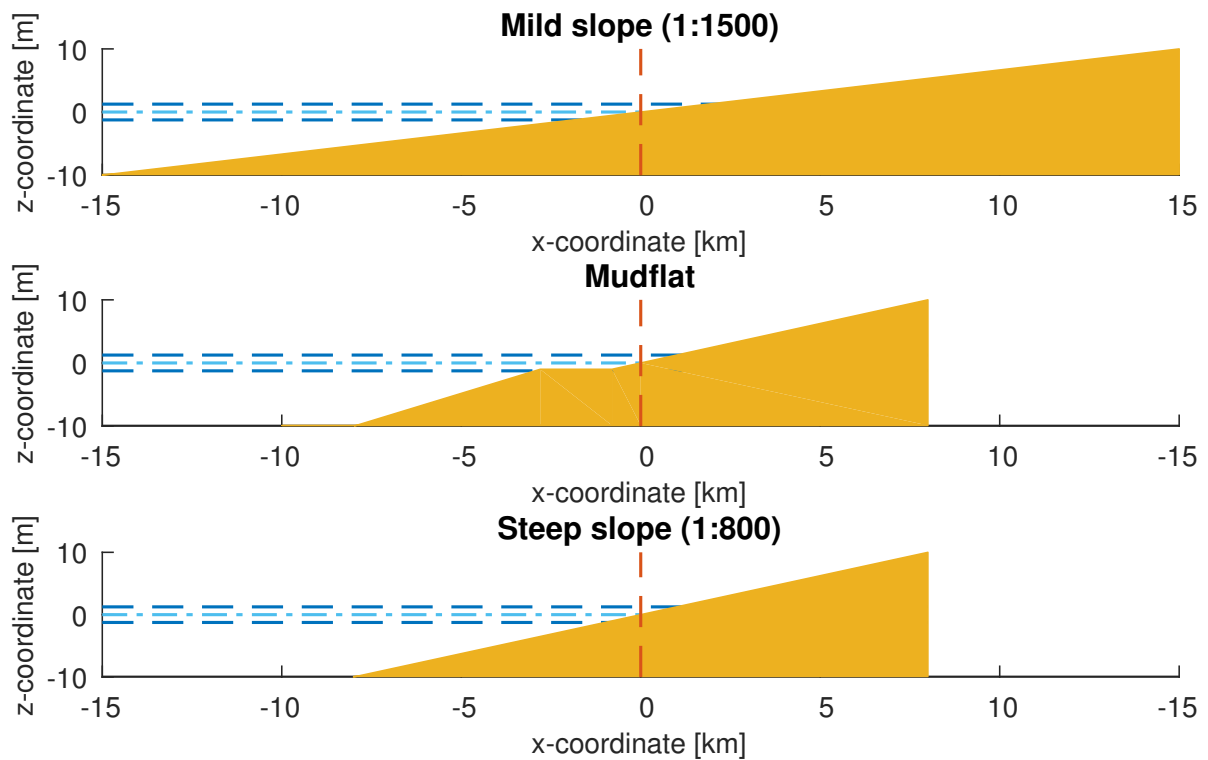


Figure 2.7: The three bathymetric profiles that will be used to model the Mekong Delta. The blue dashed lines indicate water levels (light blue for MSL, dark blue for high and low tide). The red dashed line indicates the shoreline at MSL ($x = 0$).

shore. However, in this project the bottom slope is chosen to be the same everywhere. This simplifies the comparison between bare mudflat and vegetated foreshore, but it is also the most realistic situation if the mangrove forest has to be restored. Starting from a bare foreshore, the mangrove trees grow on this mild slope. It is only when the forest becomes dense enough to influence the wave conditions, that it will start influencing the bottom slope. As there is no evolution in time included in this approach, the later stages of the mangrove forest and their effect on the bottom slope (and vice versa) are excluded.

2.4.3. Wave conditions

In contrast to the Netherlands, wave and water level data are not easily available in Vietnam. This can be explained by two reasons: first, there have not been many measurement campaigns, let alone long term measurement stations, and second, the measured data are not always available. The data are often owned by institutes who will only sell their data to a limited group of users.

Determining design conditions with large return periods is therefore very difficult. For this project, three data sources have been used: wind data for Con Dao (Tran Viet Lien et al., 2004), wave data from a wave station in Bach Ho (Hoang Van Huan and Nguyen Huu Nhan, 2006) and wave data from the NOAA wave model (National Oceanic and Atmospheric Administration, 2014).

In appendix A.1 each source has been individually analysed (appendix A.1.1), after which the data has been combined into the design conditions that will be used for the rest of this project (appendix A.1.2). The resulting design wave conditions are summarised on the next page in Table 2.2.

Return period [y]	Wind speed [m/s]	Wave height [m]	Wave period [s]
10	19.7	5.1	9.4
20	21.9	5.7	9.7
25	22.6	5.9	9.8
40	24.1	6.3	10.0
50	24.8	6.5	10.1
100	27.0	7.0	10.4
200	29.2	7.6	10.8
250	29.9	7.8	10.9
500	32.1	8.4	11.2

Table 2.2: Design wave conditions

2.4.4. Water level

Extreme water levels are a combination of a high (spring) tide and a storm surge. This storm surge can be composed of four components: wind set-up, wave set-up, a barometric effect and the effect of the shape of the land. Finally, the future water levels are also influenced by relative sea level rise. Each of these individual components are described in section A.2.

The design water level can be determined by adding all components. Since the wind set-up depends on the bathymetry and return period, and the sea level rise on the lifetime, each combination of bathymetry, return period and lifetime will have its own design water level. This is summarised in Table 2.3.

Bathymetry		Mild	Mudflat	Steep
Lifetime [y]	Return period [y]			
20	10	3.0	2.9	2.8
	20	3.2	3.0	2.8
	40	3.3	3.1	2.9
	100	3.5	3.3	3.0
50	25	3.8	3.7	3.5
	50	4.0	3.8	3.6
	100	4.1	3.9	3.7
	250	4.3	4.1	3.8
100	50	5.0	4.8	4.6
	100	5.2	4.9	4.7
	200	5.3	5.1	4.8
	500	5.5	5.2	4.9

Table 2.3: Estimated design water levels (in m above MSL) for different combinations of lifetime, return period and bathymetry.

2.4.5. Vegetation

Mangrove forests can act as a natural coastal protection, by attenuating incoming wave energy and collecting and stabilising sediments, thus preventing coastal erosion (Verhagen and Tran Thi Loi, 2012; Othman, 1994; Mcivor et al., 2012b,a, 2013). However, the mangrove forests in the Mekong Delta are disappearing at alarming rates (Anthony et al., 2015). Therefore, when modelling the coastal hydrodynamics, several scenarios should be investigated, with and without mangroves, but also for varying mangrove forest densities.

In this section, first the way SWASH approximates the wave attenuation in vegetation is described and the required parameters are listed. Subsequently, an overview of literature providing values for these parameters is given. Finally, the different scenarios that will be modelled are defined, with the corresponding values for the input parameters.

Vegetation modelling in SWASH

SWAN and SWASH use a formulation described by Dalrymple et al. (1984), in which the the amount of dissipated wave energy is expressed in terms of vegetation characteristics and wave parameters. Burger (2005) has investigated the performance of this formulation in SWAN for modelling the wave

attenuation in mangrove forests, and has found that the drag coefficient C_d is the only calibration parameter in the formulation, all other vegetation characteristics, such as vegetation diameter, density and relative vegetation height, can be measured easily. It turned out that the drag coefficient mainly depends on relative spacing. However, Burger stresses that also some non-drag related and initially neglected processes are discounted in this coefficient, and therefore, it should not be called “drag” coefficient.

This formulation allows the vegetation to be divided into different vertical segments, as shown in Figure 2.8, which is crucial in modelling wave dissipation in mangrove forests. Mangrove trees usually consist of three layers: some roots above the ground, a stem and a wide canopy. For each vertical layer, the characteristics of the vegetation are described by the following parameters: the plant height, the diameter of each plant stand, the number of plant stands per square meter and the drag coefficient (The SWASH team, 2015).

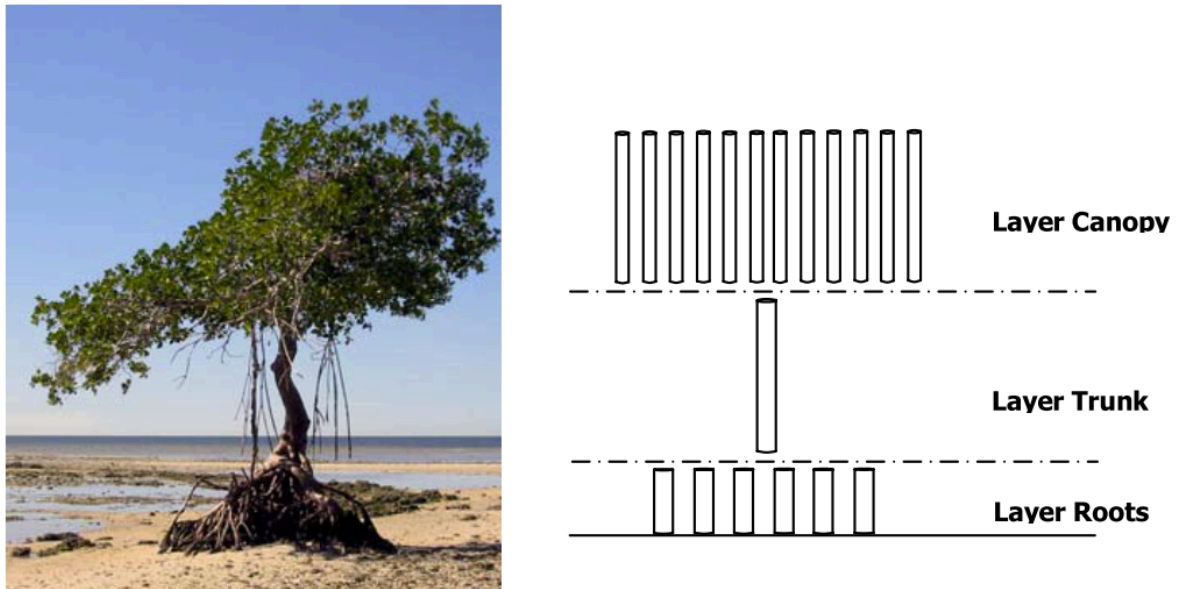


Figure 2.8: Vertical schematisation of a mangrove tree in SWASH (Burger, 2005)

Further, there is also the possibility to horizontally vary the vegetation density over the computational domain, by defining an input grid. However, of the characteristics defined for each vertical layer, only the number of plant stands per square meter is allowed to vary horizontally, by multiplying this value with the values defined in the input grid.

Literature overview mangrove characteristics

The values of the 12 parameters (4 parameters for each layer, 3 layers) will be derived from literature. Narayan (2009) has investigated the characteristics of *Rizophora* species and *Sonneratia* species in mangrove forests in India. The applicability of these parameters to mangrove forests in the Mekong Delta is defended by Phan Khanh Linh et al. (2015) because of the similarities between the mangrove species in the Mekong Delta and those in India. Phan Khanh Linh et al. (2015) also introduce different scenarios of mangrove density: sparse, average and dense, allowing for the different states of the mangrove forests along the Mekong Delta coast. This approach will also be adopted here.

Nguyen Thi Kim Cuc et al. (2015) investigated the difference in vegetation characteristics of naturally regenerated and planted mangrove forests, the main difference being a lower density in the planted forests (also a difference in height is noticeable). Therefore the different scenarios as proposed by Phan Khanh Linh et al. (2015) not only represent different states of mangrove forests, but can also represent the difference between natural and planted forests.

For the value of the drag coefficient, Burger (2005) is consulted. After a sensitivity analysis, Burger concluded that the drag coefficient is one of the most important parameters, but it is also the most difficult to determine. However, the drag coefficient can be calibrated if measurements are available. Since this is not the case here, a value of 0.25 m will be applied for every layer. Choosing a higher

value will lead to more wave attenuation, lower values give less wave attenuation, which can also be used to model flexible vegetation for instance.

Overview chosen values input parameters

A limitation of the way SWASH allows to vary the vegetation characteristics horizontally, is that only the density can be varied horizontally. However, mangrove forests consist of different zones, each accommodating different mangrove species with specific characteristics. Often, *Sonneratia* sp. can be found close to MSL, while *Rizophora* sp. will be present more landward (Phan Khanh Linh et al., 2015). However, by only varying the density of the plant stands, this difference cannot be modelled satisfactorily. Therefore, it will be assumed that the forest consists of only *Sonneratia* species. This is a limitation of the current model.

In total 4 different scenarios will be modelled: one without mangroves and three with *Sonneratia* sp. with varying density (sparse, average, dense). In Table 2.4 an overview of the input parameters for each scenario is given. For comparison, also the input parameters for *Rizophora* sp. are given.

	<i>Sonneratia</i> sp.			<i>Rizophora</i> sp.		
	Canopy	Stem	Roots	Canopy	Stem	Roots
Height [m]	2	6	0.5	2	6	0.8
Diameter [m]	0.5	0.3	0.02	0.5	0.25	0.075
Spare density [m^{-2}]	50	0.5	25	50	0.5	30
Average density [m^{-2}]	100	0.7	50	100	0.7	60
Mean density [m^{-2}]	100	1.7	100	100	1.7	130
Drag coefficient [m]	0.25	0.25	0.25	0.25	0.25	0.25

Table 2.4: Overview of the chosen values for the input parameters used to model mangrove vegetation in SWASH (Narayan, 2009; Phan Khanh Linh et al., 2015; Burger, 2005)

2.4.6. Cyclones

So far, cyclones have not been included in the boundary conditions. The first reason is that there is only limited information on cyclones in the Mekong Delta region. Cyclones rarely land in the Mekong Delta, although in 1997 Linda caused damage for more than 350 billion USD (Vo Thanh Danh and Huynh Viet Khai, 2014). Linda is actually one of the only well documented cyclones that have landed in the Mekong Delta, and has an estimated return period of 50 years (Vo Thanh Danh and Huynh Viet Khai, 2014). During the peak of the storm, wind speeds of almost 40 m/s were reached, which corresponds to a normal storm with a return period of 200 years (based on the wind data of Tran Viet Lien et al. (2004)).

The second reason that cyclones have been left out of the boundary conditions, is because of economic considerations. As the example of Linda illustrates, designing a coastal protection that can withstand cyclones would require much stronger and therefore more expensive measures. Such a dike would be prohibitively expensive for most of the Mekong Delta.²

Therefore, the author has decided not to design for cyclones in this project, but instead include investments in early warning systems and shelters. The Vietnamese government is currently setting up such a system, as was decided by Prime Minister Decision 197 (Nguyen Tan Dung, 2007).

By comparing the protection strategies designed for the boundary conditions with return period 50 and 200 years, the difference between designing with and without cyclones can be illustrated.

2.4.7. Limitations of the model input

In the above sections, all model input is listed. However, there are some limitations to this input, which will be discussed below. It is important to be aware of these limitations, even though they can not be resolved.

The biggest limitation is the lack of data. The hydraulic boundary conditions (waves, water levels) depend on extrapolation of the very limited sources of data. The larger the uncertainty in the input values,

²There is also the possibility to reduce the damage to the dikes during cyclones by designing a dike that can survive cyclones; losing its function during the cyclone, but reducing the maintenance required after the cyclone. However, because of the lack of data, this alternative will not be applied.

the lower the level of safety that can be guaranteed. Especially in the case of longer return periods (up to 500 years in this project), the uncertainty is significant. It is therefore recommended to run comprehensive measurement campaigns in the near future.

Another limitation of the chosen model input is the fact that cyclones are not included. Although cyclones do occur in the Mekong Delta, they are rare. As a result, there is little data on cyclones, which makes it impossible to determine reliable boundary conditions including cyclones. Especially since including cyclones implies a huge increase of investment, this cannot be justified by the current uncertainty range.

The effect of climate change is only accounted for through the sea level rise. Other effects, such as more intense storms or more frequent storms, have not been included, again due to a lack of information. These effects will mostly affect the longest lifetime (100 years).

The way SWASH models vegetation, makes it impossible to include zonation in mangrove forests, although research has shown this is crucial to the existence and survival of mangroves. On top of that, SWASH requires a drag coefficient, for which measurements are needed in order to be able to calibrate. However, these measurements are not available. Therefore, also the reliability of the modelled effect of vegetation is limited.

2.5. Numerical modelling

Each scenario will be numerically modelled in order to determine the wave load and overtopping of the sea dike. This section starts with a brief inventory of the requirements for the numerical model (subsection 2.5.1), after which the models that will be used are described in subsection 2.5.2. The section finishes with an overview of how the models will be set up (subsection 2.5.3).

2.5.1. Model requirements

There are two main questions related to the numerical modelling aspect of this project: what needs to be modelled and how will it be modelled?

The first question can be answered by looking at the goals of this project: to design an appropriate coastal protection. In this case, a sea dike will have to be designed for different scenarios. The numerical model is needed to determine the loads on the sea dike in each scenario. Therefore, the wave characteristics at the toe of the dike, as well as the overtopping quantities need to be modelled.

The second question boils down to a number of choices that have to be made: which model will be used and how will this model be set up? To be able to make these choices, it is necessary to understand the important processes, such that the final model represents these processes.

First of all, the model needs to be able to model the wave transformation up to the shoreline. The model should not only model the short waves, but also the long waves, since these are especially important for wave run-up. The model should also incorporate different dissipation mechanisms, such as bottom friction (important on the very mild shallow foreshores), vegetation (in mangrove forests) and wave breaking. To accurately model mangrove forests, the vegetation should be varied in vertical direction, allowing to distinguish the effects of the roots, the branches and the canopy (Mcivor et al., 2012b). Another reason why the model should be able to model the long waves accurately, is that the bottom friction has more impact on the short waves, thus closer to shore the hydrodynamics are dominated by long wave motions (Phan Khanh Linh et al., 2015).

The coasts of the Mekong Delta have always been morphologically very active, and at present a large part of the coastlines is suffering extreme erosion. However, it lies outside the scope of this MSc thesis to set up a fully morphodynamic model. Therefore, only the hydrodynamics will be modelled.

2.5.2. Model description

As morphodynamics are excluded, only the hydrodynamics will be modelled. Therefore, a hydrodynamic model is needed, which can accurately model the wave transformation nearshore up to the shoreline. For this purpose, both XBeach and SWASH are suited, but since the author has more experience with SWASH, SWASH is chosen. SWASH, which stands for Simulating Waves till Shore, is a wave-flow model for the coastal regions up to the shoreline (The SWASH team, 2015).

However, the wave boundary conditions have been defined at relatively deep water. Due to the mild bottom slopes in the Mekong Delta, the distance between the shoreline and deep water is relatively large, and in combination with the required accuracy nearshore, computing this entire domain in SWASH would be very expensive. Therefore, it is chosen to first translate the wave climate from offshore to nearshore, and in a second step to model the hydrodynamics nearshore. For this translation from offshore to nearshore, SWAN will be used. SWAN, which stands for Simulating Waves Nearshore, is a third-generation wave model for obtaining realistic estimates of wave parameters in coastal areas (The SWAN team, 2009).

Description of SWASH

SWASH is a non-hydrostatic wave model, intended for the prediction of the transformation of dispersive surface waves from offshore to the shoreline. The idea behind it is *“to provide an efficient and robust model that allows a wide range of time and space scales of surface waves and shallow water flows in complex environments to be applied.”* (The SWASH team, 2015). As such, it is perfect for this project: modelling the wave transformation from offshore up to the toe of the dike, wherever it may be located, over differently shaped foreshores.

SWASH is governed by the nonlinear shallow water equations, including the non-hydrostatic pressure term. The fact that SWASH is a non-hydrostatic model, makes it unique and especially valuable for this project. Near shore, the non-hydrostatic pressure term is no longer negligible compared to the hydrostatic pressure term. Therefore, the hydrostatic pressure assumption is no longer valid and the full vertical momentum equation should be included.

In the vertical, SWASH can be run in depth-averaged mode or in multilayered mode. In the latter case, the computational domain is divided into a number of vertical layers. The number of layers influences the accuracy of the frequency dispersion. Therefore, there is no need to increase the order of spatial derivatives, as is the case in Boussinesq-type wave models. This makes SWASH much more robust and faster than those wave models.

SWASH can model a wide range of physical phenomena, of which the following are relevant for this project: wave propagation, frequency dispersion, shoaling, refraction and diffraction; nonlinear wave-wave interactions (including surf beat and triads); depth-limited wave growth by wind; wave breaking; wave runup and rundown; moving shoreline; bottom friction; partial reflection and transmission; wave damping induced by aquatic vegetation.

Description of SWAN

SWAN is a third-generation wave model³ used to estimate wave characteristics in coastal regions. The main difference with SWASH lies in the governing equations: SWAN is a spectral wave model, based on the wave action balance equation, whereas SWASH is a non-hydrostatic wave model. As such, SWAN is a phase-averaged model and SWASH a phase-resolving model. This means that SWAN computes the statistics of the sea surface, while SWASH computes a time series of the sea surface vector.

The relevant physics modelled by SWAN are: wave propagation in time and space, shoaling, refraction due to current and depth, frequency shifting due to currents and non-stationary depth; wave generation by wind; three- (triad) and four- (quadruplet) wave interactions; whitecapping, bottom friction and depth-induced breaking; wave-induced set-up (The SWAN team, 2009).

2.5.3. Model set-up

An example of the input files of SWAN and SWASH can be found in Appendix B.

SWAN

SWAN will be run in stationary mode and in one dimension (representing one cross-section perpendicular to the coastline).

The length of the computational domain depends on the bottom slope, but the offshore boundary is located where the bottom level lies at $z = -65\text{m}$, while the landward boundary is located at $z = +10\text{m}$. The origin of the vertical axis is defined at mean sea level (MSL), while the origin of the horizontal x -axis is defined at the location of the offshore boundary. For the coordinate system the Cartesian convention will be followed. The computational domain is a regular grid with a grid cell size of 100 m.

The bathymetry is defined on a regular grid. There are three bathymetric profiles, which have been translated into a .bot file to be used as input for SWAN.

Due to the gentle slopes, wave growth due to wind cannot be neglected. Therefore, a constant wind is included. The strength of the wind depends on the boundary conditions, while the direction is always onshore.

At the offshore boundary, the wave spectrum is imposed. This will be a standard JONSWAP-shape spectrum, with a wave height and peak period as function of the return period, as determined in the previous sections. The wave direction is perpendicular to the boundary, onshore directed. At the landward boundary, a closed boundary is defined. However, this will have no effect, since the waves will never reach $z = +10\text{m}$. The water level is set at the design water level related to the corresponding return period.

SWAN will be run in third generation mode for wind input, quadruplet interactions and whitecapping (linear growth). Also triad wave-wave interactions are activated. Bottom friction will be included using a semi-empirical expression derived from the JONSWAP results. The default value for the friction coefficient of 0.038 is used. No vegetation will be included in SWAN.

SWASH

The computational grid in SWASH will be smaller than in SWAN, but at a much higher resolution. The grid cell size is 5 m. The offshore boundary lies between $z = -30\text{m}$ and $z = -10\text{m}$, depending on the location of the breaking point. The landward boundary lies at $z = +10$. In the vertical, the domain will

³In first-generation models, nonlinear wave-wave interactions are not included. Second-generation models parametrise these non-linear interactions, while third-generation models explicitly include all non-linear wave-wave interactions.

be split in three equidistant layers.

The bathymetry is defined on a regular grid. Similarly to SWAN there are three bathymetric profiles. As initial conditions, the water level and velocity components are set to zero. A spin-up time of 20 minutes is included.

At the western (offshore) boundary, waves are imposed through a wave spectrum. This spectrum has been derived from the SWAN model, although it has been enhanced to compensate for the wave height drop due to nonlinearities at the boundary. Furthermore, the boundary is weakly reflective, to prevent reflection of longer waves. At the eastern boundary (landward) boundary, no boundary condition is specified, implying the boundary is closed. However, this boundary is located at such a high level ($z = +10\text{m}$) that the waves will never reach it.

Bottom friction will be included through the Manning formula, which, although developed for quasi-steady flow conditions, provides a good representation of the surf zone wave dynamics (The SWASH team, 2015). The default value for the friction coefficient of $0.019 \text{ m}^{-1/3}\text{s}$ is applied.

Mangrove vegetation is defined in three layers, for each layer the height, diameter and number of stems is given, as well as the drag coefficient. The values of these parameters are based on work of Phan Khanh Linh et al. (2015). The mangrove vegetation grows shoreward of MSL, this is defined through a regular grid.

Due to the relatively coarse vertical resolution, wave breaking is activated. The non-hydrostatic pressure is included in the shallow water equations, because the hydrostatic pressure assumption cannot be made in case of short waves. Momentum must be conserved everywhere, and upwind discretisation is used for the momentum equations. Explicit time integration will be applied, where the Courant number is limited between 0.1 and 0.5, which is advised in case of high waves and nonlinearities.

2.6. Evaluation framework

2.6.1. Cost-benefit analysis

For each scenario, different solution strategies will be modelled. From this approach rises the need for an evaluation framework, which can be used to evaluate each individual protection strategy, and hence the results of these evaluations can be used to compare the different strategies. The evaluation and comparison of strategies will be done based on the principles of economic optimisation through a cost-benefit analysis (CBA). In this approach the investments in coastal protection are weighed against the reduction in risk (Hillen, 2008; Hillen et al., 2010). The risk can be seen as the probability of a disaster, multiplied by the consequence of such disaster, which can be expressed as the costs of the damage caused by the disaster (Mai Van Cong et al., 2008). In other words, the economic optimisation is used to evaluate the economic efficiency of the protection strategy (Albers and Stolzenwald, 2014).

Costs and benefits of coastal protection in the Mekong Delta

Looking at the coastal protection strategies for the Mekong Delta coast, all costs and benefits can actually be divided into two categories: the first category contains all costs and benefits related to the construction and maintenance of coastal protection measures, while the second category consists of all costs and benefits related to the value of land. The reason for adopting this classification, instead of the more obvious division between costs and benefits, is that this classification is more robust and straightforward. Robust, because elements will not switch between the categories just because their sign has changed, turning them from a cost into a benefit and vice versa. Straightforward, because the different components can be easily classified, even though their value might still be unknown. This classification is visualised in Figure 2.9.

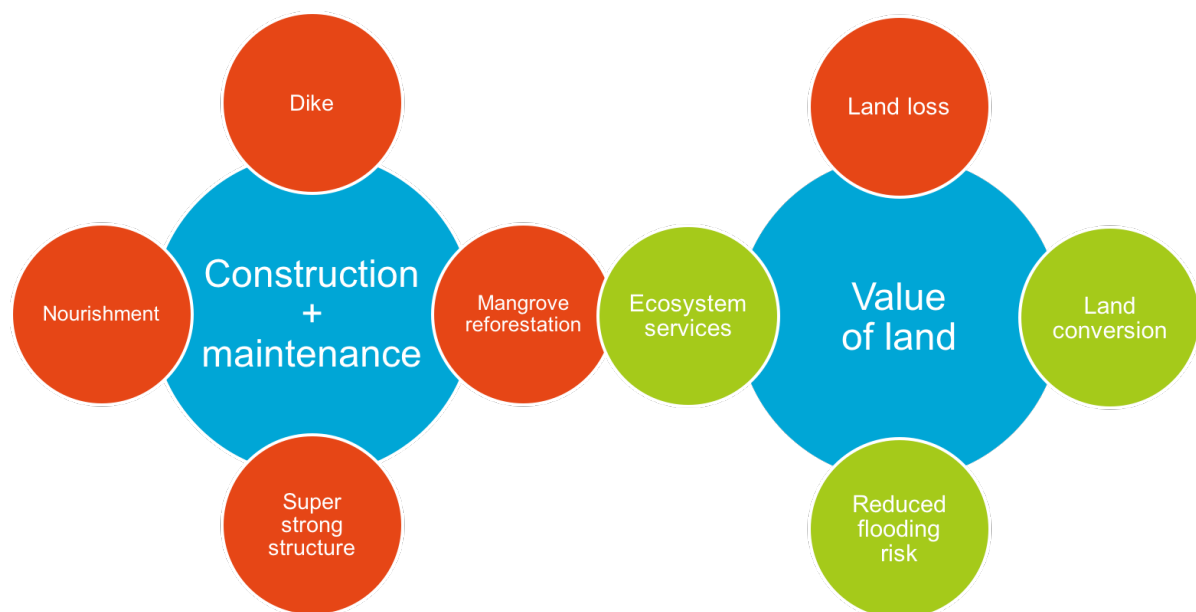


Figure 2.9: Costs and benefits of coastal protection strategies divided between costs and benefits related to construction and maintenance of protection measures and those related to the value of land.

In the first category, four different protection measures are included: sea dike, mangrove reforestation, hard solutions (super strong concrete structures) and soft solutions (nourishment). These are the protection measures applied in the various scenarios. In every scenario, a sea dike will be present, while the other three measures occur in different combinations throughout the scenarios.

In the second category the value of land is accounted for through different costs and benefits. Ecosystem services are used to translate the value of mangrove forests into an economic benefit. The avoided damage due to flooding is included as the reduced flooding risk by multiplying the reduction in flooding probability with the damage upon flooding. Furthermore, also the loss of land in case of dike retreat is included. The reference level is chosen to be the low water line, so all the area included between the low water line and the retreated dike line is considered to be lost, and the value of this lost land

is estimated as the agri- or aquacultural production of such area. In a natural situation, without any artificial protection, agri- and aquacultural activity would be possible starting from the high water level. However, the reference situation is not chosen to be the natural situation, but instead to be the preferred Vietnamese situation: a dike at low water level. By choosing the reference level thus, it can be shown for which situations it would be economically more beneficial to place the dike further inland, or in other words, the benefits of the coastal protection more than compensate the abandoned land between low water level and the dike. Although the land between the low water line and the dike is called “lost”, this does not mean its value has been reduced to zero. Through ecosystem services, or even other types of land use it can still produce benefits. These benefits are included under the term land conversion in Figure 2.9.

Unit convention

For the sake of comparison, each cost and benefit related to the protection strategies has to be expressed in the same unit. Since it is an economic comparison method, this common unit will be monetary. The currency in Vietnam is the Vietnamese Dong (VND)⁴, so all calculations will be done in VND, but the equivalent in USD will also be given, to increase the readability of the report and to make comparison with other projects possible.

In the adopted approach, only a representative cross-section is modelled. Therefore, all prices will be expressed in price per meter dike length (VND/m).

Without going into too much economic detail, the value of money evolves over time. Therefore, all costs and benefits have to be calculated at a fixed point in time, which is set at the present, when the coastal protection strategy is implemented. For costs and benefits occurring in the future, a representative present value is calculated.

Cost and benefit calculations

The total costs of each protection strategy consist of the sum of costs and benefits of each category as defined above, and is summarised by Equation 2.2. Note that negative costs represent actually net benefits gained by the protection strategy.

$$C_{tot} = C_{C\&M} + C_{VOL} \quad (2.2)$$

Where

C_{tot}	total costs protection strategy	[VND/m]
$C_{C\&M}$	costs related to construction and maintenance of protection measures	[VND/m]
C_{VOL}	costs related to value of land	[VND/m]

The costs and benefits of the first category, related to the construction and maintenance of the various coastal protection measures, are composed of two parts: an investment at present (the construction costs of the protection measures) and costs spread over the entire lifetime of the protection measures (the maintenance costs). The latter cost component needs to be translated into a present value. The total costs of the first category are given in Equation 2.4. Note that the four different measures (dike, mangrove reforestation, hard and soft solutions) are mentioned, but they will not be included in every strategy, so for each strategy only those measures that are relevant should be included.

$$\begin{aligned} C_{C\&M} &= I + PV(M) \\ &= I_D(h_D) + I_M(w_M) + I_{HS} + I_{SS} + PV[M_D(h_D)] + PV[M_M(w_M)] + PV(M_{HS}) + PV(M_{SS}) \end{aligned} \quad (2.3)$$

⁴In this report the exchange rate between Vietnamese Dong (VND) and US Dollar (USD) is set at: 1 USD = 20.000 VND.

Where

I	investments (construction costs)	[VND/m]
PV	present value of a certain cost or benefit	[VND/m]
M	maintenance costs	[VND/m/y]
$I_D(h_D)$	construction costs sea dike, as function of dike height h_D	[VND/m]
$I_M(w_M)$	mangrove reforestation costs, as function of width mangrove belt w_M	[VND/m]
I_{HS}	construction costs related to hard solution strategy	[VND/m]
I_{SS}	construction costs related to soft solution strategy	[VND/m]
$M_D(h_D)$	dike maintenance costs, as function of dike height h_D	[VND/m]
$M_M(w_M)$	mangrove reforestation maintenance costs, as function of width mangrove belt w_M	[VND/m]
M_{HS}	maintenance costs of the hard solution strategy	[VND/m]
M_{SS}	maintenance costs of the soft solution strategy	[VND/m]

The present value of the maintenance costs can be calculated with Equation 2.4.

$$PV(M) = \sum_{n=1}^{T_l} \frac{M}{(1+r')^n} \quad (2.4)$$

Where

T_l	life time of the protection strategy	[y]
M	yearly maintenance costs of the protection measure	[VND/m/y]
r'	real interest rate	[-]

The second term in Equation 2.2 contains all costs and benefits related to the value of land, see Equation 2.5. This consists mainly of four aspects: the reduced flooding risk, the benefits gained from ecosystem services, the costs related to the loss of land by placing the dike more inland and the benefits gained from converting the lost land. All four components have to be converted into a present value. The reduced flooding risk can be expressed as the reduced probability of flooding multiplied by the damage upon flooding, which is in fact the value of the land multiplied by the area that is flooded, or since the calculations are performed per meter dike length, the cross-sectional width of the flooded area. This is given in Equation 2.6. The ecosystem services are a function of the width of the mangrove belt supplying these services, as described by Equation 2.7. The costs related to the loss of land are, analogous to the flooding damage, the value of land multiplied by the distance over which the dike has been retreated, as given in Equation 2.8. The benefits related to converting the lost land are for example mangroves or alternative land use.

$$C_{VoL} = PV[D_F(w_F)] + PV[D_L(w_R)] + PV[B_E(w_M)] \quad (2.5)$$

Where

$D_F(w_F)$	damage due to flooding, as function of flooding width w_F	[VND/m]
w_F	average flooding width, cross-sectional width of area flooded per meter dike length	[m]
$D_L(w_R)$	yearly costs of land loss, as function of the retreated distance w_R	[VND/m/y]
w_R	retreated distance, distance between low water line and dike line	[m]
$B_E(w_M)$	present value of the ecosystem services, as function of width mangrove belt	[VND/m]
B_E	yearly benefits derived from ecosystem services, as function of mangrove belt width	[VND/m/y]
w_M	width of the mangrove belt	[m]

$$PV [D_F (w_F)] = \sum_{n=1}^{T_L} \frac{P_F \cdot V_L \cdot w_F}{(1 + r')^n} \quad (2.6)$$

Where

P_F probability of flooding in a year [-]
 V_L value of land [VND/m²]

$$PV [B_E (w_M)] = \sum_{n=1}^{T_L} \frac{V_E \cdot w_M}{(1 + r')^n} \quad (2.7)$$

Where

V_E value of ecosystem services, yearly benefits derived from mangrove ecosystem [VND/m²/y]

$$PV [D_L (w_R)] = \sum_{n=1}^{T_L} \frac{V_L \cdot w_R}{(1 + r')^n} \quad (2.8)$$

The values of these parameters are estimated based on literature research. A summary of the estimated values is given in Table 2.5. In Appendix C a detailed description of each estimation is given.

Construction costs			
Protection measure	Symbol	[10⁶ VND/m]	[USD/m]
Sea dike	I_D	$0.9 \cdot h_D^2 + 5.9 \cdot h_D + 0.375 + 0.125 \cdot (\sqrt{5h_D^2} + \sqrt{17h_D^2})$	-
Mangrove reforestation	I_M	$0.0015 \cdot w_M$	$0.075 \cdot w_M$
Hard solution strategy	I_{HS}	$2 \cdot I_D$	-
Soft solution strategy	I_{SS}	$0.4 \cdot A_n$	$20 \cdot A_n$
Maintenance costs			
Protection measure	Symbol	[10⁶ VND/m/y]	[USD/m/y]
Sea dike	M_D	1	50
Mangrove reforestation	M_M	see section C.1	-
Hard solution strategy	M_{HS}	2	100
Soft solution strategy	M_{SS}	$0.08 \cdot A_n$	$4 \cdot A_n$
Value of land			
Parameter	Symbol	[10³ VND/m²/y]	[USD/m²/y]
Value of land	V_L	20	1
Ecosystem services	V_E	50 (for a dense forest)	2.5
Other			
Parameter	Symbol	Value	
Average flooding width	w_F	slope * surge level	
Real interest rate	r'	0.02 (World Bank Group, 2016; Hillen, 2008)	

Table 2.5: Summary estimated parameters cost-benefit analysis

Note that especially the value of land and real interest rate are very variable over time. It is expected that the Mekong Delta will continue to develop rapidly in the future. Therefore, it would be interesting to compare different growth scenarios, however this lies outside the scope of this project.

The value of land does not only change over time, it is also very dependent on location. If the value of the hinterland is very high, other protection strategies may become favourable.

3

Results

3.1. Analysis model performance

In this section, the model performance will be critically analysed in order to assess the validity of the model. It is no real model validation, however, as there are no measurements or data available to compare the model outcome with. Therefore, the model results will be compared to the expected behaviour based on theory.

First, some very simple scenarios are modelled, for which the solutions are known (based on theory or experience). These simple scenarios will then be gradually elaborated, until the situation is representative for the Mekong Delta coast (subsection 3.1.1). The Mekong Delta situation is investigated in more detail through analysis of the variance density spectrum and the individual terms of the energy balance (subsection 3.1.2). The bottom slopes along the Mekong Delta coast are extremely gentle, outside the range of slopes for which the models have been developed. Therefore, in a small intermezzo the effect of extremely gentle slopes will be investigated, again starting from theory and elaborating different scenarios, each isolating one aspect (subsection 3.1.3). Finally, also the wave transformation inside the mangrove forest will be compared with its expected behaviour (subsection 3.1.4).

3.1.1. From linear wave theory to the Mekong Delta

In section 2.5, the adopted model approach is introduced. SWAN will be used for translating the offshore wave conditions to nearshore wave conditions, and the resulting wave spectrum is subsequently used as input for SWASH, in order to model the wave transformation up to the shoreline. The main reason for using SWAN is to reduce computational effort; modelling the entire computational domain from offshore up to the shoreline with SWASH would consume too much computational power and time, in order to guarantee sufficient accuracy nearshore.

However, in very simple (theoretical) cases, SWAN and SWASH are expected to produce the same results. This will be verified for two scenarios: a first case, in which linear wave theory should be valid, and a second case, which is no longer linear, but still the results of both models are known to be similar. From these two hypothetical cases, the input will be gradually adapted towards a situation representative for the Mekong Delta, in order to set up a validated model for the scenarios defined in section 2.3.

Linear wave theory: shoaling

Linear wave theory is the most basic theory to describe surface gravity waves (Holthuijsen, 2007). It is based on two linearised equations, a mass balance and a momentum balance equation. Combined with linearised boundary conditions, a solution to these equations is the propagating harmonic small amplitude wave. However, this theory is only applicable if the amplitudes of the waves are small, with respect to the wave length (in deep water) and with respect to the water depth (in shallow water). Based on this theory, equations have been derived describing various wave properties.¹ In the following paragraph, the relevant equations and wave properties are introduced.

Equation 3.1 defines the surface elevation of a harmonic wave. In Equation 3.2 the angular frequency

¹For the derivation of these equations, the reader is referred to Holthuijsen (2007), or any other book on wave theory.

is defined, in Equation 3.3 the wave number and in Equation 3.4 the wave celerity. Equation 3.5 gives a relation between the angular frequency, the wave number and the water depth. In Equation 3.6, a very useful ratio is introduced, the celerity of the wave group over the celerity of the individual wave. Equation 3.7 defines the wave energy flux and Equation 3.8 defines the wave energy itself.

$$\eta = a \sin(\omega t - kx) \quad (3.1)$$

$$\omega = \frac{2\pi}{T} \quad (3.2)$$

$$k = \frac{2\pi}{L} \quad (3.3)$$

$$c = \frac{L}{T} = \frac{\omega}{k} = \sqrt{\frac{g}{k} \tanh(kh)} \quad (3.4)$$

$$\omega^2 = gk \tanh(kh) \quad (3.5)$$

$$n = \frac{c_g}{c} = 0.5 \left(1 + \frac{2kh}{\sinh(2kh)} \right) \quad (3.6)$$

$$U = Ec_g = Enc \quad (3.7)$$

$$E = \frac{1}{8} \rho g H^2 = \frac{1}{2} \rho g a^2 \quad (3.8)$$

Where

a	wave amplitude	[m]
c	wave celerity	[m/s]
c_g	wave group celerity	[m/s]
E	wave energy per unit surface area	[J/m ²]
g	gravitational acceleration	[m/s ²]
k	wave number	[m ⁻¹]
H	wave height ($H = 2a$)	[m]
L	wave length	[m]
n	ratio of wave group celerity over individual wave celerity	[-]
T	wave period	[s]
t	time	[s]
U	wave energy flux per unit wave crest width	[J/ms]
x	coordinate in direction of wave propagation	[m]
η	surface elevation	[m]
ρ	water density	[kg/m ³]
ω	angular frequency	[s ⁻¹]

Equation 3.5 is also known as the dispersion relation. This relation implies that when a harmonic wave travels over a gently sloping bottom, since its frequency remains constant, its wave number will increase and its wave celerity will decrease. In other words, when a wave propagates into gradually shallower water, it will become shorter and propagate more slowly.

For the effect on the wave height, the wave energy balance is examined. In the absence of any generation or dissipation of wave energy (wind, bottom friction, wave breaking), the wave energy is conserved, therefore the energy flux, through planes between two vertical sides in wave direction, is constant. Combining the equations for wave energy and wave energy flux, a relation between wave height and water depth can be established.

$$\frac{a_2}{a_1} = \sqrt{\frac{c_{g,1}}{c_{g,2}}} = \sqrt{\frac{n_1 c_1}{n_2 c_2}} \quad (3.9)$$

Where the subscripts 1 and 2 refer to any two locations along a wave ray.

The wave height will increase when the wave travels over a gently sloping bottom. This process is called shoaling. Theoretically, the wave height could increase to infinity, but in reality the wave will break when it becomes too steep. This equation is only valid where the requirements for linear wave

theory are fulfilled (small amplitude assumption).

The first step in the process of model validation is to examine whether SWAN and SWASH can reproduce this linear shoaling. Therefore, linear wave conditions must be applied to a gently sloping bottom. A regular wave with a wave height of 2 cm and a wave length of 400 m will be applied at the offshore boundary of a computational domain with a slope of 1/400. The water depth at the offshore boundary is 30 m, the water depth nearshore is 5 m, implying the total length of the computational domain to be 10 km.

Figure 3.1 gives the wave height evolution over this domain, as modelled by SWASH and SWAN (respectively represented by the blue and orange line), compared to the shoaling equation (Equation 3.9), represented by the yellow line (which almost completely coincides with the orange line representing SWAN). The horizontal axis represents the position in the cross-section, the origin is located at the offshore boundary and the axis is positive towards the shoreline. The vertical axis gives the wave height. This coordinate system will be used for all other plots in this section. Note that the length of the domain will vary as the bottom slope varies.

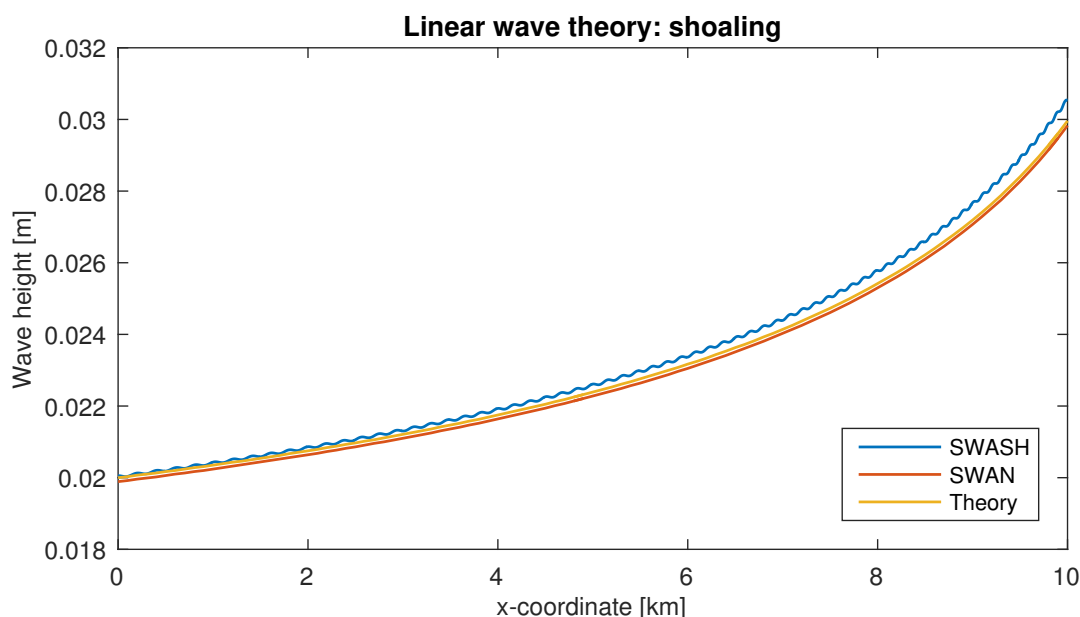


Figure 3.1: Linear shoaling, as modelled by SWASH and SWAN, compared with linear wave theory.

This figure shows that both SWAN and SWASH can reproduce shoaling according to the linear wave theory. The small difference between SWASH and the two other lines can be explained by the fact that SWASH is a nonlinear model, and can therefore not exactly reproduce the linear theory, while SWAN uses this linear theory in the model. The difference between SWASH and linear theory increases as the amplitude increases, and since linear theory is only valid for very small amplitudes, this agrees with the expectations. The models perform well enough to proceed to the next step, which is to compare SWAN and SWASH when the situation is no longer linear.

Nonlinear behaviour: shoaling and breaking

Linear wave theory is valid for small amplitudes, for example the wave modelled in the previous section. However, if the wave amplitude becomes too large with respect to water depth (or wave length), linear wave theory is no longer valid, and the shoaling equation (Equation 3.9) can no longer be applied. At a certain point, the waves will start breaking.

In such a case, there is no exact theoretical solution, instead only SWAN and SWASH can be compared. Using the same set-up as for the linear case, but now with a wave height of 4 m, the wave transformation is computed and displayed in Figure 3.2.

Analysing this wave height evolution from deep water ($x = 0$, the left hand boundary of this plot) to shallow water ($x = 10000$, the right hand boundary), one can observe that initially, the wave height increases due to shoaling. At a certain point (around $x = 7500$), the wave height stabilises and then decreases. This is the point where the waves start breaking, because the waves have become too

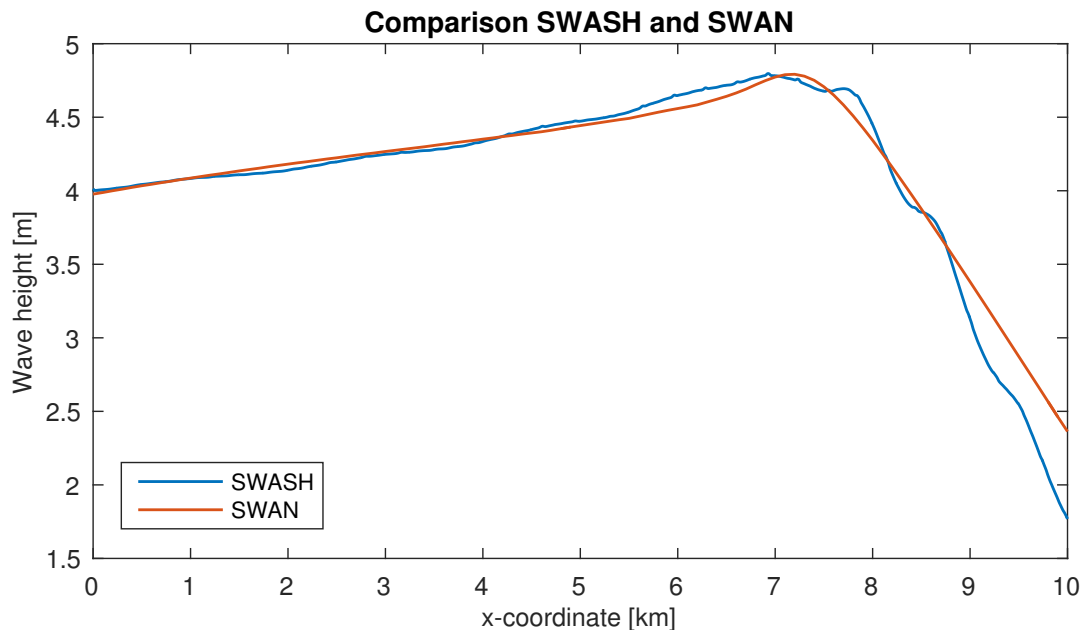


Figure 3.2: Shoaling and wave breaking, when the linear wave theory is no longer valid, as modelled by SWASH and SWAN.

steep. After the breaking point, both curves show a steep decrease in wave height. Although there are some slight divergences, the general evolution modelled by SWASH and SWAN is the same. These were two theoretical examples, where SWASH and SWAN are known to give similar results. In the next sections, the input of these theoretical examples will be adapted step by step, in order to represent the situation along the Mekong Delta coast.

From regular waves to a JONSWAP spectrum

An important difference between the theoretical case in the previous section and reality, is the imposed wavemaker boundary. Previously, a regular wave was imposed, with a single wave height and period. In reality, a wave field consists of many waves with different wave heights and periods. This means that a realistic boundary condition should not impose a single wave condition, but a whole range of wave conditions, through a wave spectrum. Measurements and experiments have shown that a JONSWAP spectrum is representative for arbitrary wind conditions in oceanic waters (Holthuijsen, 2007; Bosboom and Stive, 2015).²

In Figure 3.3, the wave transformation of this JONSWAP spectrum over the computational domain is given, as modelled by SWASH and SWAN. The general shape of these curves is the same as for a regular wave. However, when comparing Figure 3.2 and Figure 3.3, there are also some differences. First, imposing a JONSWAP spectrum in SWASH, the breaking point moves closer to shore. Second, the curve is also smoother for a JONSWAP spectrum than for a regular wave imposed at the boundary. Imposing a JONSWAP spectrum in SWAN causes some differences as well compared to the regular wave case. Offshore, the waves shoal slightly faster, and around $x = 4000$ m, the slope of the curve suddenly changes, with increased shoaling as result. Although the wave height at breaking point is larger, the breaking point itself is significantly further offshore than in the previous case, or than SWASH in the current case.

Summarised, the waves break later in SWASH than in SWAN, but the maximum wave height is higher in SWAN than in SWASH. SWASH is expected to be closer to reality, since it performs better around strongly non-hydrostatic behaviour, such as wave breaking. It can be concluded that both models perform well enough to continue to the next step: modifying the bottom slope to a more gently sloping profile, representative for the Mekong Delta.

²The JONSWAP spectrum was developed for the North Sea (JOint North Sea WAve Project), and experience has shown it could be applied to many more situations. However, there has been no close investigation of the seas off the Mekong Delta coast, nor are there sufficient measurements to verify whether a JONSWAP spectrum can represent the conditions well enough. In the absence of this information, the assumption is made that a JONSWAP spectrum is representative for the conditions encountered at the Mekong Delta coast.

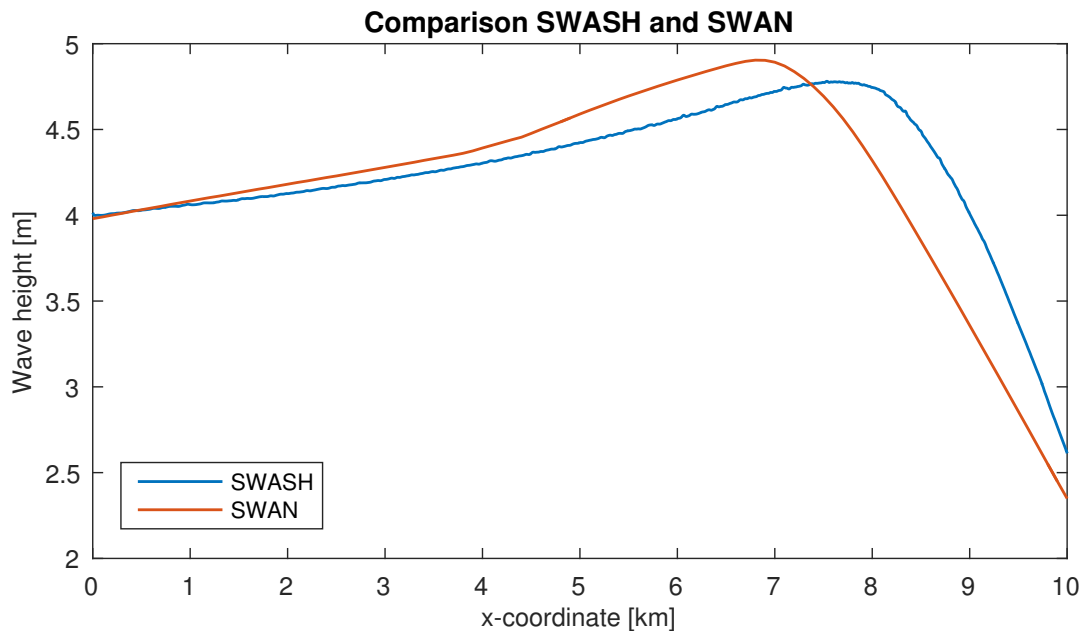


Figure 3.3: Wave transformation modelled by SWASH and SWAN, for a JONSWAP spectrum imposed at the offshore boundary.

Gentler slopes

So far, a relatively gentle slope of $1/400$ has been used, as the linear wave theory requires a gently sloping bed for the shoaling equation to be valid. However, the Mekong Delta coasts are characterised by even milder slopes, from $1/800$ up to even $1/1500$. The next step, therefore, is to introduce these mild slopes into the model set-up.

Figure 3.4 shows the results for a slope of $1/800$, while all other input parameters have remained unchanged compared to the previous set-up (see Figure 3.3). Of course, the computational domain is now twice as long.

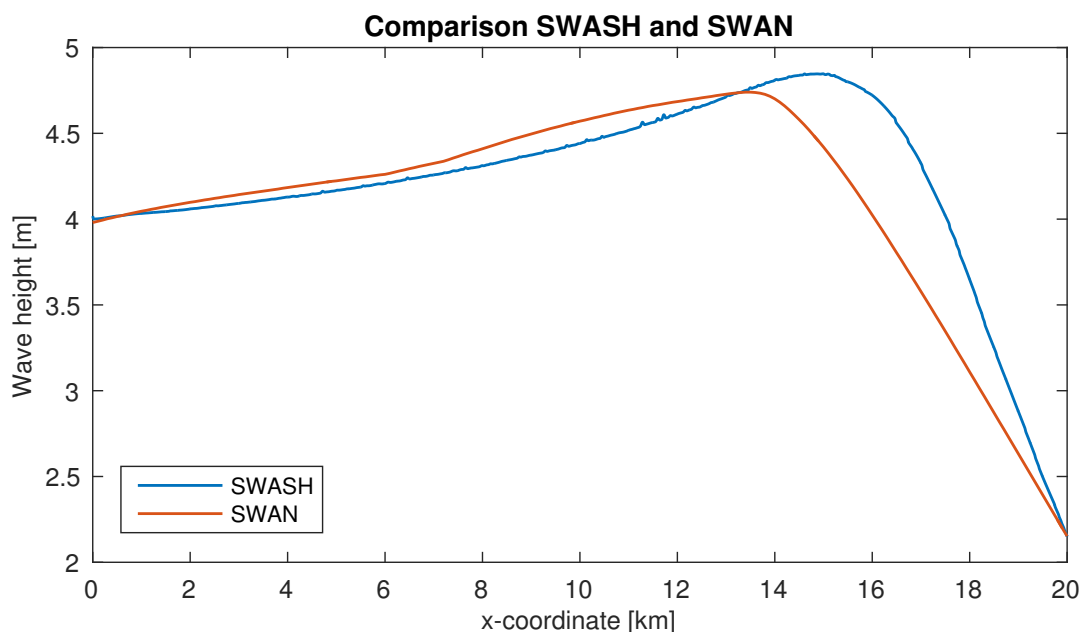


Figure 3.4: Wave transformation modelled by SWASH and SWAN, for a JONSWAP spectrum imposed at the offshore boundary, on a bottom slope of $1/800$.

What immediately strikes the eye is that, while the breaking points are at the same relative position as for the steeper slope, the breaking heights have changed. In SWASH the waves shoal more than

on steeper slopes, while in SWAN the shoaling decreases and the curve becomes almost horizontal towards the breaking point. It is expected that SWASH will be closer to reality, since on these extremely gentle slopes, the shoaling process can continue much longer before the waves reach the limit steepness.

In Figure 3.5, the same scenario is modelled, now on a bottom slope of 1/1500. It should be noted that neither SWAN nor SWASH has been developed for such extremely gentle slopes. Therefore, the exact physics on these mild slopes should be well understood, and further investigation is necessary. This will be done in subsection 3.1.3.

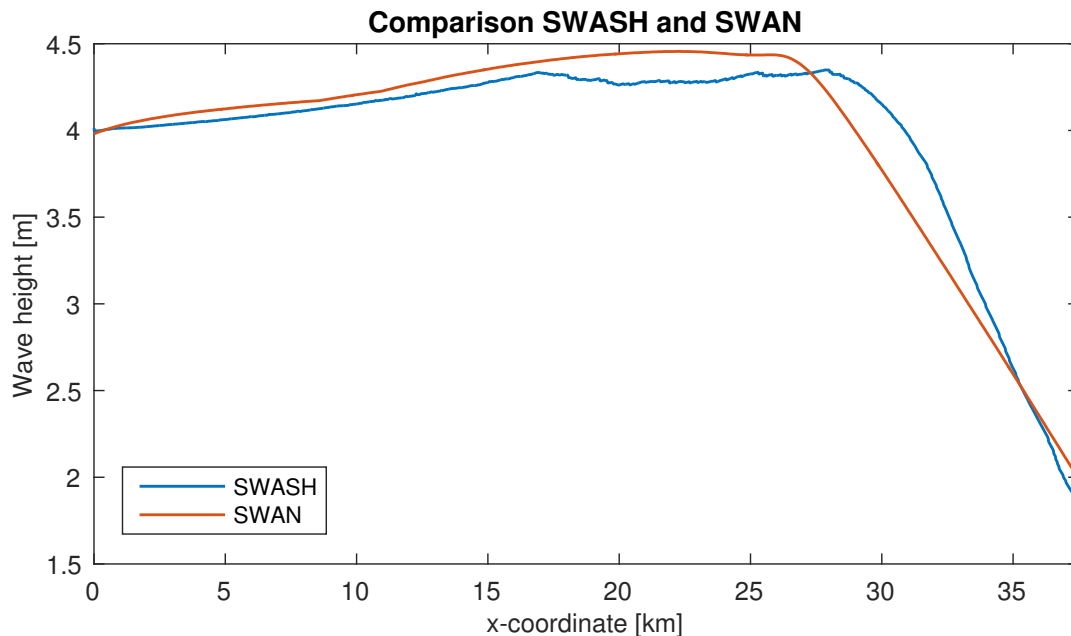


Figure 3.5: Wave transformation modelled by SWASH and SWAN, for a JONSWAP spectrum imposed at the offshore boundary, on a bottom slope of 1/1500.

The blue SWASH curve shows interesting behaviour: first, the waves shoal, until they break at a certain point. However, instead of continuously decreasing wave heights beyond the breaking point, the waves start shoaling again, until they break again. This process repeats itself several times, which results in a more or less constant wave height, until the eventual breaking point is reached and the wave height decreases until the shoreline.

SWAN also struggles with the extremely mild slope, the wave height is more or less constant and even decreases slightly before the breaking point is reached, after which the wave decreases at a constant rate.

In SWASH, the breaking point is more or less at the same depth as the previous simulations, however, in SWAN the breaking point is located closer to shore, but still further offshore than in SWASH.

However, these computations have been made for the default set-up of depth-induced breaking. For these extremely gentle slopes, it is unknown whether this default set-up is applicable. It might be possible that parameters have to be modified, to represent the different behaviour. The way SWAN and SWASH model depth-induced breaking, and the impact of each parameter, will be elaborated in subsection 3.1.3.

Introduction of wind

Due to the gentle bottom slope, the foreshore is very wide. Over such a long distance, wave growth due to wind can play an important role. Therefore, wind also has to be included in the model.

SWAN has multiple formulations, both linear and exponential, to model wind growth. SWASH, however, only includes a wind effect for large-scale wind driven circulation, tides and storm surges. This wind effect should not be used for short wave propagation. This deficiency of SWASH is another reason why SWAN should be used for the largest part of the computational domain, from offshore to nearshore, and SWASH should be used only nearshore. Apart from computational efficiency, this approach also

allows to include wind growth.

To illustrate the difference between SWAN and SWASH, in both models a wind of 25 m/s is added to the input (this wind force corresponds to a return period of 50 years). The result is given in Figure 3.6. In comparison with Figure 3.5, the waves grow faster in SWAN, which not only leads to higher waves, but also an earlier breaking point. SWASH, however, does not show any effect of the added wind, as expected.

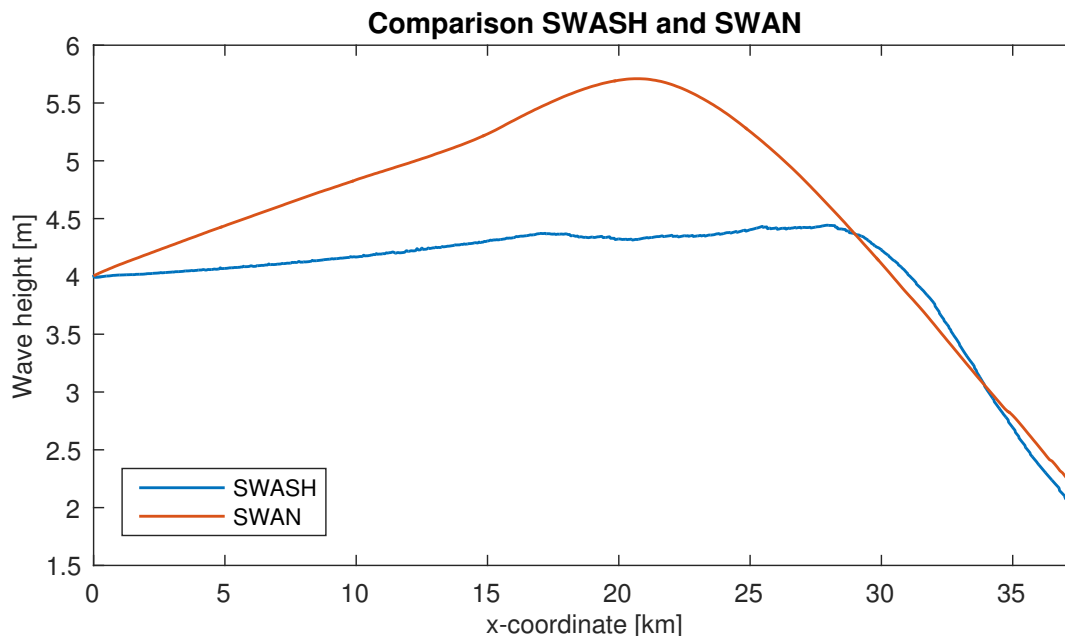


Figure 3.6: Wave transformation modelled by SWASH and SWAN, on a slope of 1/1500, with wind effect activated.

SWAN spectrum as input for SWASH

So far, SWAN and SWASH have been used to model exactly the same computational domain. Eventually, however, SWAN will be used to model the largest part of the computational domain, from offshore to nearshore, while SWASH will only model the relatively small part nearshore up to the shoreline. The exact location of this boundary still has to be determined. It should be as close as possible to the shoreline, to reduce computational effort in SWASH and to include the effect of wave growth due to wind, but not too close to shore, as SWASH is more accurate than SWAN nearshore. Therefore, the boundary should be just before the waves start breaking.

In Figure 3.7, the SWAN-SWASH boundary is placed at a water depth of 30 m. This is quite far offshore, but it places the breaking point inside the SWASH domain.³ The curves of SWAN and SWASH show large differences. This is mainly caused by the fact that the breaking point in SWASH lies close to shore, so where the wave height already reduces after the breaking point in SWAN, the waves are still shoaling in SWASH, as well as the fact that SWAN models this wave height reduction as a linear development, while SWASH shows a clearly nonlinear behaviour.

However, if one looks closely at the offshore boundary, it can be seen that the wave height in SWASH suddenly drops, resulting in a significantly lower wave height than SWAN, even though it was the exact same spectrum that was forced at the boundary.

This erroneous behaviour at the boundary is caused by the fact that SWASH requires a linear wave condition at the boundary. There is no problem with nonlinear waves in the rest of the computational domain, but at the boundary the imposed wave condition must be approximately linear. However, the imposed wave conditions are design storm conditions corresponding to high return periods, which are extremely nonlinear. Therefore, it is not possible to reduce the wave heights in order to impose relatively linear conditions.

An alternative solution, is to enhance the waves at the boundary slightly, just enough to compensate for the drop in wave height (M. Zijlema, personal communication, July 2016). In Figure 3.8, the wave

³Previous examples have shown that the breaking point in SWASH lies closer to shore than in SWAN.

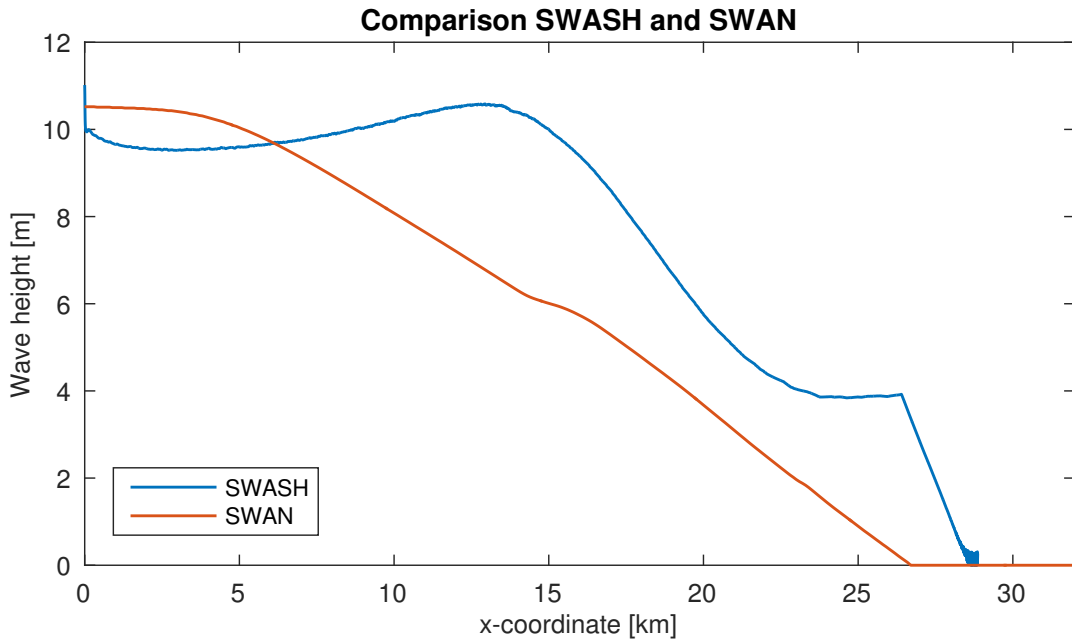


Figure 3.7: Comparison of SWAN and SWASH output, where spectrum generated by SWAN was used as SWASH input.

spectrum has been increased by a factor of 1.3 (each frequency bin is multiplied with this factor, thus preserving the spectral shape). As a result, the wave heights of SWAN and SWASH are approximately equal at a few wave lengths inside the domain.

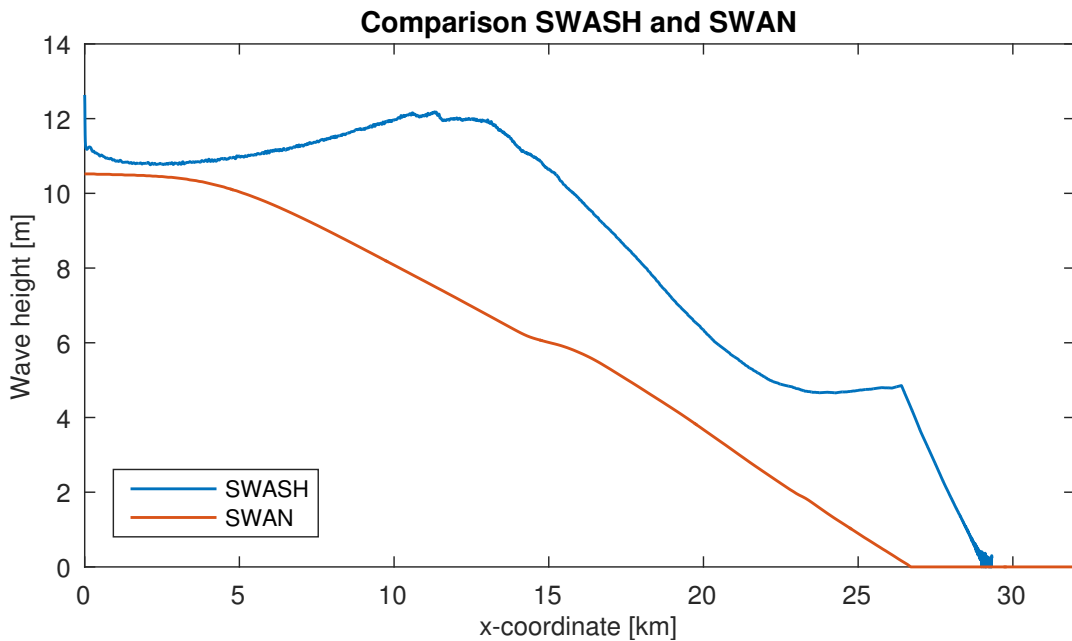


Figure 3.8: Comparison of SWAN and SWASH output, where spectrum generated by SWAN was enhanced before it was used as SWASH input.

With this trick, approximately the same boundary conditions are imposed, without any distortion caused by the boundary. The large differences between SWASH and SWAN are now clearly visible, with the continued shoaling and later breaking in SWASH, as opposed to the linear reduction in wave height in SWAN. It is also interesting to note that the wave heights close to the shoreline are unaffected by the boundary condition trick, and since this is the region of interest, this increases the robustness of the model.

Conclusion

From the previous sections, the following conclusions can be drawn. First, SWASH and SWAN can both reproduce simple cases for which the solution is known, and second, imposing irregular waves at the boundary has no negative impact on the models' performances.

The third conclusion, however, is less straightforward. The bottom slopes of the Mekong Delta are so gentle, that they may lie outside the scope of both SWAN and SWASH. The models have not been developed for this kind of slopes, and have never been validated. However, a distinction must be made between SWAN and SWASH. SWAN uses parameterisation, for example Battjes-Janssen for depth-induced breaking, which is valid for a certain range (Battjes and Janssen, 1978). Outside this range, the parameterisation may lead to wrong results and needs to be re-validated. SWASH, however, does not use parameterisations, but solves the two balance equations. Therefore, there is no reason why SWASH should be wrong. Nevertheless, measurements are necessary for validation. Using the model in this range therefore requires further investigation, which will be done in a later section (see subsection 3.1.3).

The fourth conclusion is that, as SWASH cannot model wave growth due to wind, SWAN should be used for the largest part of the domain, in order to correctly include wave growth due to wind in the model. However, this boundary should also not be too close to shore, as it can be concluded that SWASH models more accurately around the breaking point and beyond.

Finally, as SWASH requires linear wave conditions at the boundary, the imposed wave spectrum has to be enhanced in order to compensate for the drop in wave height. However, even without compensation this boundary effect only plays a role locally.

3.1.2. Variance density spectrum analysis

Another way to assess the model results is by looking at the shape of the variance density spectrum and the way it transforms when approaching the shoreline. For this purpose, the computational domain is extended to include the full domain off the Mekong Delta coast, up to an offshore depth of 65 m. At the offshore boundary, a JONSWAP spectrum is imposed. At three other locations along the computational domain, the wave spectrum is measured. The variance density spectra at these four locations are visualised in Figure 3.9: at the offshore boundary (at a depth of 65 m, blue line), at a water depth of 30 m (orange line), at a water depth of 20 m (yellow line) and at a water depth of 10 m (purple line). In this graph, the horizontal axis gives the frequency range and the vertical axis represents the variance density.

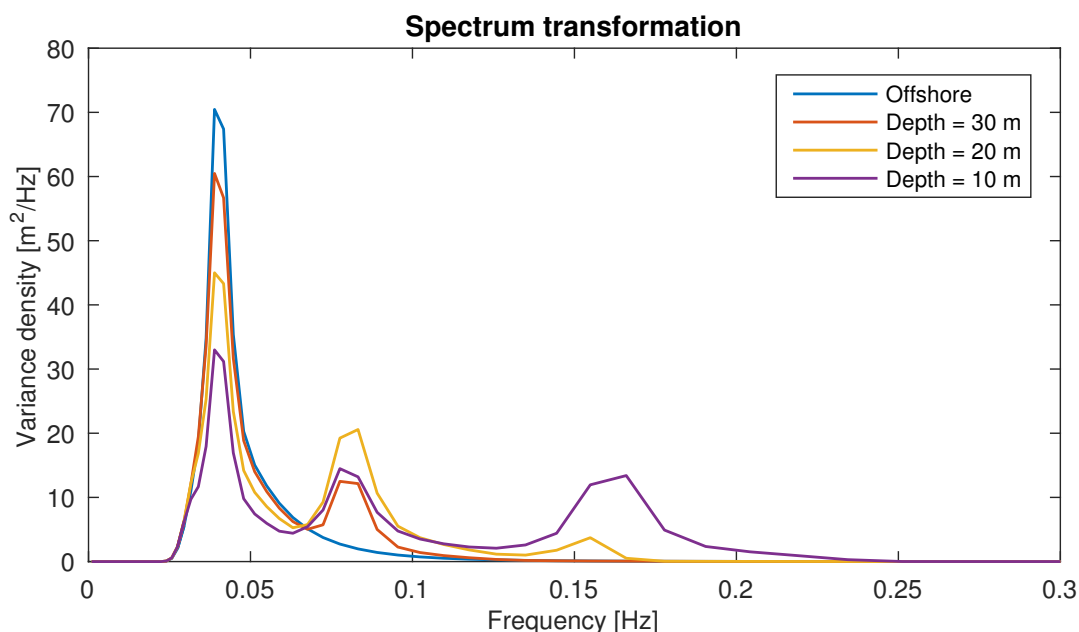


Figure 3.9: Evolution of the wave spectrum, from offshore (JONSWAP spectrum with $H_s = 4$ m and $T_p = 25$ s, at a depth of 65 m), to nearshore (at respective depths of 30 m, 20 m and 10 m).

This figure shows that the shape of the spectrum changes when the waves travel to the shore. This change in shape can be caused by three different phenomena: energy input (due to wind), energy dissipation (due to bottom friction and wave breaking) and energy transfer (due to nonlinear wave-wave interactions). Therefore, it is very useful to combine Figure 3.9 with Figure 3.10, in which the individual source terms of the energy balance are visualised. The x-axis shows the position in the cross-section, with the origin at the offshore boundary and the axis positive towards the shoreline. In other words, the horizontal axis gives the distance from the offshore boundary. As such, it shows for each location the dominant processes, and can therefore be used to explain changes in spectral shape in Figure 3.9. Note that the location of each line in Figure 3.9 is indicated on the x-axis of Figure 3.10 by an asterisk in the same colour as the corresponding line.

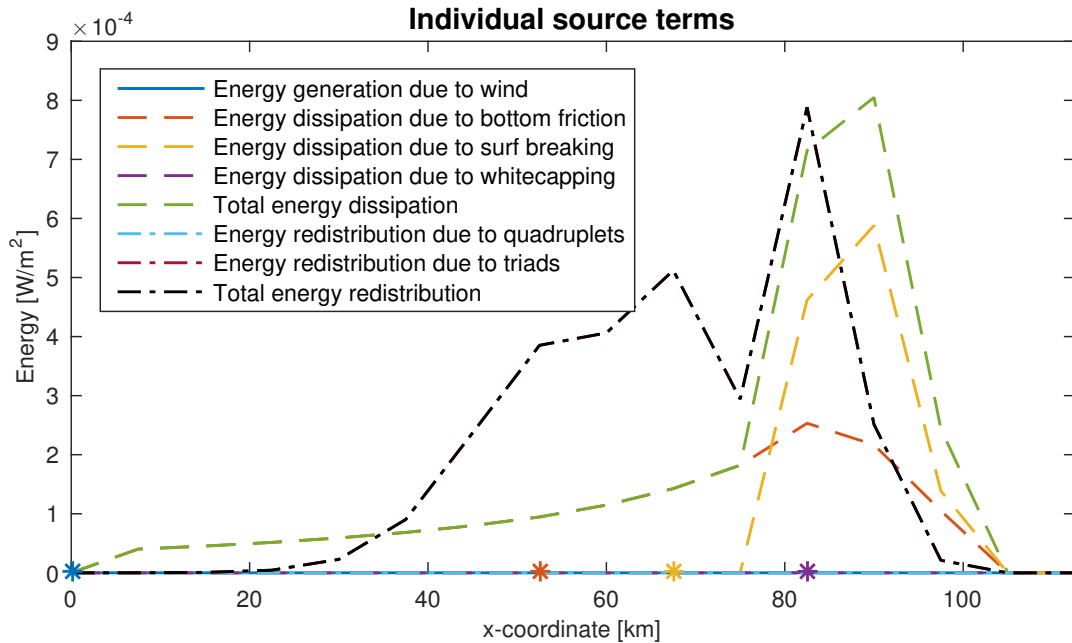


Figure 3.10: Evolution of the individual source terms of the energy balance (boundary conditions a JONSWAP spectrum with $H_s = 4$ m and $T_p = 25$ s, at a depth of 65 m).

Combined, these two figures give insight in the wave transformation and the importance of different processes in this transformation. First, Figure 3.9 is analysed. The blue line clearly forms the JONSWAP-shaped spectrum: asymmetric around the peak, steep on the low frequency side, extended tail on the high frequency side. From a depth of 65 m at the offshore boundary (the blue line) to a depth of 30 m (the orange line), some clear differences occur. Most significant is the appearance of a secondary peak. Looking at Figure 3.10, it can be seen that this peak is created by energy transfer due to nonlinear wave-wave interactions (the black dashed-dotted line). This mechanism transfers energy among the waves by resonance (Holthuijsen, 2007). In this case, the secondary peak is located at exactly twice the peak frequency, which indicates it is the result of triad wave-wave interaction with itself (which is confirmed by Figure 3.10, where the black dashed-dotted line coincides with the maroon dashed-dotted line, respectively representing the total energy transfer and the transfer due to triads, as the quadruplets are zero for this case). Triad wave-wave interaction can only occur in very shallow water. Although the water depth might seem large, it can be considered small relative to the large wave height. This is confirmed by Figure 3.10, where the energy transfer is zero offshore, where the water depth is largest, and increases for decreasing water depth. Triad wave-wave interaction requires two resonance conditions to be fulfilled:

$$f_1 + f_2 = f_3 \quad (3.10)$$

$$k_1 + k_2 = k_3 \quad (3.11)$$

In this case, the wave component interacts with itself, so $f_1 = f_2$, and therefore a new peak is generated at $f_3 = 2f_1$. Note that some energy of the primary peak is transferred to create the secondary peak, and while this peak is superposed on the existing energy at that frequency, it represents bound waves,

that travel at the same speed as the primary peak. However, in SWAN each frequency bin is computed separately, and therefore all frequencies move independently (dispersion). This means that there are no bound waves, the transferred energy will move at the same speed as the other wave energy in this frequency bin.

In a similar fashion, a new peak can be created at $4f_1$, which is clearly visible at a depth of 10 m (purple line).

A second difference that can be noticed in Figure 3.9 between the different water depths, is the height of the primary peak. At a water depth of 30 m, the height of the peak is slightly lower than offshore, and while most of this energy is actually transferred to the secondary peak through triad wave-wave interaction, some energy is also dissipated. The green dashed line in Figure 3.10 visualises the total energy dissipation. Offshore, this energy dissipation is solely caused by bottom friction, and increases when the water depth decreases.

At a depth of 10 m (the purple line in Figure 3.9), the primary peak is significantly lower, while not all energy has been transferred to secondary peaks. Figure 3.10 shows that most energy is dissipated through surf breaking, which implies that this location is inside the surf zone. Further, there is also some energy dissipation through bottom friction.

Eventually, all waves will break in the surf zone and the peaks will disappear quickly as the entire spectrum disappears.

The previous case was highly simplified and served both to introduce the method of analysis, as well as to validate the model. In this simple case, a JONSWAP spectrum with a significant wave height of 4 m and a peak period of 25 seconds is applied to a constant bottom slope of 1/1500. The model shows the behaviour that can be expected from theory (Holthuijsen, 2007). However, in the Mekong Delta, the situation is more complex. First, the waves are mostly wind waves, much steeper and higher than the swell waves used in the first case (wave heights in the order of 6 m, wave periods in the order of 10 s). Second, there is a strong wind blowing over the entire computational domain. Third, quadruplet wave-wave interactions and whitecapping were not activated in the first example (these processes are only activated when wind is activated). In the next paragraphs, these elements will be introduced step by step, and the performance of the model will be analysed according to the method introduced here.

Mekong Delta conditions: wind and steep waves

In the previous example, not all terms of the energy balance have been included. Energy dissipation through whitecapping and energy transfer through quadruplet wave-wave interactions can only be included in SWAN if also wind is activated. Therefore, the first step is to complete the energy balance by applying a constant wind to the domain (in the order of 25 m/s, corresponding to a return period of 50 years). The variance density spectra corresponding to this model run are given in Figure 3.11 and the behaviour of the individual source terms is given in Figure 3.12.

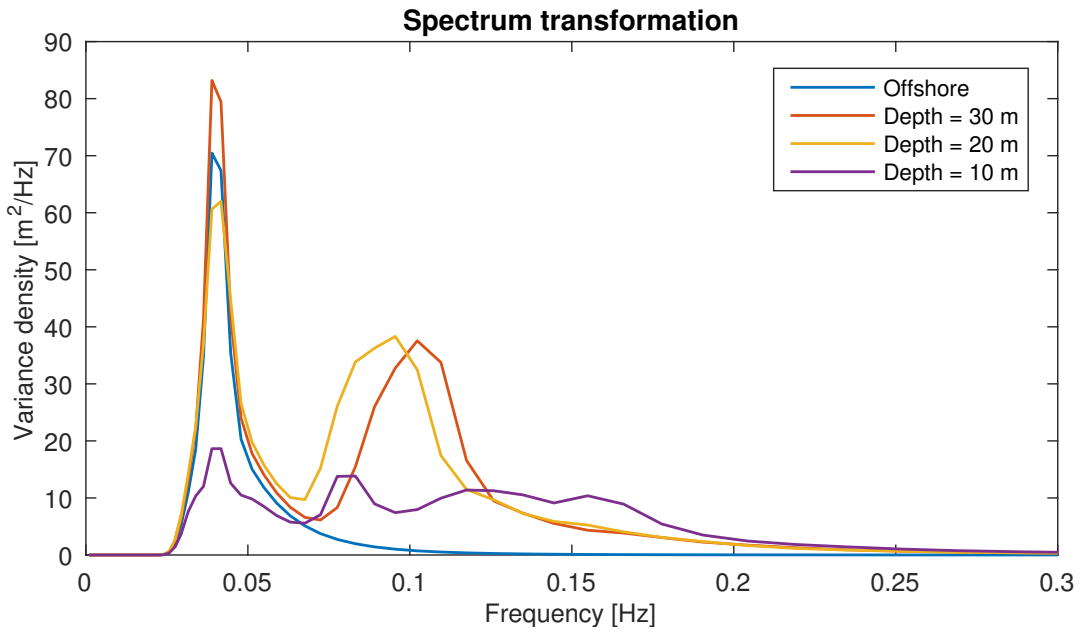


Figure 3.11: Evolution of the wave spectrum, from offshore (JONSWAP spectrum with $H_s = 4$ m and $T_p = 25$ s, at a depth of 65 m), to nearshore (at respective depths of 30 m, 20 m and 10 m), with a wind of 25 m/s.

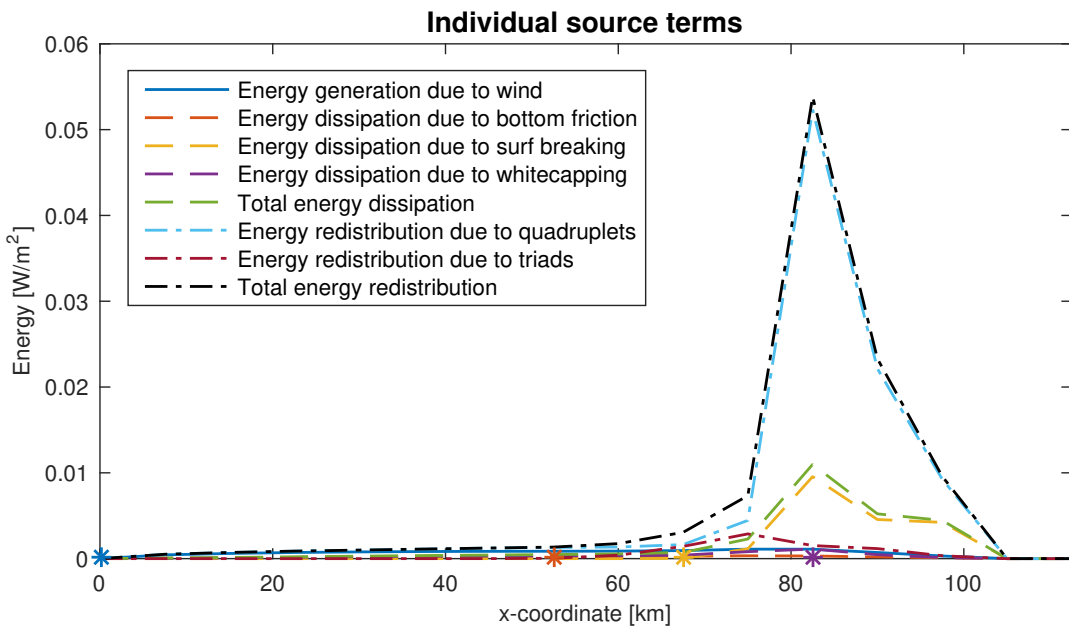


Figure 3.12: Evolution of the individual source terms of the energy balance (boundary conditions a JONSWAP spectrum with $H_s = 4$ m and $T_p = 25$ s, at a depth of 65 m and a constant wind of 25 m/s over the entire domain).

The first thing that strikes the eye in Figure 3.11 is the occurrence of a secondary peak around 0.1 Hz at depths of 30 m and 20 m. There is no clear relation between the location of this secondary peak and the location of the primary peak, at 0.04 Hz. Strangely enough, when looking at Figure 3.12, there is not one clear cause of this deviant behaviour (also when zooming in around $x = 52.5$ km and $x = 67.5$ km). However, due to the extreme peak in quadruplet wave-wave interactions inside the surf zone, all other source terms are barely visible. Not only is this amount of energy transfer unrealistic, also the location of this energy transfer through quadruplets is questionable. According to Holthuijsen (2007), quadruplets are active in deeper water, while in very shallow water triads dominate the energy transfer.

It is clear that the model is not performing as it should, and further investigation is required. This becomes even more obvious when the applied wave spectrum is modified to steeper, higher waves, representing the Mekong Delta wave conditions: the results are visualised in Figure 3.13 and Figure 3.14.

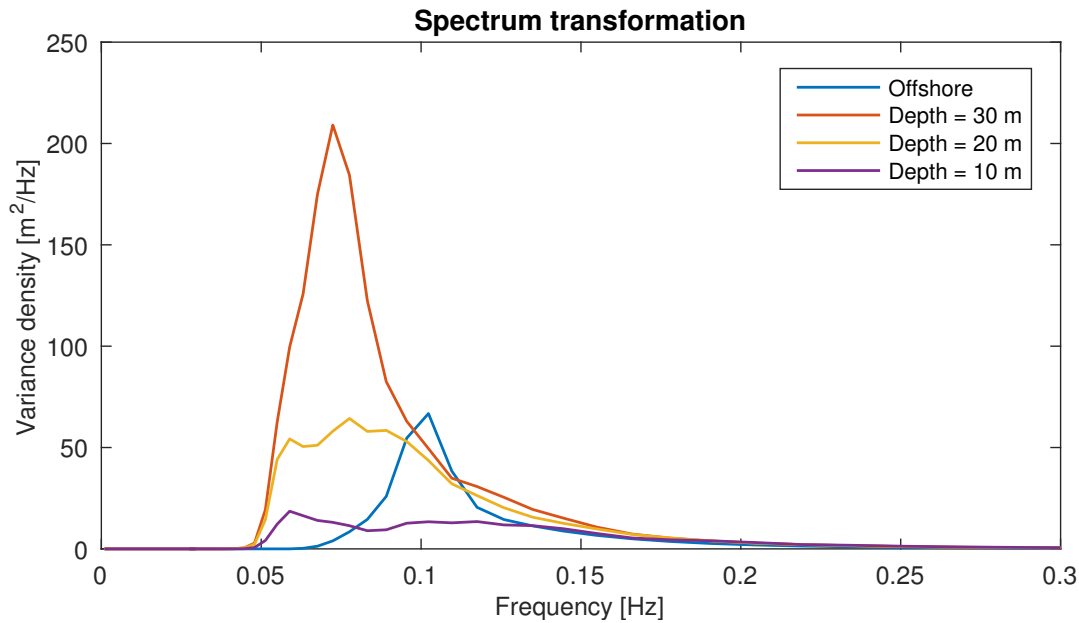


Figure 3.13: Evolution of the wave spectrum, from offshore (JONSWAP spectrum with $H_s = 6$ m and $T_p = 10$ s, at a depth of 65 m), to nearshore (at respective depths of 30 m, 20 m and 10 m), with a wind of 25 m/s.

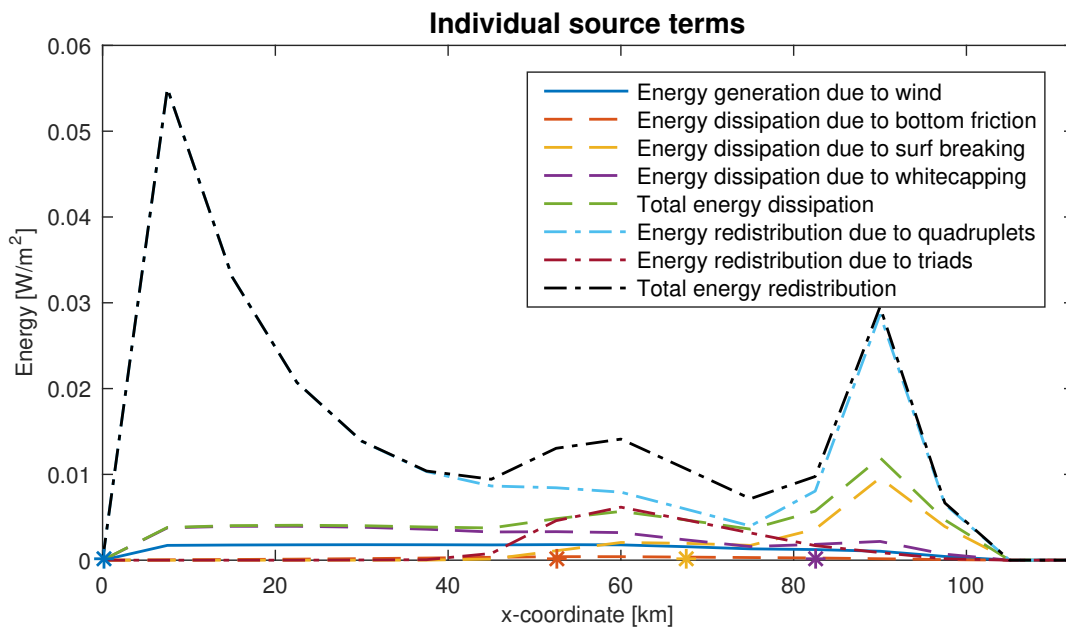


Figure 3.14: Evolution of the individual source terms of the energy balance (boundary conditions a JONSWAP spectrum with $H_s = 6$ m and $T_p = 10$ s, at a depth of 65 m and a constant wind of 25 m/s over the entire domain).

In Figure 3.13 an explosive increase in variance density can be observed between the offshore boundary and a depth of 30 m. Not only does the peak shift to lower frequencies, it also becomes four times as high. In Figure 3.14 this is accompanied by an extreme peak in quadruplet wave-wave interactions. Although these interactions are expected to occur in this region, and quadruplets tend to shift energy to lower frequencies, they should not add energy to the spectrum. There is some energy input through

wind, but this cannot be responsible for this enormous increase of energy from offshore to the 30 m line.

It is paradoxical that the numerical approximation used in SWAN to model quadruplet wave-wave interactions (the Discrete Interaction Approximation, DIA, of Hasselmann et al. (1985)), which is supposed to conserve wave variance, momentum and action when the frequencies are geometrically distributed (as is the case in SWAN according to The SWAN team (2015)), in this case apparently adds energy to the spectrum (M. Zijlema, personal communication, July 2016).

In the preceding paragraphs, first a simplified case was analysed and validated, after which the set-up has been modified to be representative for the Mekong Delta (steeper waves and wind). However, for this set-up, SWAN shows some deviant behaviour, generating energy at unexpected frequencies, over-active quadruplet wave-wave interactions etc. Therefore, the model set-up should be scrutinised, to understand what is causing these deviations, and why they occur (in other words, is this realistic or a numerical artefact). This will be done in the following paragraphs.

Analysing the individual impact of the each source term

At the beginning of this section on variance density spectrum analysis, with Figure 3.9 and Figure 3.10, the model was validated for a simple case. In this simple case, energy dissipation due to bottom friction and surf breaking, as well as energy redistribution due to triad wave-wave interactions was included, for a swell-wave spectrum. However, when adding energy generation due to wind, energy transfer due to quadruplet wave-wave interactions and energy dissipation due to whitecapping, for a wind-wave spectrum, the model showed some serious deviations. Therefore, these 4 aspects will be analysed individually, in order to trace down the cause of the deviations.

Steeper waves To start with, the set-up from Figure 3.9 and Figure 3.10 is taken, and only the JONSWAP spectrum at the boundary is changed: instead of $H_s = 4$ m and $T_p = 25$ s, $H_s = 6$ m and $T_p = 10$ s is imposed. The resulting wave spectra at the four fixed locations are given in Figure 3.15, the individual source terms are visualised in Figure 3.16.⁴

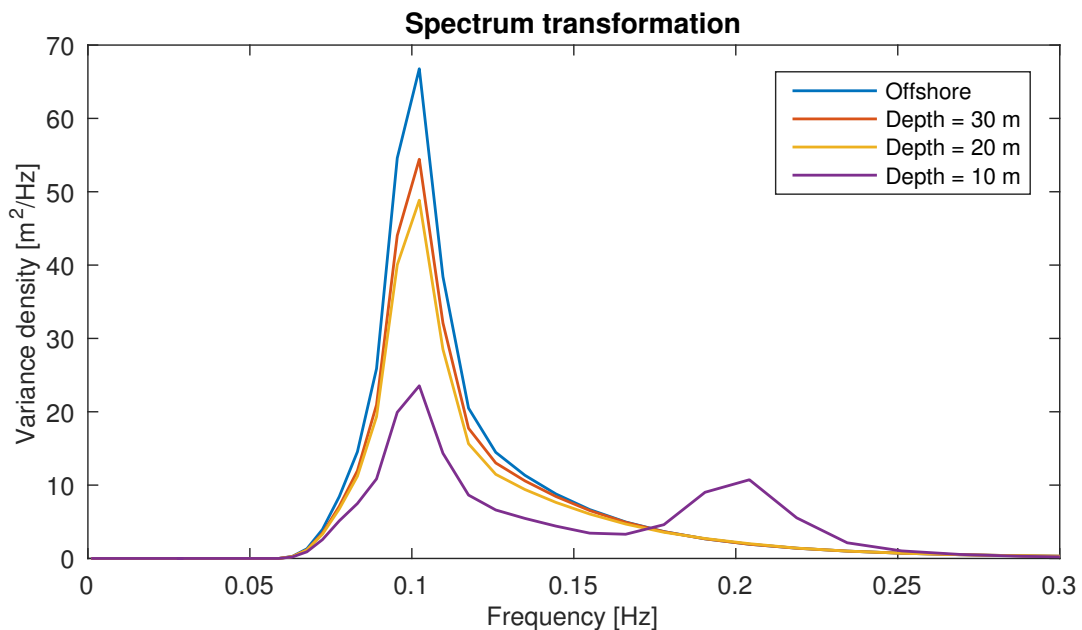


Figure 3.15: Evolution of the wave spectrum, from offshore (JONSWAP spectrum with $H_s = 6$ m and $T_p = 10$ s, at a depth of 65 m), to nearshore (at respective depths of 30 m, 20 m and 10 m).

Comparing Figure 3.15 with Figure 3.9 (the difference between both being the wave boundary: swell waves or higher, steeper waves), there are several differences. First of all, the location of the primary peak of the variance density spectrum lies at a different frequency, which is of course the peak frequency imposed at the boundary, respectively 0.1 Hz and 0.4 Hz.

⁴Wind input, whitecapping and quadruplets are non-active.

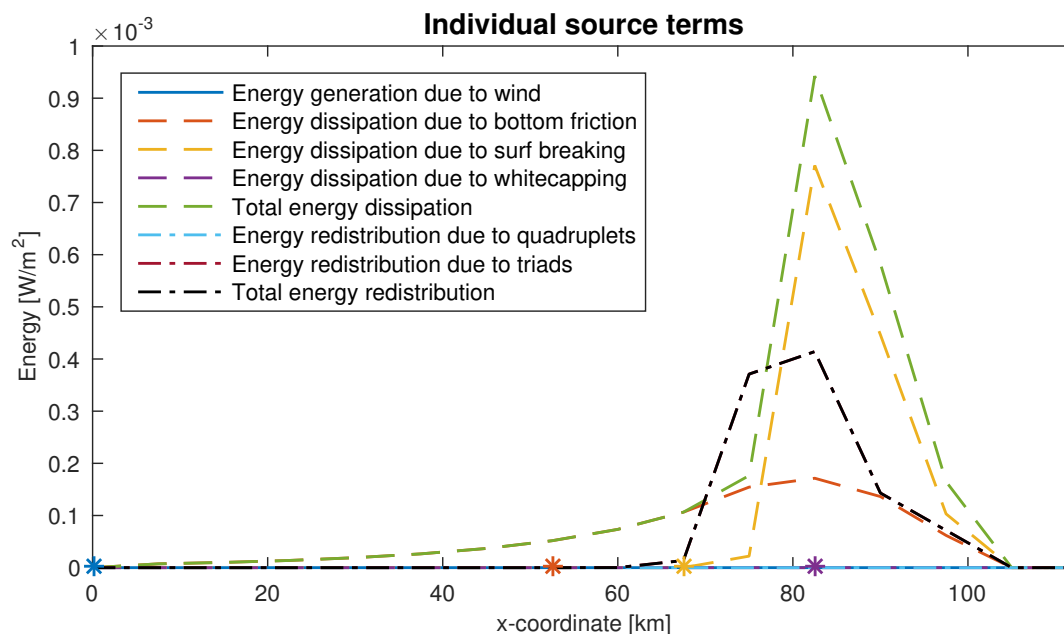


Figure 3.16: Evolution of the individual source terms of the energy balance (boundary conditions a JONSWAP spectrum with $H_s = 6$ m and $T_p = 10$ s, at a depth of 65 m).

Second, there is only one secondary peak for the steeper wave spectrum, and it only occurs close to shore at a depth of 10 m. Looking at the individual source terms in Figure 3.16, this is supported by the black dashed-dotted line, which represents the total energy redistribution (in this case only containing triad wave-wave interactions). The triads only become active inshore of the 20 m depth line (represented by the yellow asterisk on the x-axis). This behaviour is in line with theory, since triads only become active in shallow water.⁵

It can be concluded that the model behaves according to theory for steeper waves.

Whitecapping So far, the only energy dissipation in deep water is through the small amount of bottom friction. Therefore, before adding another source of energy through wind, first the whitecapping mechanism is activated. SWAN only allows whitecapping to be activated if there is also wind, so a negligible wind of 0.01 m/s is added to the model. The resulting variance density spectra are given in Figure 3.17 and the individual source terms are shown in Figure 3.18.

Figure 3.15 and Figure 3.17, respectively without and with whitecapping, show a very similar image. The main difference is the height of the peak at a depth of 30 m, which is lower in the latter case. This is exactly the expected behaviour, since whitecapping is an energy dissipation mechanism acting also in deeper water where the other dissipation mechanisms are negligible. This is confirmed by Figure 3.18. There is also some whitecapping inside the surf zone, but this is compensated by less energy dissipation through surf breaking. Finally, also an increase in triad wave-wave interactions is observed, however this transferred energy is quickly dissipated through wave breaking.

It is expected that whitecapping is not the main cause of the deviations observed in the first simulations. However, the different source terms have strong interactions, therefore a small change in one term may have significant impact on other terms, resulting in a completely different wave transformation.

⁵The terms shallow and deep water are relative and depend on the wave characteristics. Water that is considered deep for a small wave, can be shallow for higher waves. On the other hand, water can be shallow for a long wave, but deep for a steep wave. Apparently, the swell wave spectrum applied in Figure 3.10 “feels” the bottom earlier than the spectrum applied here.

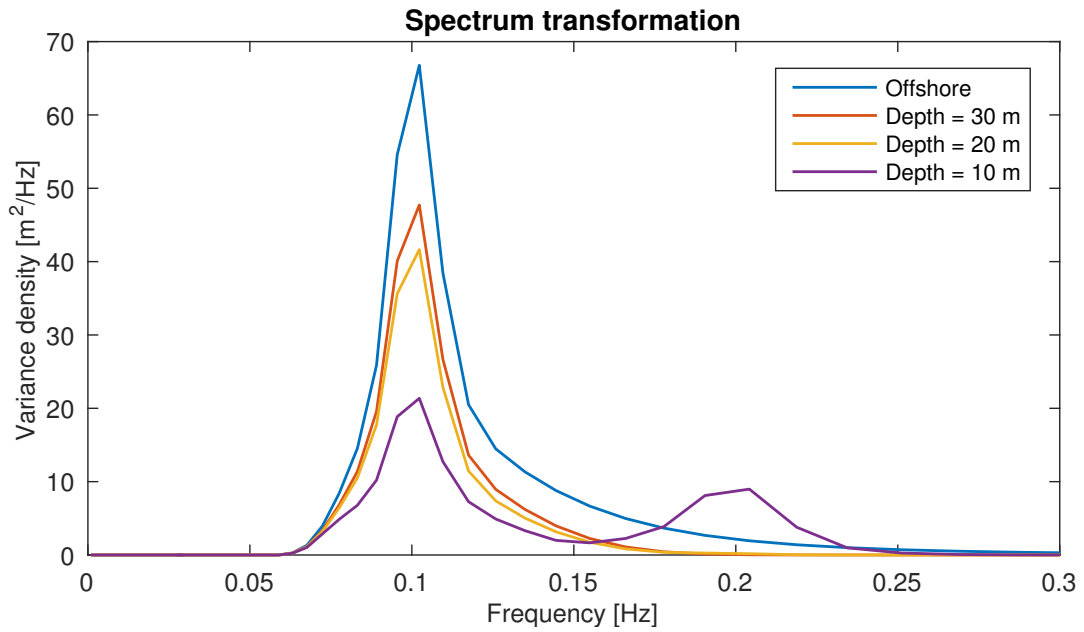


Figure 3.17: Evolution of the wave spectrum, from offshore (JONSWAP spectrum with $H_s = 6$ m and $T_p = 10$ s, at a depth of 65 m), to nearshore (at respective depths of 30 m, 20 m and 10 m), including whitecapping.

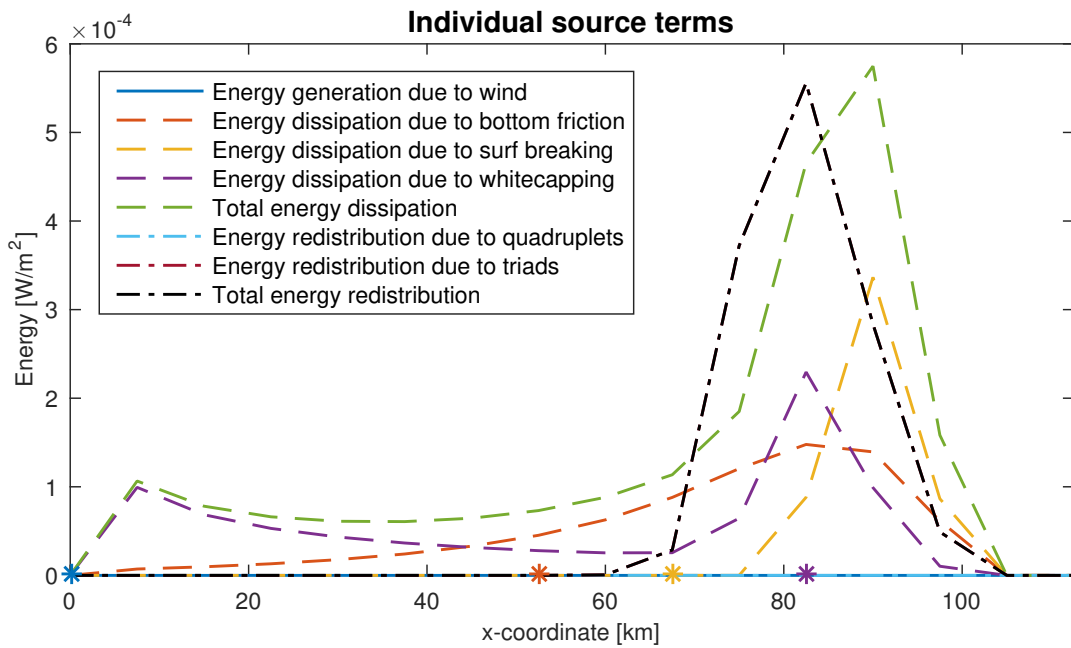


Figure 3.18: Evolution of the individual source terms of the energy balance (boundary conditions a JONSWAP spectrum with $H_s = 6$ m and $T_p = 10$ s, at a depth of 65 m), including whitecapping.

Wind input The Mekong Delta is characterised by extremely gently sloping foreshores. The climate is characterised by two monsoon seasons, one northeastern and one southwestern, each one relevant to a side of the Mekong Delta. On these wide foreshores, the effect of wind input can be quite significant. Whether and how SWAN models this effect is investigated in this paragraph by adding a constant onshore directed wind of 25 m/s to the model set-up of the previous paragraph.

Figure 3.19 shows the importance of wind on these gentle foreshores: the height of the peak in the variance density almost doubles between the offshore boundary and the depth of 30 m. It is interesting to see in Figure 3.20 that although the energy generation due to wind is high, the energy dissipation due to whitecapping is also significant. In other words, much of the energy generated by the wind

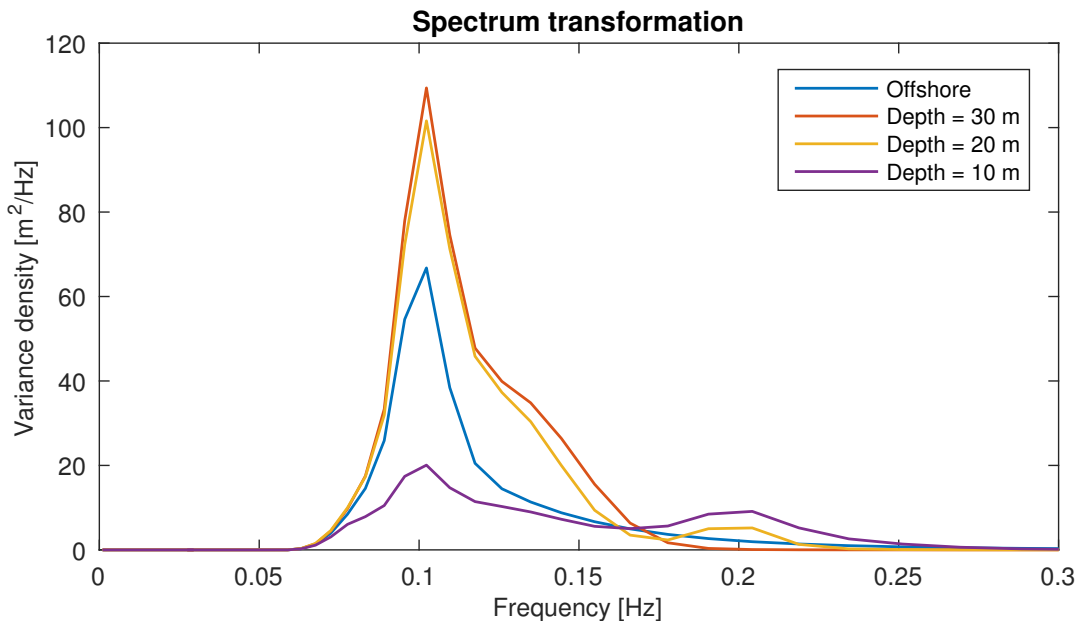


Figure 3.19: Evolution of the wave spectrum, from offshore (JONSWAP spectrum with $H_s = 6$ m and $T_p = 10$ s, at a depth of 65 m), to nearshore (at respective depths of 30 m, 20 m and 10 m), with an onshore directed wind of 25 m/s, including whitecapping.

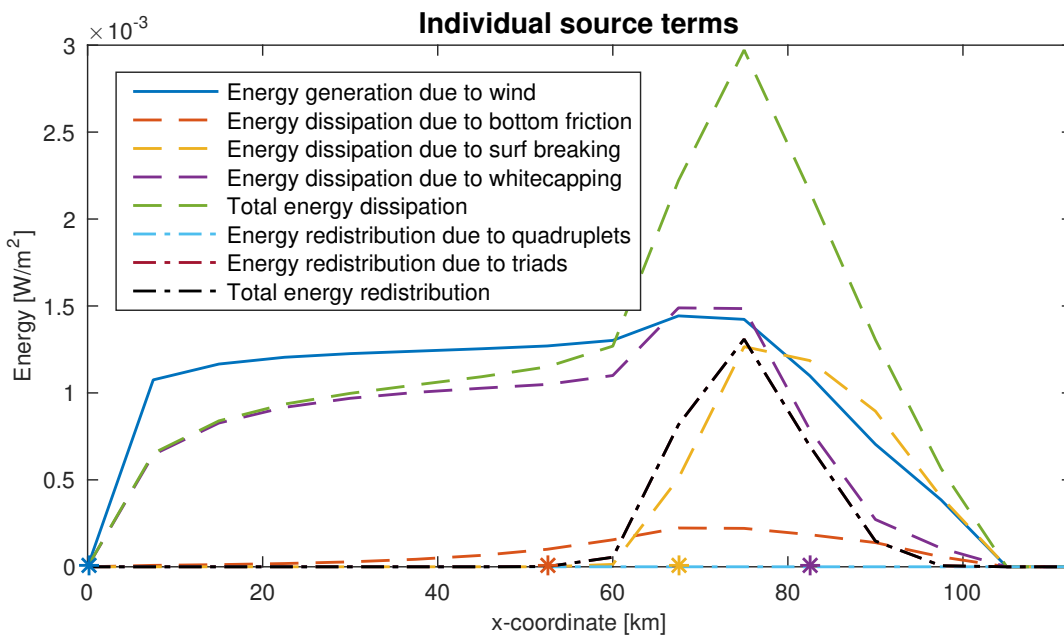


Figure 3.20: Evolution of the individual source terms of the energy balance (boundary conditions a JONSWAP spectrum with $H_s = 6$ m and $T_p = 10$ s, at a depth of 65 m), with an onshore directed wind of 25 m/s, including whitecapping.

is immediately dissipated through whitecapping. Nevertheless, the remaining energy is enough to generate the increase in variance density depicted in Figure 3.19.

Between the yellow and orange asterisks in Figure 3.20, the total energy dissipation exceeds the energy generation due to increased whitecapping and the start of surf breaking, which explains the reduction in variance density between the depths of 30 m and 20 m in Figure 3.19. Between these two depths, also the triads become active, and indeed a secondary peak is formed.

Finally, the depth of 10 m lies deep into the surf zone, where the energy dissipation becomes dominant and the wave spectrum is dissipated over all frequencies.

Another interesting aspect to notice in Figure 3.19 is the shape of the spectrum around a water depth of 30 m. The frequencies above the peak frequency, until about twice the peak frequency, contain

relatively more energy than in a normal JONSWAP spectrum. This change in shape is caused by both wind input and whitecapping. Relatively more energy is generated in this range by wind input, while whitecapping mostly affects frequencies below and around the peak frequency. It can be concluded that the model performs well under significant wind input.

Quadruplet wave-wave interactions The final element to be added to the model input are the quadruplet wave-wave interactions. These interactions are strongest in deep water and become more important for steeper waves. Adding quadruplets to the set-up of the previous case, the model set-up has become equal again to Figure 3.13 and Figure 3.14. While the latter figure showed a complete explosion of quadruplet wave-wave interactions, the former figures revealed an enormous increase in variance density.

As the previous paragraph showed, the energy generation through wind can be significant, doubling the density in that example. However, in Figure 3.14, it can be seen that the energy dissipation through whitecapping is actually larger than the energy generation through wind. Therefore, it cannot be correct that the variance density almost quadruples. This must be caused by a numerical effect related to the quadruplet wave-wave interactions.

Conclusion

Although quadruplet wave-wave interactions are a very important mechanism in wave transformation, its effects in the SWAN model set up for the Mekong Delta are more than doubtful (see Figure 3.13 and Figure 3.14). Since they dominate all other source terms in the wave energy balance, the results of the model become also extremely uncertain. On the other hand, when excluding quadruplets from the model set-up, as was done in Figure 3.19 and Figure 3.20, the model performs exactly as expected from theory.

Therefore, quadruplets will be excluded from the model set-up for the rest of this project. Although this has some serious consequences, it is the belief of the author that the consequences of excluding the quadruplet wave-wave interactions are smaller than the negative impact of the most likely erroneous behaviour of the current quadruplet modelling in SWAN.

Due to excluding quadruplets, there will be no energy transfer to lower frequencies, and less energy transferred to higher frequencies (only in shallow water through triads). As a result, the peak frequency might be slightly too high and the mid-frequencies might contain slightly too much energy. However, all other source terms act exactly according to theory (Holthuijsen, 2007). Therefore, there is enough confidence to use this model for the intended purpose.

It is not the goal of this project to investigate the cause of this behaviour any further. However, throughout this model validation the belief has grown that some of the deviations are caused by the extremely gentle bottom slopes. There is currently no literature available on wave transformation on these slopes. Therefore it is highly recommended to perform more research on both the physical behaviour of waves on these slopes, as well as the numerical reaction to these slopes in wave models. Another possible cause of the strange quadruplet wave-wave interactions might be the fact that a 1DV (one dimensional vertical) approach is followed, since quadruplets also tend to spread energy, which is not possible in 1DV.

3.1.3. Extremely gentle slopes

Mangrove coasts, and especially the coasts along the Mekong Delta in Vietnam, are characterised by extremely gentle slopes. Numerical models such as SWAN and SWASH, however, have been developed for the steeper sandy coasts, as can be found in the Netherlands. Although these models have been validated extensively, they have never been validated for slopes in the order of 1/1000, which is the range along the Mekong Delta coasts. Before the models can be applied to such mildly sloping foreshores, some research must be done to find answers to the following questions. What can wave theories tell about wave transformation on foreshores? Can the models reproduce this behaviour? How do SWAN and SWASH model depth-induced breaking and is there a way to tweak these models in order to optimise their performance on extremely gentle slopes? In the next sections, answers to these questions will be sought. With these answers in mind, two simple test cases will be modelled and analysed.

Physics of waves on gentle slopes

As a first step, a small literature research has been carried out. There is some material on wave transformation on very gentle slopes, such as Divoky et al. (1970), however, as it turns out, these slopes are still not as gentle as those found along the Mekong Delta. One very useful article by Alagan Chella et al. (2015) investigates the breaking characteristics of spilling breakers on slopes. Since spilling breakers occur for mild slopes, it is assumed that their conclusions can be extended to the Mekong Delta. Therefore, as a next step, these conclusions will be tested in the SWAN-SWASH model.

According to Alagan Chella et al. (2015), for a certain offshore wave steepness and water depth, the distance over which the waves shoal is longer on milder slopes. In other words, milder slopes slow down the wave breaking process, and as a result the breaking point moves shoreward. Figures 3.3 and 3.4 have the same boundary conditions imposed at the same offshore water depth, but a bottom slope of respectively 1/400 and 1/800. However, looking closely at the location of the breaking point, it is hard to say whether the breaking point in the latter case lies closer to shore. Both breaking points have approximately the same relative location, around the same water depth. This lack of difference is probably caused by the fact that both slopes can be considered “very gentle”.

Another conclusion by Alagan Chella et al. (2015) is that for a certain bottom slope and offshore water depth, waves with a lower offshore steepness break closer to shore. This will be tested by applying two different wave periods at the offshore boundary. The offshore boundary is located at a water depth of 65 m, the bottom slope is 1/800. First, a wave with a wave height of 6 m and a wave period of 15 s is applied, next, a wave with the same wave height but a wave period of 10 s is applied. The only difference between the two runs is the wave period, and therefore the wave steepness. The result is given in Figure 3.21.

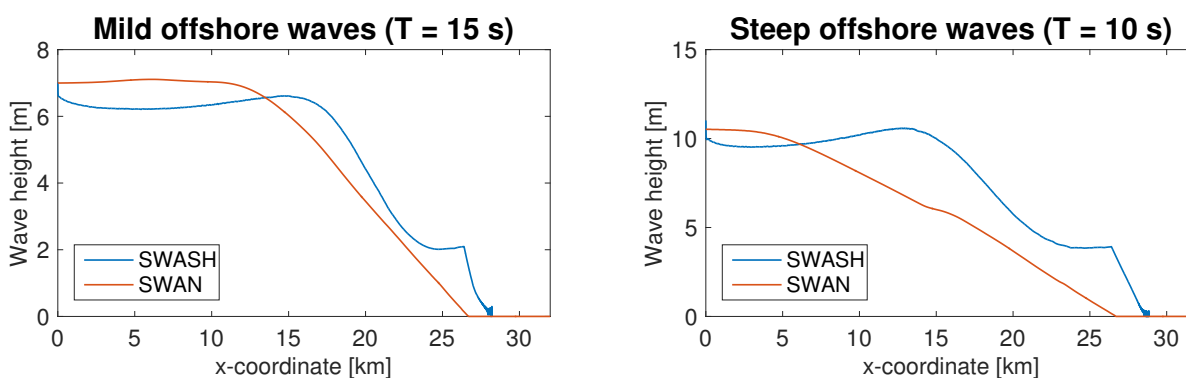


Figure 3.21: Location of breaking point for waves with different offshore steepness (left: $T = 15$ s, right $T = 10$ s).

This confirms the conclusion of Alagan Chella et al. (2015), the breaking point lies closer to shore in the case of the lower offshore steepness (left picture, $T = 15$ s).

According to theory, the shoaling distance and therefore the location of the breaking point depends on the offshore wave steepness and the bottom slope. The breaking point will lie closer to shore for waves with a lower steepness and for milder bottom slopes. This is confirmed by both models.

Depth-induced wave breaking in SWAN

Depth-induced breaking is one of the 6 processes included in the source term of the spectral action balance equation in SWAN (The SWAN team, 2015).⁶ Depth-induced breaking occurs when waves propagate towards the shoreline. Due to shoaling, the waves become steeper, until a certain limit is exceeded and the waves break.

Unfortunately, the process of wave breaking itself is still poorly understood. However, by comparing a breaking wave with a bore, the total energy dissipation and global properties of breaking waves can be determined. Following the bore model of Battjes and Janssen (1978), SWAN determines the maximum wave height with the following equation:

$$H_{max} = \gamma d \quad (3.12)$$

⁶The other 5 processes are: wave growth by wind, nonlinear energy transfer through quadruplets and triads, and energy dissipation through whitecapping and bottom friction The SWAN team (2015).

Where

H_{max}	maximum possible individual wave height	[m]
γ	breaker parameter	[-]
d	total water depth (incl. set-up)	[m]

In SWAN, there are two approaches to the breaker parameter γ (The SWAN team, 2015). Either it is a constant value (default value: 0.73), or it can be a function of the bottom slope β and the dimensionless water depth kd (the so-called β - kd -approach). While the constant value is default, for this project it is more appropriate to use a variable breaker parameter, as the bottom slope plays an important role. In case of a variable breaker parameter, a reference value for horizontal slopes has to be defined (default value 0.53).

Figure 3.22 shows the effect of a constant and variable breaker parameter in SWAN. For comparison also the SWASH wave transformation curve is given.

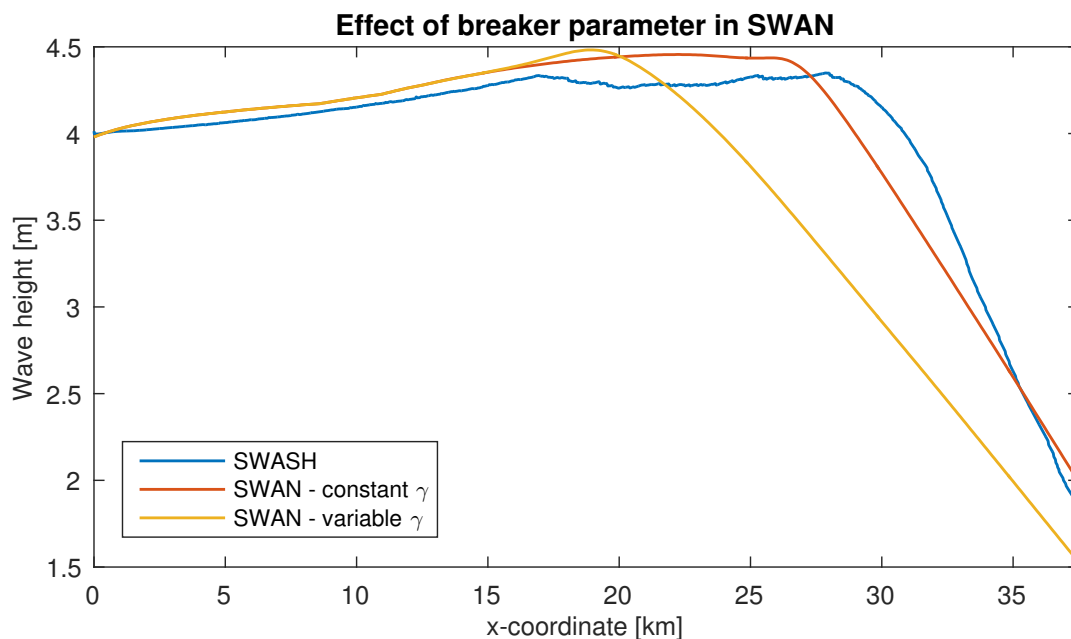


Figure 3.22: Effect of constant and variable breaker parameter in SWAN.

The yellow curve shows the wave transformation modelled by SWAN with a variable breaker parameter. As can be seen, the waves break earlier than in the case of a constant breaker parameter. This is caused by the low value of the breaker parameter on these extremely gently sloping, shallow foreshores. The value of the breaker parameter is probably very close to the reference value for horizontal slopes. In the case of a constant breaker parameter, the wave height already decreases long before the breaking point, in fact it starts decreasing at the location of the breaking point in the case of a variable breaker parameter. Therefore the location of the new breaking point seems realistic. There is still a large difference between the behaviour in SWAN and SWASH, but it can be concluded that the variable breaker parameter is more appropriate for this project.

Depth-induced wave breaking in SWASH

Like SWAN, SWASH cannot model the details of breaking waves. In fact, none of the current spectral or non-hydrostatic models can model this, since the essential processes of breaking are not included in these models (The SWASH team, 2015). However, following the same bore-analogy, SWASH can approximate the integral properties of breaking waves.

In case of sufficient vertical resolution (10 or more vertical layers), SWASH can accurately determine these properties. However, in case of a coarse vertical resolution (which is the case in this project, with 2-4 vertical layers), the horizontal velocities near the wave crest may be underestimated.

A solution is to use the BREAK command, which enforces a hydrostatic pressure distribution at the

front of the wave. SWASH labels a grid point for hydrostatic computation if the local surface steepness exceeds a certain value α (default value 0.6). In order to represent the persistence of wave breaking, the neighbouring grid points are labelled also for hydrostatic computation if the local surface steepness exceeds a certain value β , which is lower than α (default value 0.3).

It is hypothesised that wave breaking can be postponed or expedited by respectively increasing or lowering the α -value. The effect of β is less clear, but is expected that this influences the wave height beyond the breaking point. Figure 3.23 shows the effect of various α and β values in SWASH.

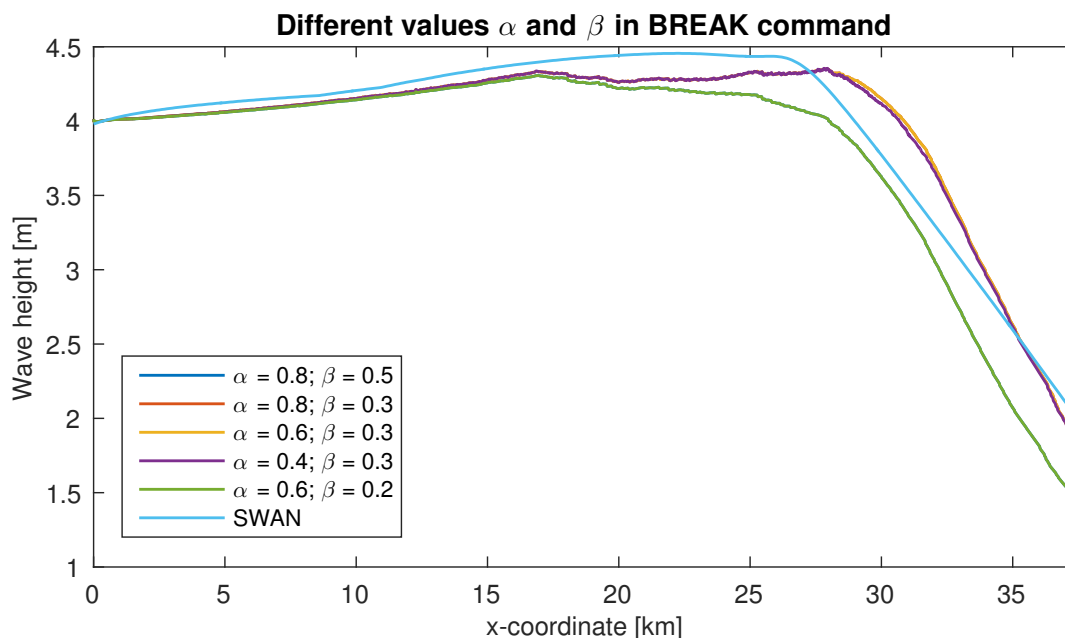


Figure 3.23: Effect of various α and β values in BREAK command SWASH.

The default values are represented by the yellow line, which is barely visible, only after the final breaking point. Lowering the α -value (represented by the purple line), has nearly no effect, and neither has increasing the α -value (represented by the invisible orange line, which is completely covered by the purple line). Changing the β -value has more effect, as can be seen by the green line ($\beta = 0.2$). Oddly enough, increasing the β -value has exactly the same effect as lowering the β -value, since the green line completely coincides with the dark blue line, representing $\beta = 0.5$.

Since the effect of changing the value of α is negligible, and the effect of changing the value of β is ambiguous, the default values ($\alpha = 0.6$ and $\beta = 0.3$) will be used throughout the rest of the project.

Case 1: Imposing a regular wave on a 1/1500 slope

Since it is unsure how well SWAN and SWASH perform on these extremely gentle slopes, two additional cases will be modelled to verify the model behaviour. In the first case, a regular wave will be imposed on a slope of 1/1500. The results are given in Figure 3.24. In the same figure also the model results are given for a run with the same input, except the wave boundary condition, where a JON-SWAP spectrum was imposed.

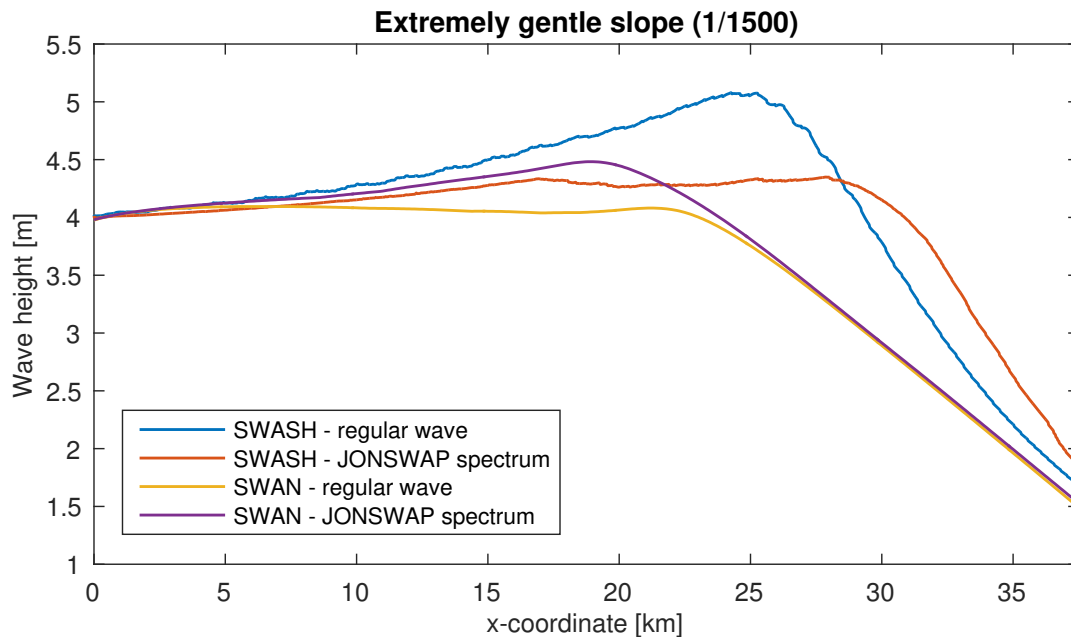


Figure 3.24: Comparison of the wave transformation of a regular wave and a JONSWAP spectrum on a slope of 1/1500

First, the results of SWASH will be analysed. For a regular wave, SWASH shows globally the expected behaviour: increasing wave height due to shoaling, until the breaking point is reached, after which the wave height decreases rapidly. The curve is not smooth however, showing repeatedly breaking and re-shoaling. Nevertheless, this is the shape which can be expected based on theory, and therefore increases confidence in the model. However, when a JONSWAP spectrum is imposed at the boundary, the waves do not manage to shoal so high. This is probably caused by the fact that, in contrast to a regular wave, a spectrum consists of countless waves with different amplitudes and frequencies. Therefore, part of that spectrum will start to break long before other waves will break, which results in a lower significant wave height overall. The closer to shore, the more the two curves coincide, which further increases confidence in the model.

Looking at the results of SWAN, there is hardly any difference between the curves. It can be concluded that the effect of a wave spectrum is not as large in SWAN as in SWASH, this is probably caused by the fact that SWAN is a Boussinesq-type model, as opposed to the non-hydrostatic model SWASH. This first case gives confidence in the model, since it performs still rather well for a relatively simple case on an extremely gentle slope.

Case 2: Complete model set-up on a 1/200 slope

In the second case, the opposite of the first case will be examined. Instead of a simple set-up on an extremely gentle slope, the full design set-up will be tested on a normal slope of 1/200. The boundary conditions correspond to a design storm with a return period of 50 years (see section 2.4). SWAN will be used to model the wave transformation from deep water (65 m) to nearshore, where it will generate a wave spectrum, which will be used as input for SWASH. However, due to the required linear wave boundary condition in SWASH, this spectrum will first be enhanced, before it is applied (as was explained above). The eventual wave transformation nearshore is given in Figure 3.25.

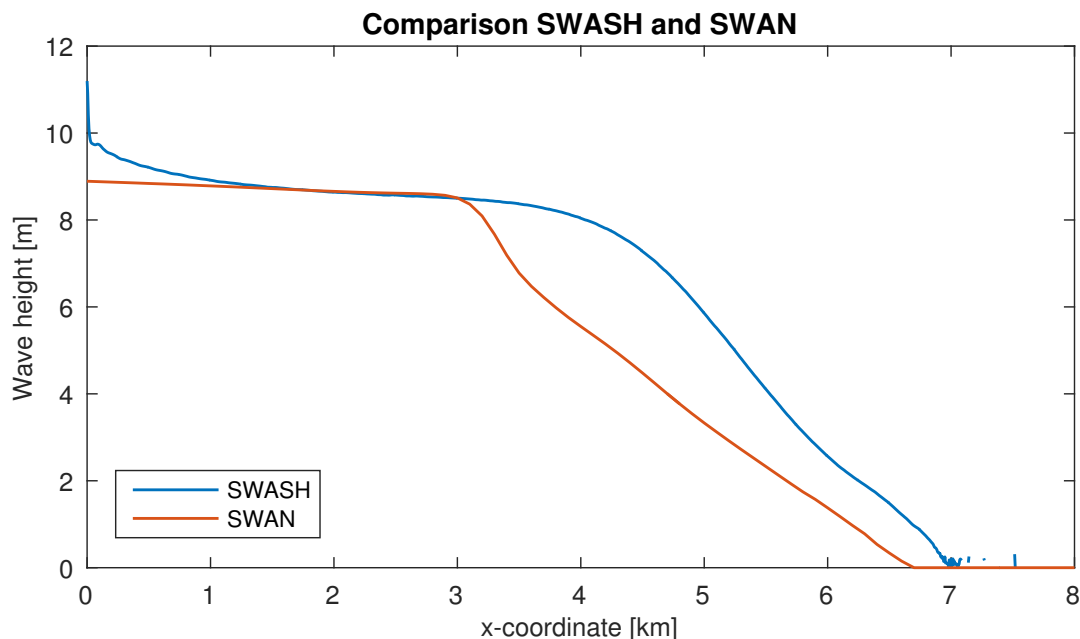


Figure 3.25: Wave transformation for full model set-up on a slope of 1/200.

The shape of both curves is very similar. In SWASH, however, the waves propagate further before they break, compared to SWAN. The wave height reduction rate after the breaking point is comparable for both models. This second test case gives sufficient confidence in the model to continue towards modelling the design scenarios.

Conclusion

The goal of this section was to determine whether SWAN and SWASH can be used with sufficient confidence to model design storm conditions along the Mekong Delta coast, which is characterised by extremely gentle slopes. As a first step, literature on wave transformation on gentle slopes was consulted. However, in most of these sources, the gentle slopes turned out to be a lot steeper than the slopes in question. Assuming the conclusions from literature can be extrapolated to the gentler slopes of the Mekong Delta, it was tested whether SWAN and SWASH could reproduce the described behaviour. Although not every aspect came out equally clearly, at least the models did not contradict the theory. Therefore, it is concluded that the models can be applied to these gentle slopes.

In a next step, it was investigated how SWAN and SWASH model depth-induced breaking, and how these settings could be optimised for extremely gentle slopes. Both SWAN and SWASH use a bore analogy to approximate the integral properties of breaking waves. In SWAN, the maximum individual wave height is determined on the basis of a breaking parameter γ . By default, this parameter is constant, but it is also possible to make it a function of bottom slope and dimensionless water depth. This latter is preferable on these mild slopes. In SWASH, wave breaking can be influenced through two parameters, α and β , which also influence the limit wave steepness. However, varying these parameters has no clear impact on the model behaviour. Therefore, it is opted to continue with the default values ($\alpha = 0.6$ and $\beta = 0.3$).

Finally, two simplified test cases were modelled. The first test case imposed a regular wave on a slope of 1/1500, in order to examine whether the model was capable of modelling on such extremely gentle slopes. Especially the results in SWASH were encouraging, which gives confidence that the model can be applied to such foreshores. In the second test case, the opposite was investigated, whether the full design conditions on a normal slope (1/200) would produce realistic results. The results of SWAN and SWASH were comparable, which proved that the models are able to deal with the full design conditions. Combining the results of both test cases, it can be concluded that the models can be applied to extremely gentle slopes, and that the models are able to deal with extreme design conditions. This gives confidence that also the combined input of extreme design conditions on extremely gentle slopes will give realistic results.

3.1.4. Wave transformation inside mangrove forests

So far the models have been validated for a situation without any vegetation. However, in all scenarios also the effect of mangrove forests will be investigated. Mangrove trees grow between mean sea level and spring high tide, and since SWAN is only used for the offshore part of the computational domain, vegetation will only be modelled in SWASH.

In order to assess and validate the effect of the mangrove forest on the hydraulic conditions, four situations will be compared: a first situation without vegetation (blue line), and three situations with vegetation, but with different vegetation densities (sparse, average and dense, respectively the orange, yellow and purple lines), following the approach of Phan Khanh Linh et al. (2015).

In Figure 3.26, these four situations are modelled on a bottom slope of 1/800 for boundary conditions corresponding to a return period of 100 years. In the same figure, also the wave attenuation as defined by the Technical Standards for Seadike Design in Vietnam (Tran Quang Hoai et al., 2012) is visualised by the green dashed line. The left boundary of the x-axis represents the start of the mangrove forest, which is at MSL, however due to a storm surge the current water level is above MSL. The right boundary of the x-axis represents the shoreline.

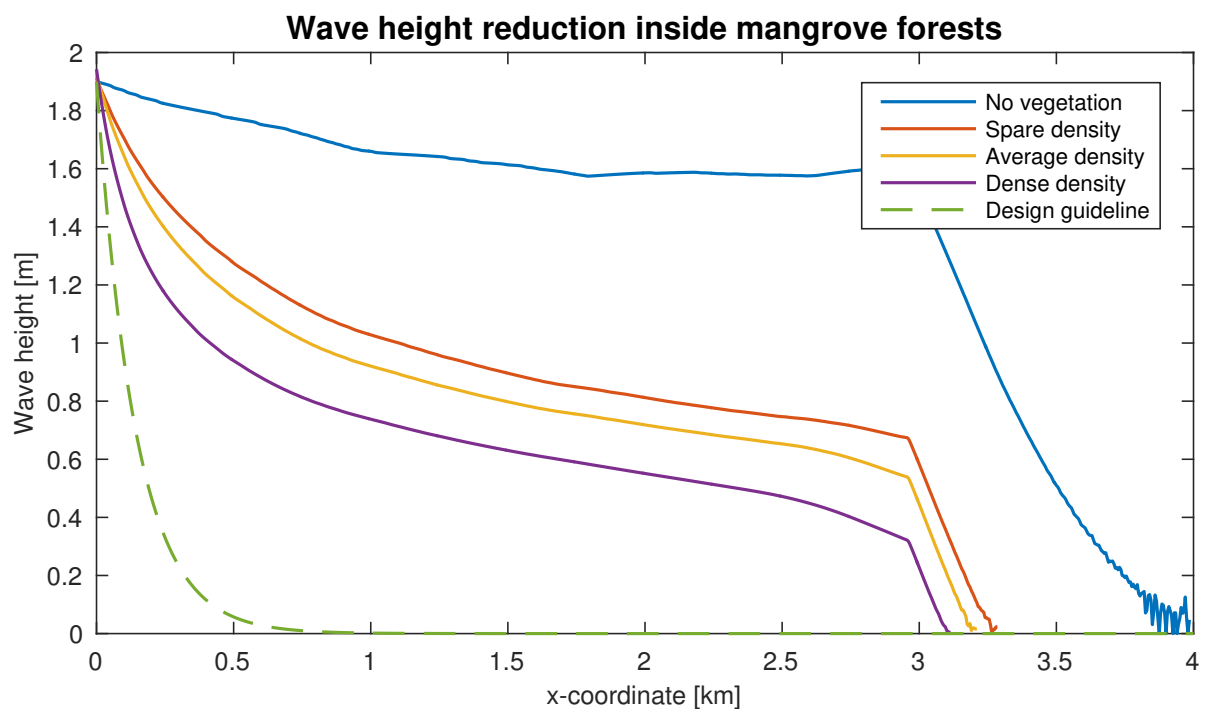


Figure 3.26: Wave height reduction nearshore, for different mangrove densities, on a bottom slope of 1/800 for boundary conditions with a return period of 100 years.

As expected, the effect of vegetation is to increase the wave height attenuation. This effect is largest in the first 500 m of the forest and shows an exponential decline. Further inside the mangroves, the smaller waves are barely affected, and they only fully reduce near the shoreline. This strong wave attenuation is absent in the case without vegetation, and as a result much higher waves reach the shoreline.

The green dashed line shows an extremely strong wave height reduction. This amount of wave height reduction (from a wave height of 2 m to a couple of centimetres in less than 500 m) is much higher than what SWASH models, and seems unrealistic. In the design guidelines, no details are given on how this formula has been derived.

The amount of wave attenuation also depends highly on the water level. In this case, a storm surge of 3 m has been included. As a result, the waves no longer travel through the highly dissipating root network, but instead they travel through the stems of the mangrove trees, which provide less resistance. Furthermore, also the type of mangrove species plays an important role, through its structure and density of each vertical layer. The species vary through the forest, which makes it even more difficult to summarise the wave attenuation inside a mangrove forest in just one simple formula.

Conclusion

Due to the large difference between the design guidelines and the model results, in the rest of the project, the model results will be followed, since this is on the safe side. However, in order to reduce the uncertainty in the design of the coastal protection, more knowledge is required on the precise effect of mangrove vegetation on wave transformation nearshore.

3.2. Analysis model results

The SWAN-SWASH model, that has been optimised in the previous section, will now be used to model the range of situations representative for the Mekong Delta. This range of situations includes 3 bathymetries, 3 lifetimes with each 4 return periods and 4 vegetation densities, as defined in section 2.4.

In the following sections, first the general wave transformation will be analysed (subsection 3.2.1), after which the effect of the bathymetry (subsection 3.2.2), the lifetime and return period (subsection 3.2.3) and the vegetation will be investigated (subsection 3.2.4).

3.2.1. General wave transformation

In order to assess the general behaviour of the model, one specific situation is chosen (randomly) for investigation. For this, the relatively steep bathymetry (bottom slope 1:800) is chosen, to which a lifetime of 50 years and a return period of 100 years is applied. This specific situation is used as illustration, however the conclusions drawn here are valid for all situations defined in section 2.4.

Wave transformation in SWAN

For each situation first SWAN is used to model the wave transformation from offshore (at a depth of 65 m) to nearshore. This wave transformation is visualised in Figure 3.27.

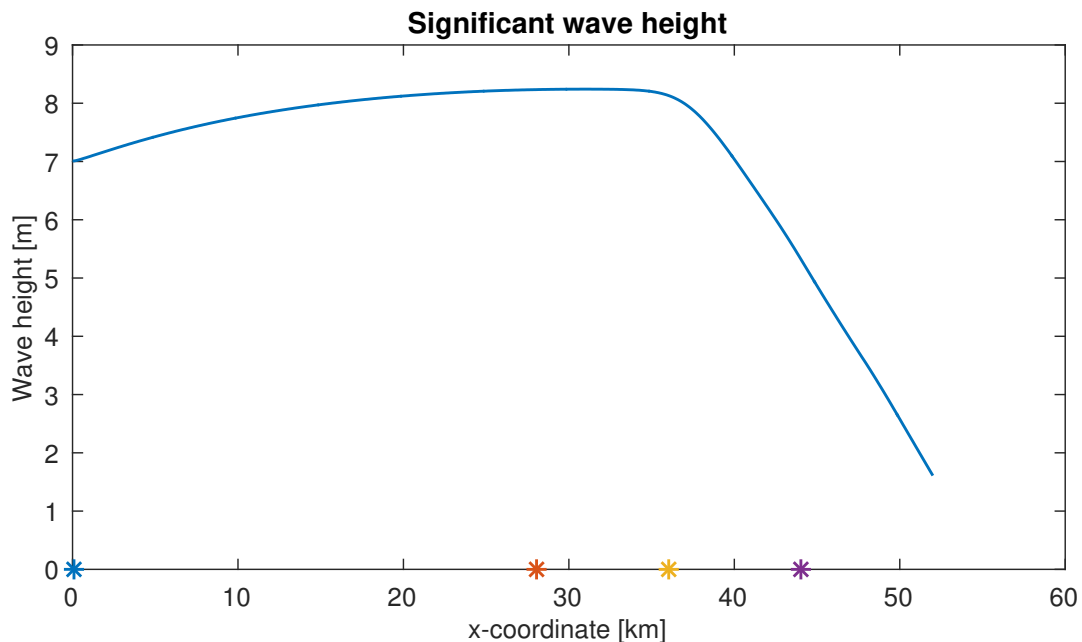


Figure 3.27: Wave transformation as modelled by SWAN on a relatively steep bathymetry (bottom slope 1:800) for a lifetime of 50 years and design conditions with a return period of 100 years.

At the boundary, a significant wave height of 7 m is applied. When moving into the domain, the wave height increases due to shoaling. However, this shoaling process reduces, until the wave height remains more or less constant for a couple of kilometers. The final breaking point is reached around $x = 37$ km, after which the wave height decreases linearly. This is in accordance with the expected behaviour as discussed in section 3.1.

It is also interesting to analyse the transformation of the wave spectrum. In Figure 3.28 four wave spectra are visualised, at depths of 65 m (the offshore boundary), 30 m, 20 m and 10 m (respectively the blue, orange, yellow and purple lines). These locations are also indicated by asterisks in the respective colours on the x-axis of Figure 3.27.

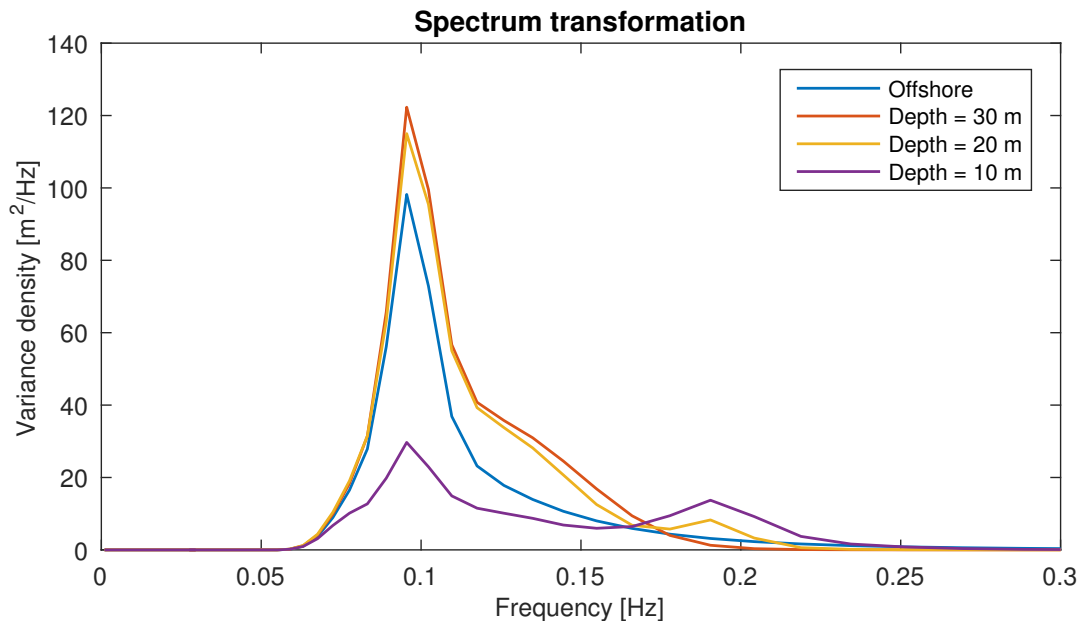


Figure 3.28: Evolution of the wave spectrum, from offshore (at a depth of 65 m) to nearshore (with respective depths of 30 m, 20 m and 10 m).

The blue spectrum is clearly the JONSWAP spectrum, as imposed at the offshore boundary. Further, it can be noticed that the spectra closer to shore not only change shape, but also that the total amount of variance density varies. To assess the causes of these changes, the individual source terms will be analysed. The evolution of these source terms is visualised in Figure 3.29.

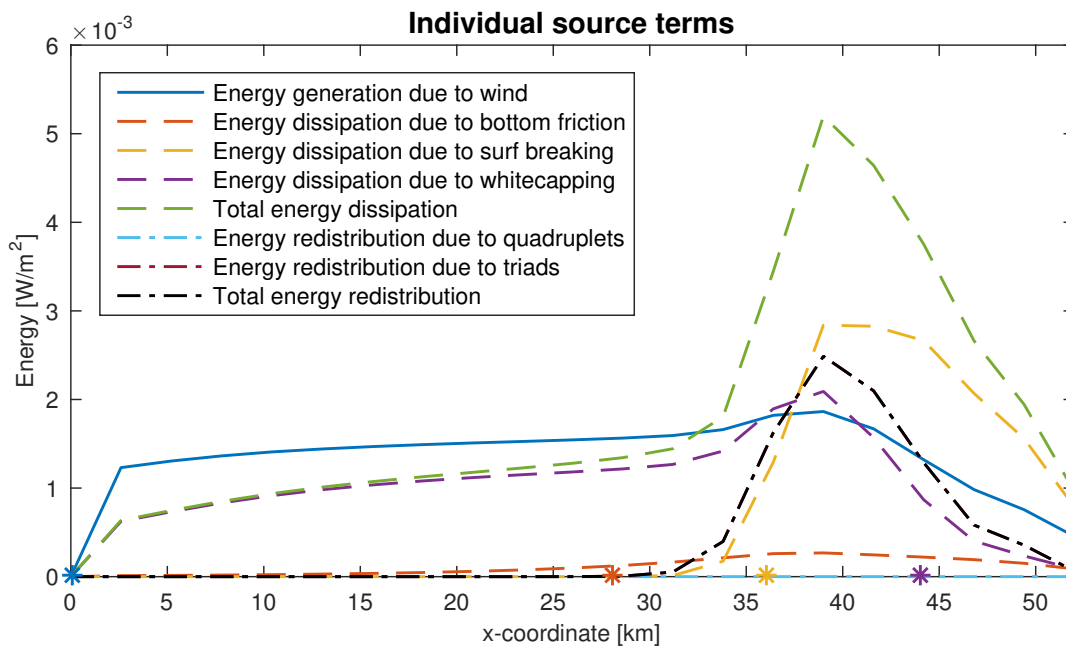


Figure 3.29: Evolution of the individual source terms of the energy balance

From this figure it can be derived that energy generation due to wind is responsible for the increased peak height between the offshore boundary and the 30 m depth. Inshore of the 30 m depth, the peak starts to decrease again, which can be explained by increased energy dissipation, exceeding the energy generation due to wind. Also inshore of the 30 m depth line, energy redistribution due to triads occurs, which explains the emergence of a secondary peak around a frequency twice the peak frequency. Finally, the energy is rapidly dissipated inshore of the 20 m depth line, as the surf zone starts

around $x = 35$ km.

During the model validation, it was concluded that the location of the SWASH boundary should be offshore of the breaking point. In the current situation, the surf zone starts around $x = 35$ km. Therefore, the choice to locate the SWASH boundary at a depth of 30 m is correct, as this is at $x = 27.5$ km. In the next section, the wave transformation nearshore, as modelled by SWASH, will be analysed.

Wave transformation in SWASH

Between a water depth of 30 m and the shoreline, SWASH will model the wave transformation. The boundary conditions at a depth of 30 m are derived from SWAN. However, the spectrum produced by SWAN first needs to be modified, in order to compensate for the wave height drop at the boundary due to nonlinear wave conditions (for more information read subsection 3.1.1). In this case, a relatively high factor is needed to compensate for the deviation. This is illustrated in Figure 3.30. The blue line represents the wave transformation as modelled with SWASH, while the orange line represents the nearshore part of the SWAN results.

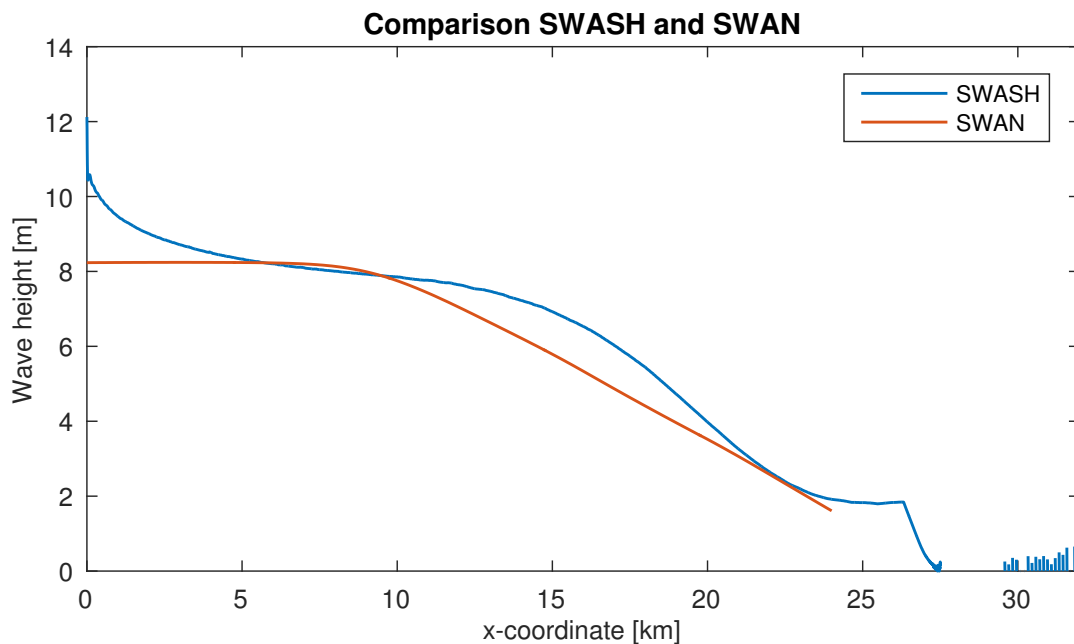


Figure 3.30: Wave transformation nearshore as modelled by SWASH and SWAN on a relatively steep bathymetry (bottom slope 1:800) for a lifetime of 50 years and design conditions with a return period of 100 years.

At the left hand boundary, the trick applied to the spectrum file to compensate for the drop in wave height is very obvious. However, it is the right hand side of the domain that is of importance, and thanks to this boundary trick, the results at the right hand side are not influenced by boundary effects. It can also be noticed that the breaking point lies inside the nearshore domain, and that the breaking point in SWASH is located closer to shore than in SWAN. This is in agreement with section 3.1.

It is also interesting to compare the behaviour beyond the breaking point. In SWAN, the wave height reduces linearly. In SWASH, however, the wave height initially reduces linearly, but this reduction decreases as the shoreline approaches, where the wave height remains more or less constant for a short distance. Eventually, the wave height rapidly decreases to zero at the shoreline.

3.2.2. Effect of bathymetry on wave transformation

The Mekong Delta can be represented by three bathymetric profiles: a very mildly sloping foreshore (1:1500), a relatively steep foreshore (1:800) and a relatively steep foreshore with a mudflat of 2 km at 1 m below MSL. These profiles represent respectively the east coast, west coast and southern tip of the Mekong Delta. In this section, the effect of these different bathymetries is analysed.

Figure 3.31 shows the wave transformation on the three types of bathymetry. To each bathymetry, the same offshore boundary conditions are applied: a lifetime of 50 years with a return period of 100 years. The origin of the x-axis is located at a depth of 20 m, and is positive towards the shoreline.

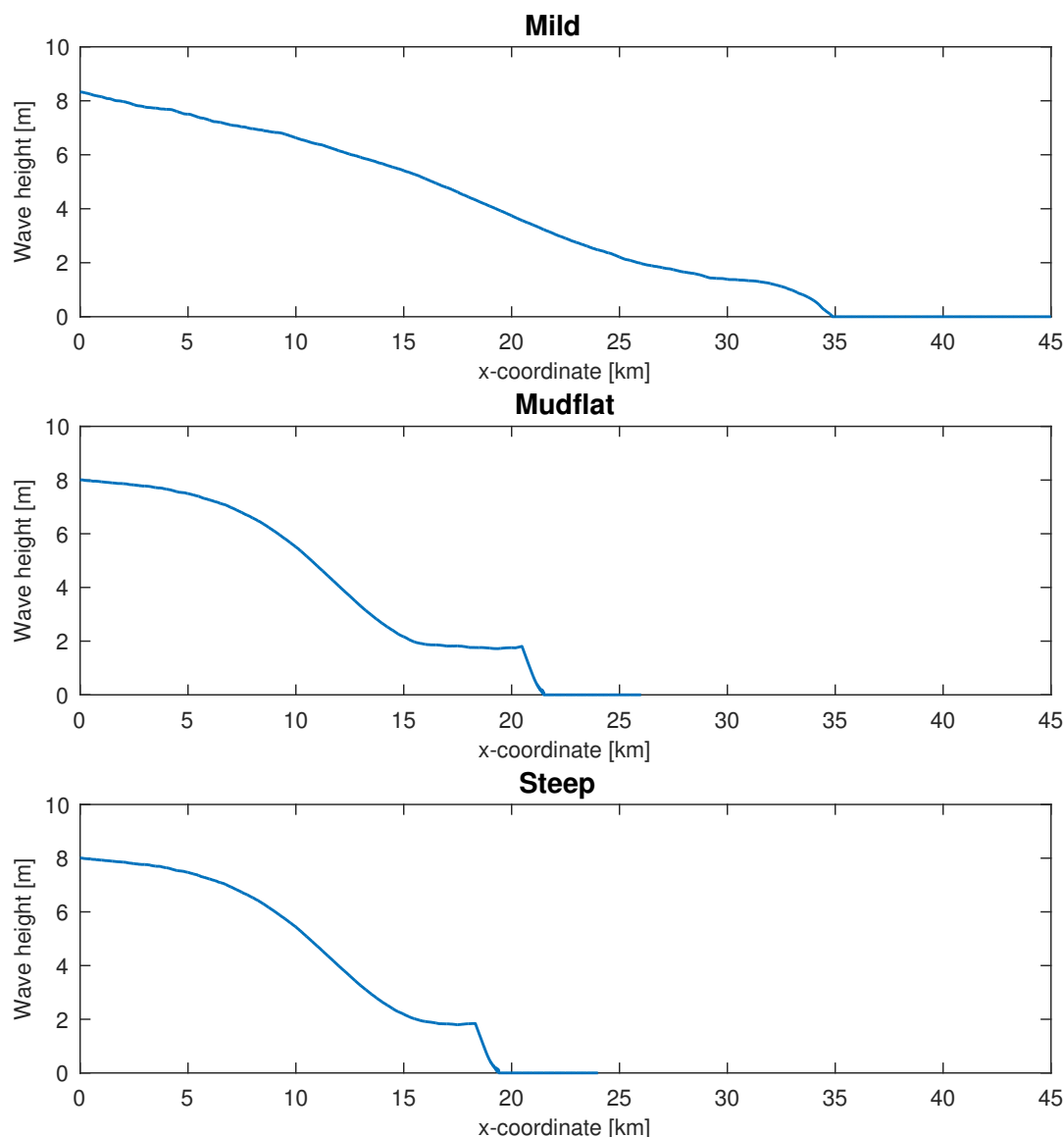


Figure 3.31: Wave transformation nearshore for different bathymetries (from top to bottom: mild, steep with mudflat and steep). To each bathymetry, the same offshore boundary conditions are applied, corresponding to a lifetime of 50 years and a return period of 100 years.

Near the left hand boundary, the wave height decreases most strongly on the mild bathymetry, while on the two other bathymetries, the wave height remains almost constant, indicating the vicinity of the breaking point. However, further inside the domain, the wave height decreases more rapidly on the latter two bathymetries. This reduction continues until a wave height of about 2 m is reached, after which the wave height remains more or less constant up to the shoreline, where a rapid reduction to zero is observed. On the mild bathymetry, however, the wave height reduces steadily until a lower wave height, around 1 m, is reached. After a short distance, the wave height reduces at the same slope to zero.

Since the focus of this project lies nearshore, it is the behaviour close to the shoreline that matters most. On the relatively steep foreshore, with and without mudflats, waves with a wave height around 2 m reach the shoreline, while on the mild foreshore, waves with a wave height around 1 m approach the shoreline, and the wave height is reduced gradually before the shoreline is reached. For a coastal protection strategy, this latter case is more favourable, as the load on a possible construction will be significantly lower.

It can be concluded that the effect of the bottom slope is most strongly felt close to the shoreline. The

steeper the foreshore, the higher the waves that reach the shoreline. For milder slopes, the waves approaching the shoreline are not only lower, they also reduce gradually before reaching the shoreline. The effect of the mudflat is rather negligible nearshore, perhaps the waves reaching the shoreline are slightly lower.

3.2.3. Effect of lifetime and return period on wave transformation

Lifetime and return period cannot be separated, as it is the combination of both that determines the probability of failure. In this project, the return periods are even expressed as a function of the lifetime: $0.5T_l$, T_l , $2T_l$ and $5T_l$.

Figure 3.32 shows three plots, one for each lifetime (20 years, 50 years and 100 years). For each lifetime, four return periods are compared ($0.5T_l$, T_l , $2T_l$ and $5T_l$).

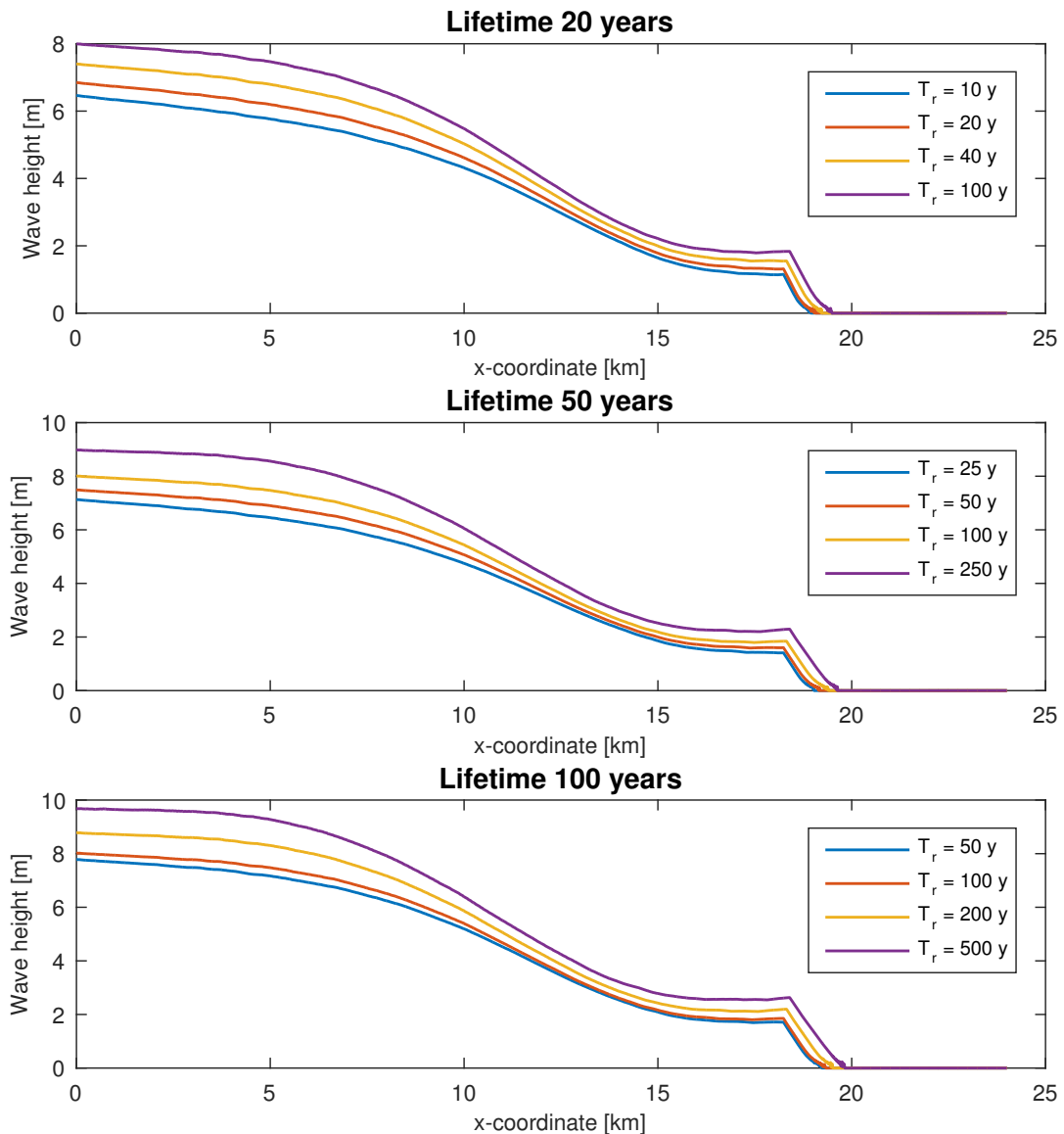


Figure 3.32: Wave transformation nearshore for different lifetimes (from top to bottom: 20 years, 50 years and 100 years) and different return periods ($0.5T_l$, T_l , $2T_l$ and $5T_l$).

The consequence of expressing the return periods as function of the lifetimes, is that for longer lifetimes, heavier design conditions occur. It is therefore impossible to isolate the effect of the lifetime. However, the lifetime directly influences the design water level, through the relative sea level rise of 21 mm/y. Over a period of 50 years, this is an increase of 1 m in water level. On a slope of 1/800, this means that the shoreline will move 800 m inland. In the case there is a sea dike, the dike needs to be able

not only to withstand the higher water level, but also the increased wave loading, as higher waves can reach the dike since the water in front of the dike has become deeper.

It is difficult to observe these effects, but when zooming in around the shoreline, it can be seen that this position moves inland in the lower plots. Further, it is also visible that the wave height close to the shore becomes higher. This is due to the higher offshore wave conditions, but also due to the increased water level.

Nevertheless, the effect nearshore of increased lifetime and return period is much smaller than the effect offshore. A difference in wave height of 2 m at a water depth of 20 m is reduced to a difference in wave height in the order of 0.1-0.2 m at the shoreline. However, the further away from the shoreline, the larger the difference. This means that the further inland the sea dike (or other coastal protection measure) is constructed, the lower the additional costs are for longer lifetimes/return periods related to the wave load.

3.2.4. Effect of vegetation on wave transformation

Finally, also the effect of the mangrove forest on the wave transformation is analysed. Mangrove forest starts around MSL and can grow up to the highest spring tide levels. Therefore, the effect is expected to be concentrated in the area between MSL and the shoreline. Further, also the effect of the vegetation density is investigated, since large parts of the remaining mangrove belts in the Mekong Delta are declining, both in size and in density.

Figure 3.33 shows the wave transformation nearshore (starting at a depth of 10 m) for 4 different mangrove situations: no vegetation (blue line), spare density (orange line), average density (yellow line) and dense density (purple line). The bottom slope is relatively steep (1:800) and for the boundary conditions offshore a lifetime of 50 years and a return period of 100 years is chosen.

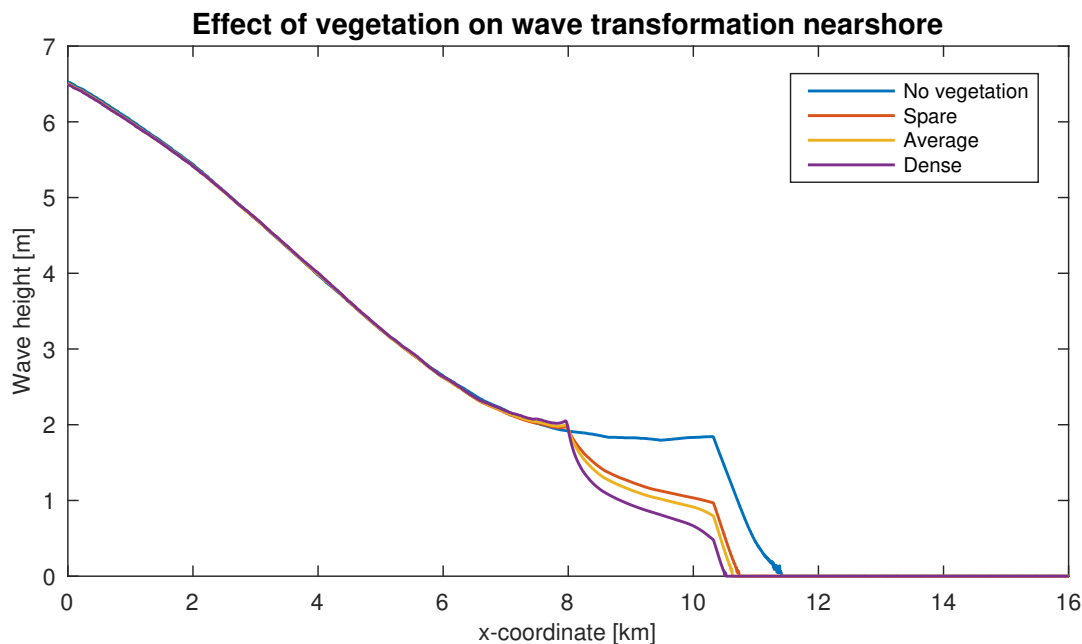


Figure 3.33: Wave transformation nearshore for different vegetation densities (no vegetation, spare density, average density, dense density) on a steep bottom slope (1:800).

The first element that can be derived from this plot is that the effect of vegetation is very local. There is some reflection just outside the mangrove forest, but this is negligible. Inside the mangrove forest, a large difference can be noticed between the situation without vegetation and the situations with vegetation. The wave height remains more or less constant without vegetation, resulting in high waves reaching the shorelines, while with vegetation the wave height decreases exponentially. As a result, the wave run-up is much lower, and the shoreline is located further offshore than in the case without vegetation.

The effect of density is also clearly visible. However, the difference between spare and average density is rather small. The difference between the dense forest and the two others is significant, leading to

almost twice the wave height reduction near the shoreline in the latter case. In other words, a healthy mangrove forest can attenuate a large amount of wave energy, however, as soon as the forest is affected and the density starts to decline, the waves are much less attenuated. Still, a sparsely forested mangrove belt provides twice as much wave height reduction as a bare mudflat.

Subsection 3.2.2 revealed a significant difference in the wave transformation close to the shoreline for the different bathymetries. Therefore, the effect of vegetation is not only investigated on a relatively steep bottom slope (1:800, previous example), but also on a mild bottom slope (1:1500).

Figure 3.34 shows the wave transformation nearshore (starting at a depth of 10 m) for the same 4 mangrove situations: no vegetation (blue line), spare density (orange line), average density (yellow line) and dense density (purple line). The bottom slope is extremely mild (1:1500) and for the boundary conditions offshore a lifetime of 50 years and a return period of 100 years is chosen.

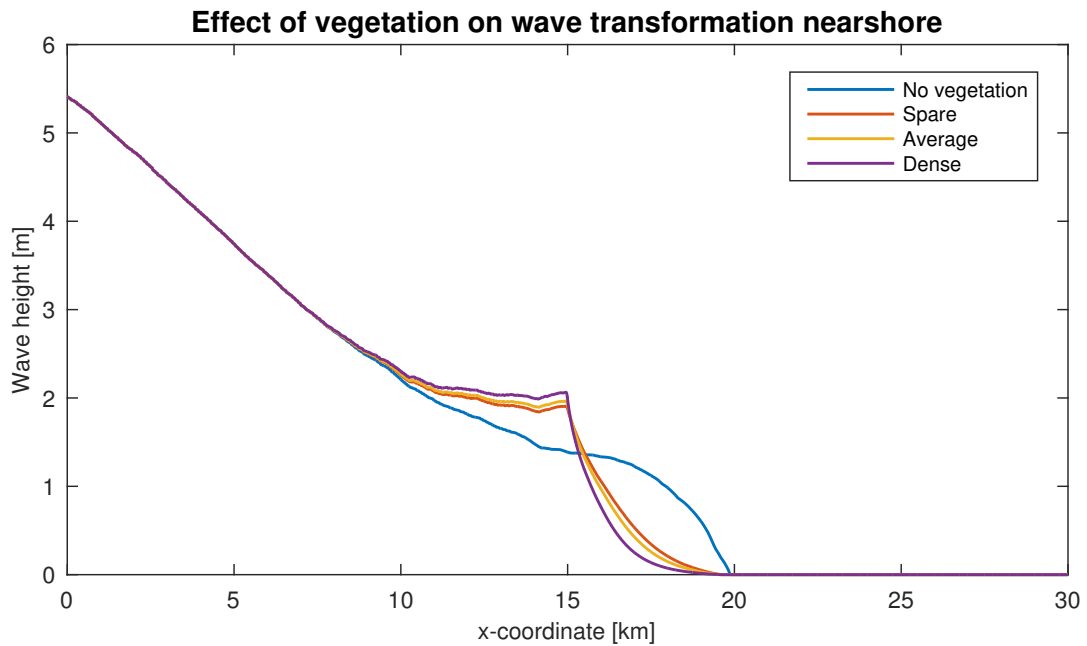


Figure 3.34: Wave transformation nearshore for different vegetation densities (no vegetation, spare density, average density, dense density) on a mild bottom slope (1:1500).

Compared to the previous example, the effect of vegetation is felt over a larger area, but still it is limited to the very nearshore. However, the effect of vegetation is now also clearly visible offshore of the mangrove forest. Compared to the situation without vegetation, the wave height is significantly larger in front of the forest, this indicates some wave reflection against the seaward border of the mangrove vegetation.

Inside the mangrove forest, the waves are strongly attenuated, and within a relatively short distance, the wave heights have become lower than in the case without vegetation. However, the difference between the three densities is almost negligible.

In the case without vegetation, the wave height curve does not show an exponential shape, but instead a logarithmic shape. This implies that the strongest wave height reduction takes place closer to the shoreline, contrary to the cases with vegetation, where the strongest wave height reduction takes place in the first part of the mangrove forest. This implies that, in the case without vegetation, it is wise to locate the dike further inland. However, the vegetation also shows that on these extremely mild slopes, reflection can be significant. This should be carefully investigated in the final design stages.

Although the strongest wave attenuation takes place in the first part of the mangrove forest, this does not mean that the sea dike can be located further seaward. Mangrove forests require a certain minimum width in order to survive (this is also known as mangrove squeeze, more information can be found in Phan Khanh Linh et al. (2015)). With a cost-benefit analysis, both options can be compared: sacrificing land for a healthy mangrove forest, versus sacrificing mangrove forest for more land behind the dike.

3.2.5. Conclusion

After a thorough analysis of the model results, it can be concluded that SWAN and SWASH perform in accordance with the expected behaviour, as determined in section 3.1. A range of situations has been modelled, with 3 different bathymetries, 4 different vegetation densities and 3 different lifetimes with each 4 different return periods. The effect of each of these parameters has been analysed, and the conclusions of these analyses are summarised here.

The Mekong Delta can be represented by three bathymetric profiles: a very mildly sloping foreshore (1:1500), a relatively steep foreshore (1:800) and a relatively steep foreshore with a mudflat of 2 km at 1 m below MSL. Offshore, waves are attenuated more on the mild foreshore than on the steeper profiles. This wave height reduction continues almost linearly until the shoreline is reached on the extremely gentle profile. On the steeper profiles, however, the waves are damped over a shorter distance, close to shore, until a wave height in the order of 2 m is reached. These waves then continue almost up to the shoreline, where they are finally damped over a short distance. On the steep profiles, significantly higher waves are measured close to the shoreline, which implies that coastal protection structures, such as dikes, are more heavily loaded. On mild slopes, these structures benefit from continuous energy dissipation over the entire foreshore. The effect of the mudflat on the wave height reduction is rather negligible.

The effect of lifetime and return period cannot be considered separately, as it is the combination that determines the probability of failure. The lifetime influences the water level through relative sea level rise, while the return period both influences the water level and the wave conditions offshore. Nearshore, the effect of heavier boundary conditions decreases with the distance to the shoreline, which implies that the further inland the coastal protection measure is located, the lower the additional costs are for longer lifetimes or higher return periods.

Finally, also the effect of the presence of vegetation and possible variations in vegetation density is analysed. The effect of vegetation is to reduce significantly the wave height inside the mangrove forest. However, on extremely mild slopes, mangrove forests can cause reflection, leading to a significantly increased wave height in front of the forest. The effect of density is relatively small, especially the difference between sparse and average density.

4

Discussion

The Mekong Delta is characterised by a large range of situations, and for each situation there are countless possible coastal protection strategies. In order to determine the optimal strategy for each situation, an evaluation framework is necessary. This framework was set up in section 2.6 and follows the principles of a cost-benefit analysis. All costs and benefits can be distributed over two categories: 'Construction and maintenance', for all costs and benefits related to the construction and maintenance of coastal protection measures, and 'Value of land', for all costs and benefits related to the value of land.

In the following sections, this cost-benefit analysis will be executed. In section 4.1 the individual components of the cost-benefit analysis will be investigated. After this, the CBA will be applied to the three different situations, based on the erosion rate: a stable coastline (no net erosion or accretion, section 4.2), accretion (section 4.3) and erosion (section 4.4).

4.1. Individual analysis components cost-benefit analysis

The individual costs and benefits were determined in section 2.6 and summarised in Table 2.5. However, so far it has all been hypothetical. In the following sections, these costs and benefits are applied to the Mekong Delta reality. First, each individual element of the two categories (see Figure 2.9, the first category contains construction and maintenance costs and the second all costs and benefits related to the value of land) will be analysed. Afterwards, this knowledge will be used to apply the cost-benefit analysis to each situation and scenario.

4.1.1. Construction and maintenance costs of sea dikes

The construction costs of a sea dike are a function of the size of the dike. Since a standard cross-section is used in this project, the size of the dike can be expressed through one single parameter: the dike height. The height of the dike depends on the hydraulic boundary conditions. In section C.1 these boundary conditions were translated into dike dimensions and the costs of the dike were expressed as function of the dike height.¹

Although the maintenance costs of sea dikes also depend on the size of the dike, in this project fixed yearly maintenance costs are assumed, independent of the dike dimensions. This assumption can be justified by the fact that a significant part of maintenance costs consists of monitoring and small repairs, which is the same for smaller and bigger dikes. It is only in the case of severe damage that the repair costs will be significantly higher for larger dikes. However, the objective of regular maintenance is exactly to prevent such severe damage to occur. Therefore, the budget for dike maintenance only depends on the lifetime of the dike.

In Figure 4.1 the construction costs of a sea dike, as function of the dike height, are visualised in the upper plot. A distinction is made between the construction costs of a dike with a revetment (standard design, full line) and without a revetment (optimised design behind mangroves, dashed line). The lower

¹In this project, the hydraulic boundary conditions only influence the dike design through the dike height. In reality, they also influence other aspects of the design, for example the design of the revetment to protect against wave attack. However, to simplify the cost-benefit analysis a standard design, containing a standard revetment, is used.

plot shows the maintenance costs, as function of the dike lifetime. All costs are expressed in million VND per meter dike length.

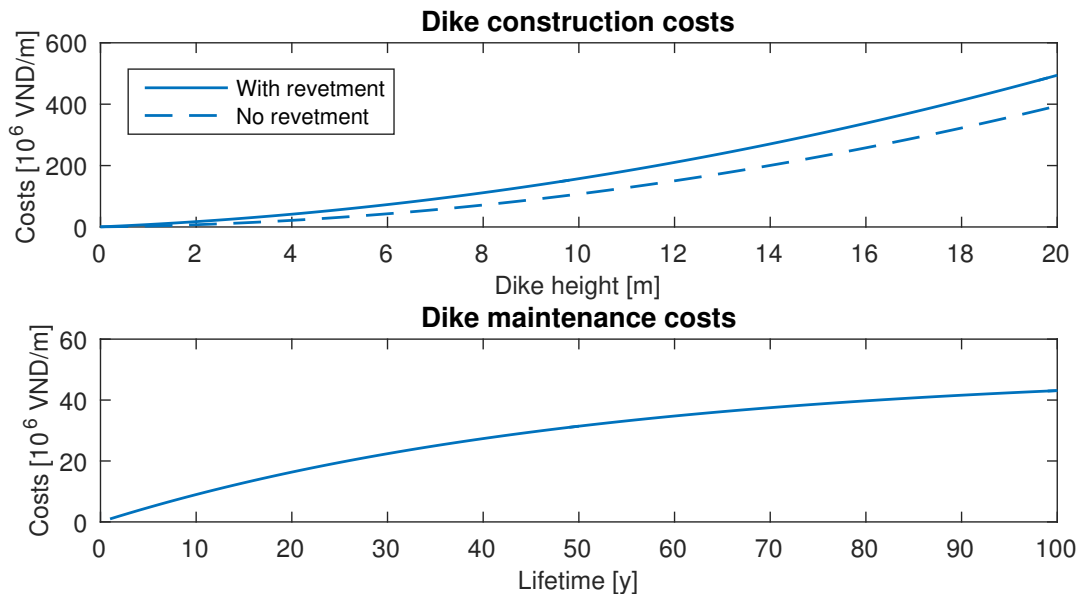


Figure 4.1: The upper plot shows the construction costs of a sea dike, as function of the dike height. The lower plot shows the maintenance costs of a sea dike, as function of the dike lifetime. All costs are expressed in million VND per meter dike length.

In the upper plot, the dashed line represents the construction costs without a revetment. Especially for low dikes, the revetment costs represent a significant part of the total costs. In scenarios where there is a sufficiently wide mangrove belt present in front of the dike, the construction costs can be reduced significantly. However, for this project it is assumed that if there are mangroves present in the scenario, these mangroves first have to be restored. Therefore, in the first phase of the lifetime, they cannot provide the required wave damping and a revetment is still necessary. In reality, however, optimisation is possible.

Note that the maintenance costs are expressed as present value (with Equation 2.4, for more information read subsection 2.6.1). The vertical axis of both plots shows that the present value of the maintenance costs is about ten times smaller than the construction costs.

4.1.2. Mangrove reforestation and maintenance costs

Mangroves can significantly contribute to coastal protection, through, amongst other effects, wave attenuation and erosion protection. Therefore, it is very useful to include mangrove forests in the coastal protection strategy. However, at many locations along the Mekong Delta coast (and other mangrove coasts over the entire world), mangrove forests are disappearing at alarming rates. Therefore, in many cases the mangrove forest first needs to be brought back to the system, before the coast can rely on its protection services. The costs of mangrove reforestation were estimated in section C.1 as $1.5 \cdot 10^3$ VND/m².

Since mangrove forests are in essence natural ecosystems, maintenance is only required during the first years of the mangrove reforestation project. After 10 years, it is assumed that the mangrove forest has build up enough resilience (provided the external boundary conditions allow this, so no squeeze or extreme erosion shortage for example). The present value of 10 years of mangrove maintenance is about $4 \cdot 10^3$ VND/m². In contrast to sea dikes, where the maintenance costs were 10 times smaller than the construction costs, the maintenance costs of mangrove reforestation are 2.5 times higher than the construction costs. This is caused by the fact that the monitoring and maintenance of mangrove reforestation projects is very labour-intensive.

These construction and maintenance costs represent a successful reforestation project. In practice, however, a significant part of these project fails. Although in some cases, the causes of failure are quite clear (wrong abiotic conditions, wrong type of vegetation planted, ...), there is still a lot to be understood in order to guarantee reforestation success. As a result of these failures, the eventual re-

forestation costs lie often higher. In this project, it is assumed that the reforestation is successful, and the costs mentioned above can be applied. However, if the reforestation fails, the additional costs for a new reforestation project are significantly lower than the additional costs for a dike without mangrove protection. Through monitoring, the success rate of the reforestation project can be kept track off and if necessary additional trees may be planted. Therefore, monitoring reforestation projects is crucial in order to limit additional costs.

4.1.3. Ecosystem services

Mangrove forests provide a wide range of (indirect) services, these are called ecosystem services. The exact value of those ecosystem services was defined in section C.1, based on literature. A healthy, densely vegetated mangrove forest provides $50 \cdot 10^3$ VND/m² per year (see Table 2.5). This proves that mangrove reforestation is an extremely profitable investment, as the total investment costs (including maintenance) are almost 10 times lower than the benefits gained from the mangroves.

However, it is difficult to really grab the value of these ecosystem services. Not only is it quite complex to quantify the value of the ecosystem services, it is also not a direct value that stakeholders can grab. Nevertheless, even if the real benefits appear to be lower than the value currently accepted, the difference between the costs and benefits is sufficiently large that the conclusion remains valid that mangrove reforestation is a wise investment. Furthermore, another ecosystem service of mangrove forests is to reduce wave energy, which directly leads to a reduction in the construction costs of sea dikes protected by mangroves.

4.1.4. Reduced flooding risk

The main purpose of a coastal protection system is to reduce the flooding risk. The flooding risk is defined as the probability of flooding times the consequence of flooding. The coastal protection system reduces the risk by lowering the probability of flooding. The consequence of flooding is the damage when flooding occurs. In this project, the flooding damage is defined through the parameter "Value of land" (see Table 2.5). The value of land in the Mekong Delta is $0.02 \cdot 10^6$ VND/m².

This is the value of one square meter of land, therefore, it is also required to determine the area that is protected by the sea dike. Since this project follows a generic approach, it is assumed that the land above the water line has a constant bottom slope of 1/1000, so the total protected area can be found by multiplying the storm surge water level with the bottom slope.

The reduced flooding risk can thus be found by multiplying the reduction in flooding probability with the value of land and the area of land protected by the coastal protection measure.

Note that the value of land is subject to change over time, especially in a rapidly developing region as the Mekong Delta, therefore, the reduced flooding risk may actually increase over time. For this project, however, all values are constant over time.

4.1.5. Costs of land loss

In Vietnam it is common practice to place the dike at the low water line, as this is the location furthest seaward where the dike can be easily constructed. From that point of view every dike location higher than the low water line abandons the land between the low water line and the dike location. To account for this viewpoint, this "lost land" is included as a cost element, by multiplying the "lost" area with the same value of land as mentioned in the previous section. By including this in the cost-benefit analysis, it can be investigated whether placing the dike at the low water line is the best choice, based on economic considerations.

4.1.6. Costs and benefits of land conversion

In the previous section, the land in front of the dike, between the toe and the low water line has been called "lost land", because, from the viewpoint of common Vietnamese practice, this land has been given back to the sea, instead of being protected by a dike. However, this does not mean it is completely lost. First of all, it serves an important coastal protection service, by reducing the wave height at the toe of the dike. As a consequence, the dike design becomes cheaper. Furthermore, this protection can even be increased by using this "lost land" (the part above MSL) for mangrove reforestation, and as such provide ecosystem services. For this, the costs of mangrove reforestation and maintenance have to be included, but as discussed above, these costs are significantly smaller than the benefits provided

by the mangrove forest.

These costs and benefits are included in the analysis, and may even outweigh the costs of “land loss” from the previous section.

4.1.7. Overview individual cost and benefit components

To place all components in perspective, Figure 4.2 gives, for some randomly chosen situation, the value of each of the components discussed above. For simplicity, the construction costs and maintenance costs have been combined per subject. The x-axis represents the location of the sea dike in the cross-section, the origin is located at the low water line, as this is the most seaward location a dike can be easily built. For each x-coordinate, all costs and benefits are calculated as if the dike were to be constructed at that location. The vertical axis shows the net benefits, so costs are negative and benefits are positive. In other words, the plot shows how the costs and benefits of the coastal protection vary with the location on the dike, as the location of the dike is represented by the horizontal axis and the costs and benefits by the vertical axis.

The only purpose of this plot is to give an idea of the order of magnitude of each component. Conclusions with respect to the choice of protection strategy will be discussed in the following sections.

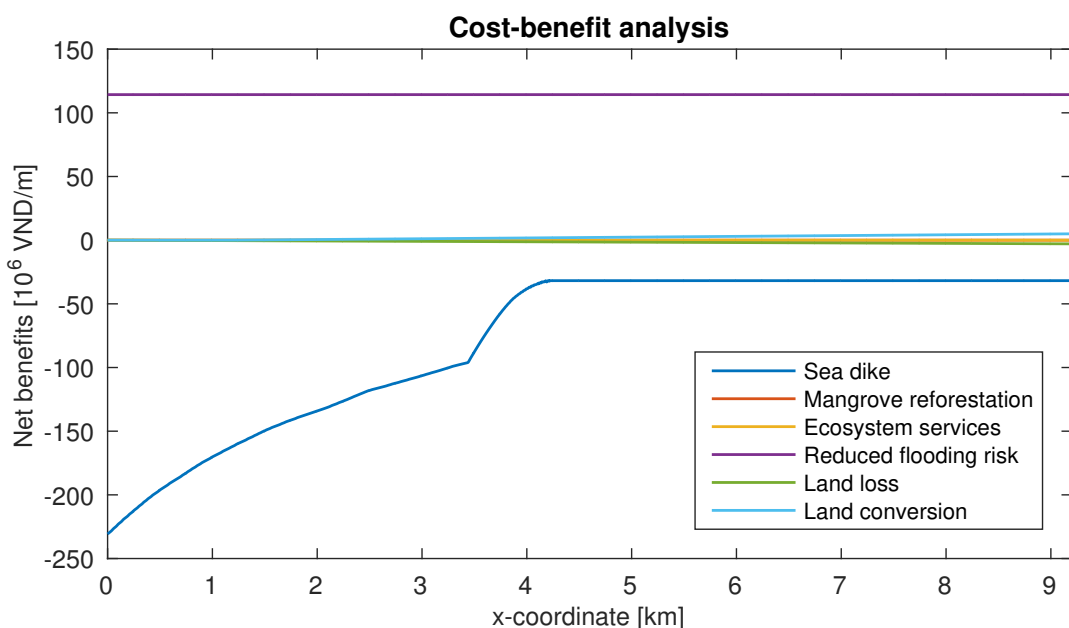


Figure 4.2: In this graph the individual components of the cost-benefit analysis of a random situation are given as function of the location of the dike.

It immediately strikes the eye that two components are dominant: the construction and maintenance costs of dikes, and the reduced flooding risk. As the other components are much smaller than these two dominant factors, their behaviour cannot be analysed based on this plot. Therefore, a second plot has been generated (see Figure 4.3), showing each individual component in a separate graph, with adapted scaling of the y-axis. The x-axis still represents the location of the dike and is the same for each graph in Figure 4.3.

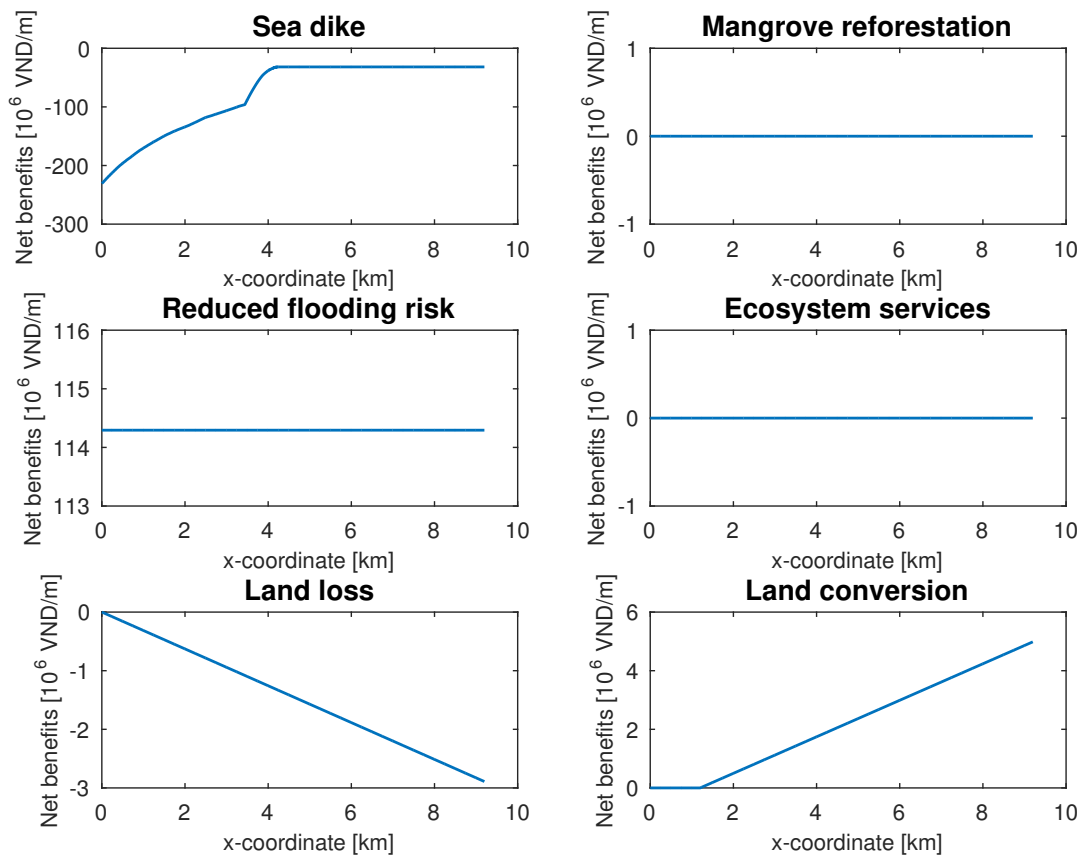


Figure 4.3: In these six plots the behaviour of each individual component of the cost-benefit analysis is visualised.

The costs of the sea dike reduce when the location of the dike is further inland (x-coordinate increases), because further inland the hydraulic boundary conditions become calmer and therefore the dike needs to be less strong and high.² On the other hand, the costs of mangrove reforestation increase as the dike is located further inland, because the area available for mangrove reforestation in front of the dike increases. It is for the same reason that the ecosystem services provide more benefit as the dike moves inland. The reduced flooding risk is independent of the dike location, because no matter where the dike is located, it should provide a certain level of safety. The costs related to land loss increase as the dike is placed above low water level, since the “lost land” is defined as the land between the low water line and the dike toe. In this specific situation, the costs and benefits of land conversion are zero. This is because the land in front of the dike is already a mangrove forest, so there are no additional costs for turning this area into mangroves, and the ecosystem services are already included in the plot above.³

²The construction costs include a revetment. Further inland, the wave attack is lower and eventually a revetment may become unnecessary. This additional cost reduction is not included in the calculation, but in practice this will result in a sudden step in construction costs (a reduction between 30% and 60%) and even lower costs further inland.

³If in the original situation there had been no mangrove forest, the ecosystem services component would have been zero, but the land conversion plot would have shown a net benefit, as it would have included both the costs for mangrove reforestation and maintenance, as the ecosystem services generated by this new mangrove forest.

4.2. Cost-benefit analysis for a stable coastline

Based on the erosion rate, three situations have been defined. In this section, the most straightforward situation from a coastal protection viewpoint will be discussed: a stable coastline. In the following two sections, the situation will be more complex by accounting for respectively accretion and erosion.

With the combined SWAN/SWASH model the hydraulic boundary conditions nearshore have been computed. This has been done for different foreshore geometries (different bathymetries, different vegetation densities). These conditions will now be used to determine the required dike dimensions at each location in the cross-section. With the cost-benefit analysis, the costs and benefits of each possible dike location will be compared, in order to determine the optimal coastal protection strategy. In the following sections, first the effect of each of the parameters defining the scenarios (bathymetry, lifetime, return period and vegetation) on the costs and benefits will be investigated. After that, the effect of allowing some overtopping will be analysed.

4.2.1. Effect of bathymetry on costs and benefits

Three bathymetric profiles have been defined to represent the Mekong Delta coasts. In subsection 3.2.2 the effect of bathymetry on the wave transformation was investigated. It was concluded that the effect of the bottom slope is most strongly felt nearshore. For milder slopes, the waves approaching the shoreline are not only lower, they also reduce gradually before reaching the shoreline, whereas on steeper slopes the wave height is significantly larger near the shoreline. The effect of the mudflat appeared to be negligible.

In Figure 4.4, the cost-benefit analysis is visualised for the three bathymetric profiles. The hydraulic boundary conditions applied to this example correspond to a lifetime of 20 years and a return period equal to the lifetime. However, the conclusions drawn from this example are also valid for all other combinations of lifetime and return period under consideration in this project.

All costs and benefits have been divided over two categories: all costs and benefits related to the construction and maintenance of the protection measures, and all costs and benefits related to the value of land. In Figure 4.4, these categories are represented by respectively the orange and yellow lines. Combining both categories gives the net costs, this is visualised by the blue line. Like in the previous section, the x-coordinate represents the location of the dike in the cross-section. Therefore, the net benefits at a certain x-coordinate represent the net benefits related to a dike located at that precise x-coordinate. For all three bathymetries, the origin of the x-axis is located at the low water line. The vertical axis represents the net benefits, so a negative value implies costs and a positive value benefits.

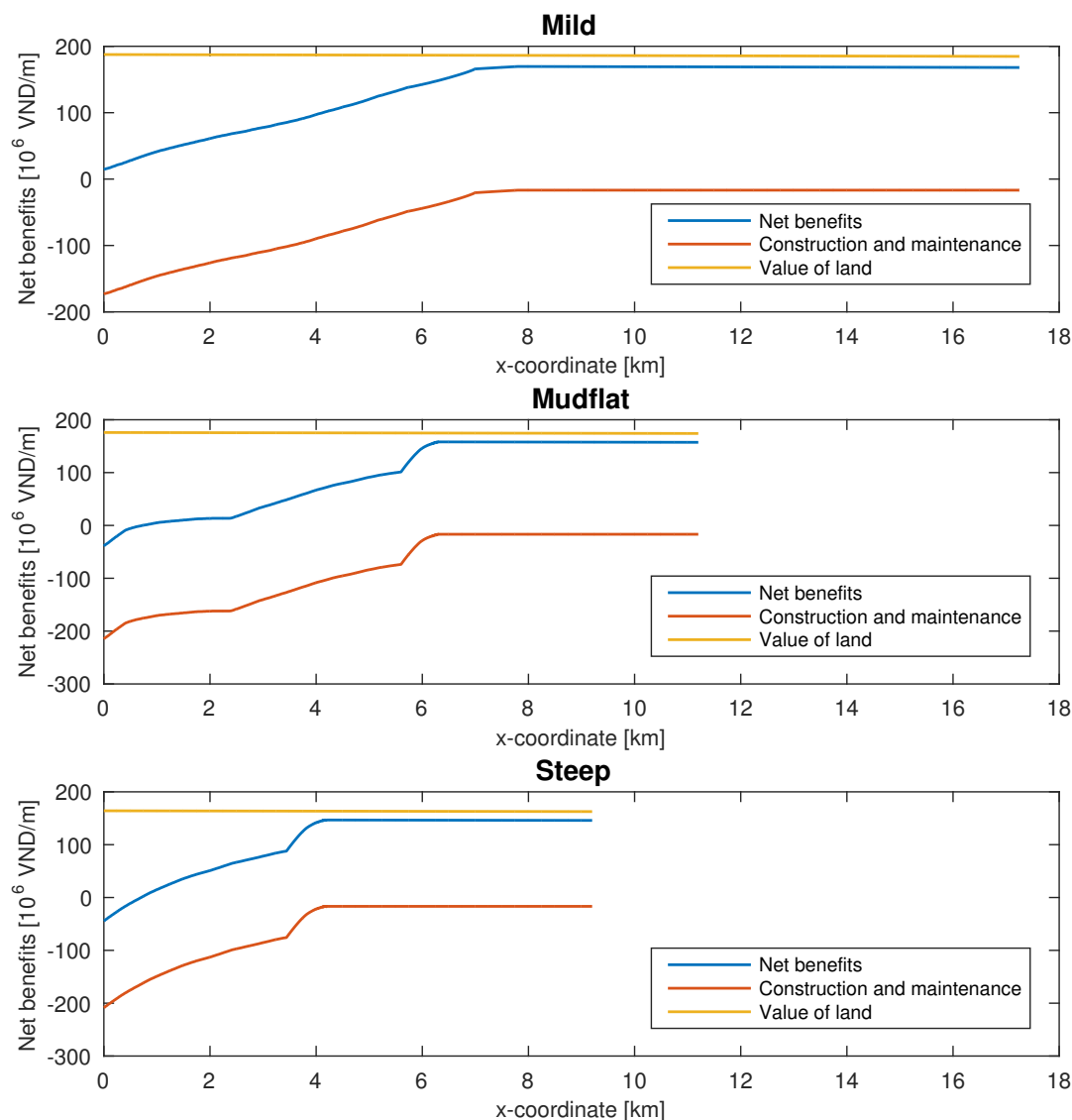


Figure 4.4: Costs and benefits of coastal protection, as function of the location of the dike in the cross-section, for different bathymetries, from top to bottom: a constant mild slope (1:1500), a steeper slope (1:800) with a mudflat and a constant steeper slope (1:800). The boundary conditions correspond to a lifetime of 20 years and a return period equal to the lifetime. The horizontal axis, with its origin at the low water line, shows the location of the dike in the cross-section, and the vertical axis gives the net benefits for each dike location.

In subsection 3.2.2 it was concluded that the waves nearshore are lower on a milder bottom slope. This is reflected in Figure 4.4, as the costs of construction and maintenance are lower in the upper plot corresponding to the mild bathymetry. Although the effect of the mudflat on the hydraulic conditions was not very clear in subsection 3.2.2, the effect becomes more visible when looking at the construction costs. The mudflat appears to lower the costs, but not significantly. Finally, on the steepest foreshore, the costs reduce relatively fast, however, compared to the mild bathymetry, the costs remain higher. The effect of bathymetry on the cost and benefit category related to the value of land is smaller than on the first category. However, the benefits are slightly higher for the mildest bottom slope. Also the presence of a mudflat creates some more benefits, compared to the steep profile without mudflats. This small difference is caused by the difference in storm surge level. Although the offshore boundary conditions are the same, the nearshore design water level is a function of the bathymetry through the wind set-up. Therefore, a milder bottom slope causes a higher water level. The damage in case of flooding would be higher, as this is a function of the flooding water level. Therefore, the reduced flooding risk, the dominant benefit in this cost-benefit analysis, is higher for milder bottom slopes.

One of the objectives of this thesis is to assess the effect of the foreshore geometry on the wave load and overtopping of the dike. With this knowledge, the design load on the dike can be influenced through nourishing the foreshore. This cost-benefit analysis shows that nourishing the foreshore is beneficial for the wave load, as it dampens more wave energy, but it will also lead to higher storm surges, thus requiring a higher dike.

4.2.2. Effect of lifetime on costs and benefits

The effect of lifetime and return period on the hydraulic boundary conditions is difficult to separate, as together they determine the flooding probability, and the return period is expressed in terms of the lifetime. However, the purpose of this thesis is to help make decisions on appropriate lifetime and return period. Therefore, the two aspects are analysed separately based on costs and benefits.

In Figure 4.5 the three lifetimes (20 years, 50 years and 100 years) are compared for the same set of boundary conditions. The return period of the hydraulic boundary conditions is chosen to be equal to the lifetime for each of the three lifetimes, while the bathymetric profile is the steep profile without mudflats. The x-coordinate is again the location of the dike in the cross-section and the vertical axis shows the net benefits.

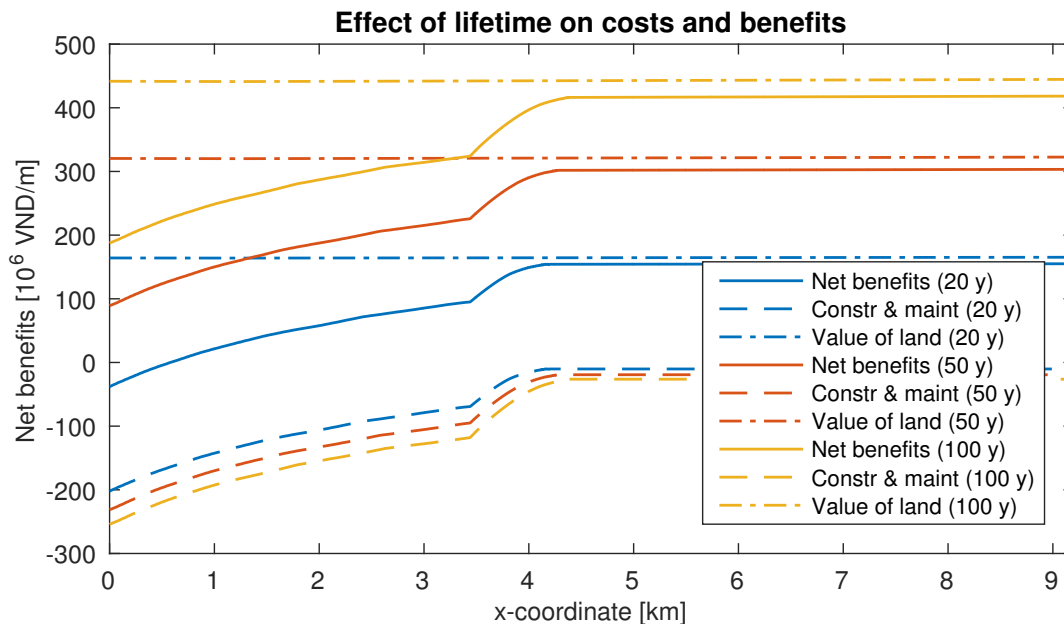


Figure 4.5: Costs and benefits of coastal protection, as function of the location of the dike in the cross-section, for different lifetimes (20, 50 and 100 years, respectively blue, orange and yellow). The return period of the boundary conditions is equal to the respective lifetimes. The bathymetry is the steep profile with a bottom slope of 1:800. The construction and maintenance costs are represented by the dashed line, the costs and benefits related to the value of land are represented by a dashed-dotted line and the net costs are represented by a full line. The horizontal axis, with its origin at the low water line, shows the location of the dike in the cross-section, and the vertical axis gives the net benefits for each dike location.

A longer lifetime corresponds to higher construction and maintenance costs (represented by the dashed line). The higher construction costs are caused by the longer return period of the hydraulic boundary conditions, as the return period is set equal to the lifetime in order to guarantee the same level of safety. The maintenance costs of the dike, however, only depend on the lifetime. Longer lifetimes therefore imply higher maintenance costs. However, the total increase in construction and maintenance costs is relatively small.

On the other hand, longer lifetimes result in significantly higher benefits. This is mainly caused by the fact that the reduced flooding risk can be guaranteed for a much longer time.

It can be concluded that designing a dike for a longer lifetime requires only a small additional investment, but the total benefits are significantly higher.

4.2.3. Effect of return period on costs and benefits

The same analysis as in the previous section is executed, this time regarding the effect of the return period. In this project, for each lifetime, four return periods are defined: half the lifetime, equal to the lifetime, twice the lifetime and five times the lifetime. By defining the return period as function of the lifetime, the same flooding probability is valid for different lifetimes, therefore allowing comparison between the different lifetimes.

For the analysis of the effect of the return period, a lifetime of 50 years is chosen. The bathymetry, as for the previous section, is the steep bathymetry (bottom slope 1:800). In Figure 4.6 the costs and benefits are again divided into two categories: construction and maintenance costs (represented by the dashed line in the graph) and all costs and benefits related to the value of land (represented by the dashed-dotted line in the graph). The net costs are represented by the full line. The different colours represent the different return periods: blue for a return period of 25 years (half the lifetime of 50 years), orange for a return period of 50 years (equal to the lifetime), yellow for a return period of 100 years (twice the lifetime) and purple represents a return period of 250 years (five times the lifetime). The x-coordinate represents the location of the dike in the cross-section, while the vertical axis gives the net benefits.

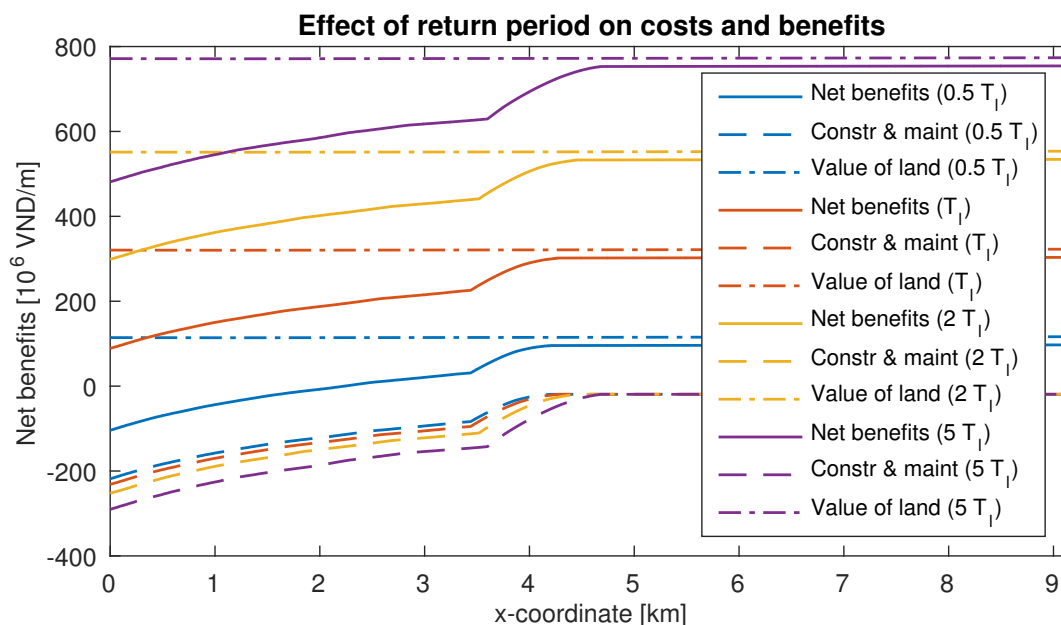


Figure 4.6: Costs and benefits of coastal protection, as function of the location of the dike in the cross-section, for different return periods (25, 50, 100 and 250 years). The lifetime is 50 years and the bathymetry is the steep profile with a bottom slope of 1:800. The construction and maintenance costs are represented by the dashed line, the costs and benefits related to the value of land are represented by a dashed-dotted line and the net costs are represented by a full line. The horizontal axis, with its origin at the low water line, shows the location of the dike in the cross-section, and the vertical axis gives the net benefits for each dike location.

Similarly to the effect of the lifetime, the effect of the return period on the construction and maintenance costs is relatively small. The increase is caused by higher construction costs, due to higher wave load and water level. The maintenance costs are the same for the different return period. Especially for the shortest return periods, the additional costs for longer return periods are very small.

The benefits related to the value of land increase significantly with longer return periods. This can be explained by the fact that longer return periods result in a stronger reduced flooding risk.

Again it can be concluded that the additional investment for higher return periods is significantly smaller than the increased benefits of the coastal protection strategy. From a cost-benefit point of view, it is wise to choose a relatively long return period.

4.2.4. Effect of vegetation on costs and benefits

So far, vegetation has not been included in the cost-benefit analysis. In section 4.1 the individual components of the cost-benefit analysis have been discussed. It was concluded that the costs of mangrove reforestation and maintenance are negligible compared to the construction and maintenance of dikes, and that the ecosystem services provided by the restored mangrove forest are even four times higher than the investment required for reforestation.

Besides the ecosystem services component, mangroves also influence another important cost component: the construction and maintenance costs of sea dikes, through attenuating wave energy. This is actually the most significant effect on the cost-benefit analysis, and in contrast to the ecosystem services, this reduction in construction costs is directly felt by the investors.

The overall effect of vegetation on the costs and benefits is visualised in Figure 4.7. The boundary conditions correspond to a lifetime of 50 years and a return period equal to the lifetime. The bottom slope is steep (1:800), without mudflat. The different colours represent the different vegetation densities: blue is no vegetation, orange for spare density, yellow for average density and purple for dense density (see subsection 2.4.5 for the exact definition of the vegetation densities). While the horizontal axis still represents the location of the dike, the origin has now been placed at MSL instead of the low water line, as mangrove vegetation only occurs shoreward of MSL. The vertical axis still represents the net benefits.

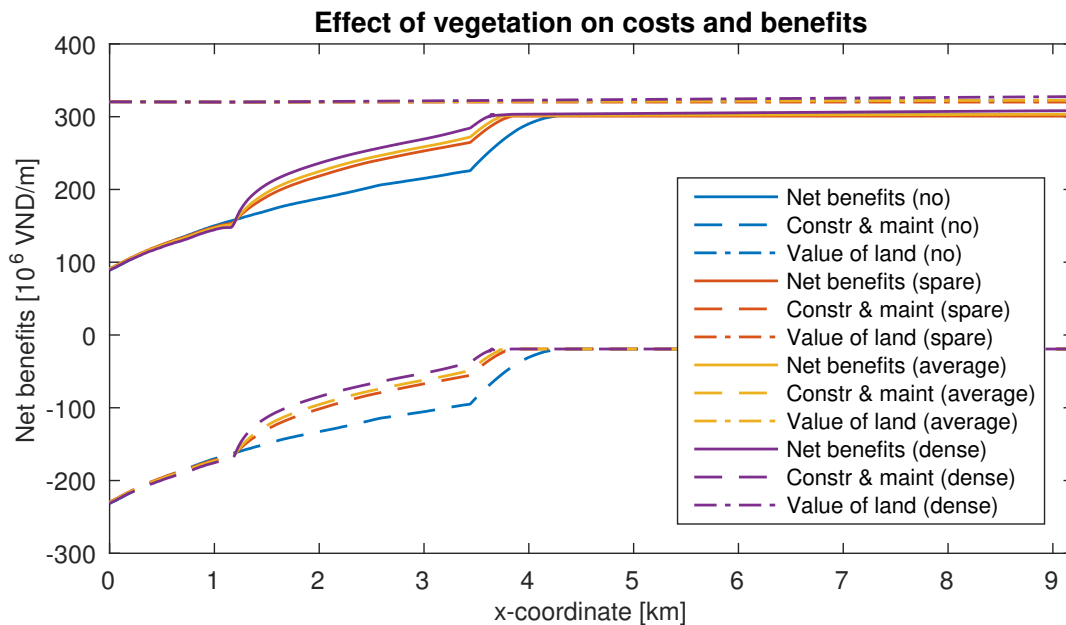


Figure 4.7: Costs and benefits of coastal protection, as function of the location of the dike in the cross-section, for different vegetation densities (no vegetation, spare, average and dense). The lifetime and return period are 50 years and the bottom slope is steep (1:800). The construction and maintenance costs are represented by the dashed line, the costs and benefits related to the value of land are represented by a dashed-dotted line and the net costs are represented by a full line. The horizontal axis, with its origin at MSL, shows the location of the dike in the cross-section, and the vertical axis gives the net benefits for each dike location.

As discussed in subsection 3.2.1, the effect of vegetation is concentrated nearshore. The construction and maintenance costs are lower inside the mangrove forest, as the mangrove trees attenuate wave energy. However, the benefits provided by the mangrove forest (the ecosystem services) are negligible compared to the benefit of reduced flooding risk. Only for extremely wide mangrove forests, the dashed lines of the category value of land no longer coincide.

Note that the reduction in costs can be even higher in reality, because the mangrove forest, if sufficiently wide, can render a revetment unnecessary, and as discussed in appendix C.1.2, revetments make up 20% to 60% of the total dike construction costs. In Figure 4.7 this would result in a stepwise reduction in construction and maintenance costs, as well as a stepwise increase in net benefits.

It can be concluded that the main effect of vegetation on the costs and benefits of a coastal protection strategy is through attenuating wave energy inside the forest. The indirect benefits through ecosystem

services are negligibly small compared to the reduced flooding risk. Nevertheless, these benefits are still larger than the investment required for mangrove reforestation, so the combined direct and indirect benefits of mangrove reforestation prove the value of this measure.

4.2.5. Effect of allowable overtopping on costs and benefits

So far, no overtopping has been allowed⁴. However, as discussed in section C.1, this imposes rather strict requirements on the dike design. By allowing some overtopping, the dike can be lower, resulting in a significant cost reduction. Whether some overtopping can be allowed, depends on the land use behind the dike. By adapting the land use and opting for an activity that can withstand some salinity from time to time (for example aquaculture), an overtopping discharge of $q = 1$ l/s/m (orange line) can be allowed. The effect on the cost-benefit analysis of this smart land use is investigated below.

In Figure 4.8 the construction costs have been visualised for a case without overtopping (blue line) and a case with an overtopping discharge of $q = 1$ l/m/s. The lifetime and return period are 50 years, the bathymetry is the mildest profile (bottom slope 1:1500). The horizontal axis shows the location of the dike, its origin is again located at the low water line.

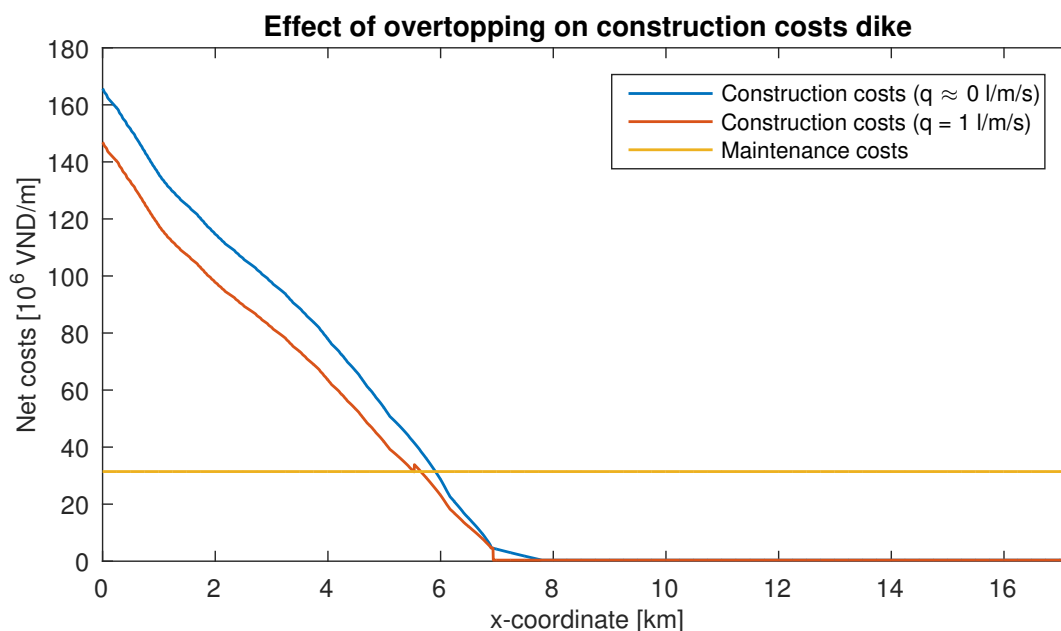


Figure 4.8: Construction costs of a sea dike without overtopping (blue line) and with some overtopping (orange line). Also the maintenance costs are given (yellow line). The lifetime and return period are 50 years, the bottom slope is 1:1500. The horizontal axis, with its origin at the low water line, shows the location of the dike in the cross-section, and the vertical axis gives the net benefits for each dike location.

From this figure it is clear that allowing some overtopping gives a significant reduction in construction costs. For all situations in this project, the possible cost reduction varies between 5% and 15%. Furthermore, for a small overtopping discharge, such as $q = 1$ l/m/s, no additional investments, such as inner slope protection for example, are required. Therefore, smart land use behind the dike can save money.

4.2.6. Designing for cyclones

When setting up the boundary conditions, it has been decided to leave cyclones out (see subsection 2.4.6). This was mainly due to a lack of available information on cyclones in the Mekong Delta, but also because it was expected that designing for cyclones would become too expensive. However, there has been one cyclone, Linda in 1997, that has been well documented. A cyclone with the strength of Linda has a return period of 50 years, and the hydraulic conditions occurring during the cyclone correspond to “normal” boundary conditions with a return period of 200 years. Therefore, it is interesting

⁴An overtopping of $q = 0$ l/m/s cannot be guaranteed, in the same way that a failure probability of 0% cannot be guaranteed. No overtopping therefore means $q \approx 0$ l/m/s

to compare those two scenarios.

In Figure 4.9, the construction costs have been calculated for two cases. In the first case, the boundary conditions have a return period of 50 years, in the second case they have a return period of 200 years. The second case therefore corresponds to the boundary conditions of a cyclone with a return period of 50 years. The lifetime of the construction is 100 years, and the bottom slope is 1:800. No vegetation is included. The horizontal axis shows the position of the dike, with the origin at the low water line.

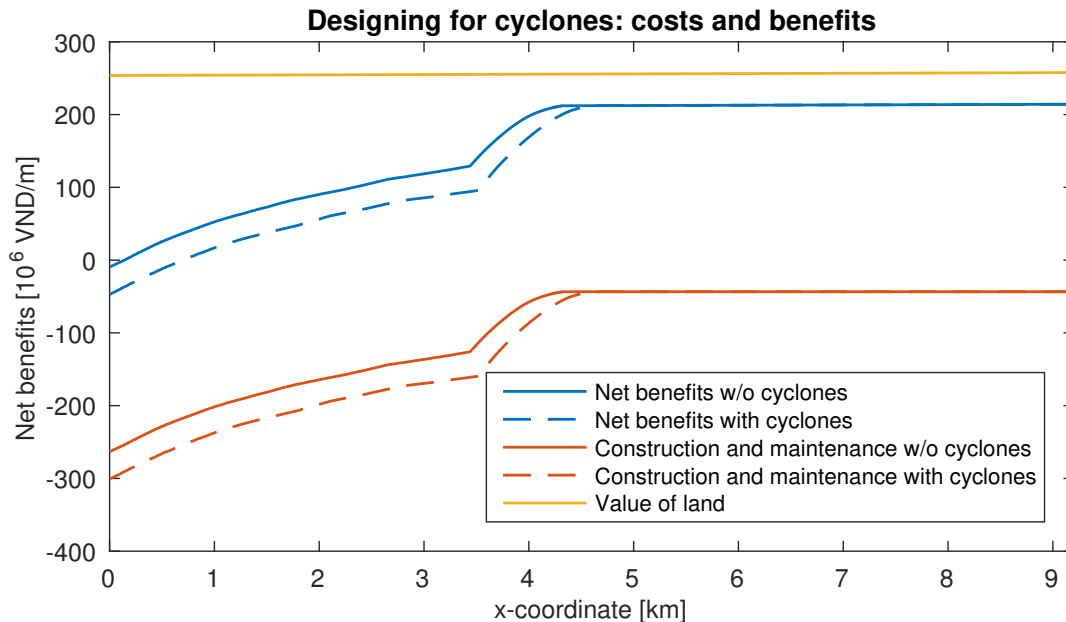


Figure 4.9: Costs and benefits of designing with and without cyclones (respectively the dashed and full lines). The lifetime is 100 years and the bottom slope 1:800. The horizontal axis, with its origin at the low water line, shows the location of the dike in the cross-section, and the vertical axis gives the net benefits for each dike location.

The additional investment for including cyclones in the boundary conditions is about 50 million VND/m. This is a significant investment, and can only be justified if the value of the land behind the dike is high enough (for example in the case of a city). Nevertheless, the cost-benefit analysis shows that even for lower values, it can be beneficial, if the dike is placed far enough inland.

4.2.7. Conclusion

A milder bottom slope reduces the net costs by attenuating wave energy, thus lowering the hydraulic conditions at the toe of the dike, which leads to lower construction costs, but also by increasing the reduced flooding risk, which leads to higher benefits.

The analyses of the effects of lifetime and return period have both revealed that for a higher lifetime or return period the additional investments are minor compared to the additional benefits. Therefore, from a cost-benefit point of view, in the case of a stable coastline, it is always wise to design for longer lifetimes and return periods.

The effect of vegetation is only minor, mostly by attenuating wave energy inside the forest, which lowers the hydraulic conditions at the toe of the dike. However, the costs for mangrove reforestation and maintenance are four times smaller than the ecosystem services provided by the mangrove forest, so if it is possible to reforestate, it should always be done.

Finally, it was discovered that by allowing a limited overtopping discharge, which does not require additional protection of the dike, 5% to 15% of the construction costs of the dike can be saved. Wise land use, which can survive some salinity from time to time, can therefore lead to a significant cost reduction.

4.3. Cost-benefit analysis in case of accretion

An accreting coastline is a very favourable situation for coastal protection. The ever growing foreshore will provide increasing protection. From a technical point of view, the protection strategies for a stable coastline can simply be applied to accreting coastlines. However, from a cost-benefit point of view, optimisations are possible. As the foreshore will provide increasing protection over time, the coastal protection system will become overdimensioned. Therefore, two approaches to this situation will be investigated and compared. In the first approach, a short lifetime is chosen, and after the lifetime has passed the whole system is redesigned, leading to a new dike more seaward (subsection 4.3.1). In the second approach (subsection 4.3.2), the dike remains at the first location, and the foreshore is put to use (for example through extensive aquaculture).

4.3.1. Redesign after short lifetime

For a stable coastline, it was concluded that it is almost always more beneficial to design a dike with a longer lifetime. However, in the situation of an accreting coastline, this may lead to a seriously overdimensioned dike. Therefore, it is investigated whether it would be cheaper to design a dike for a short lifetime, and design a new dike after the lifetime, which can be placed further seaward as the coastline accretes. The advantage of such an approach is that the investments are spread over time, and that more land becomes available inside the dike. Material from the previous dike can be recycled, thus further reducing the construction costs of the later dikes.

4.3.2. Alternative use foreshore

In a natural environment, the accreting foreshore will be colonised by mangrove trees. As the forest becomes wider, it may become possible to use (part of) the foreshore for new activities. An example of an activity that is possible on the foreshore is aquaculture. However, the mangrove forest should remain strong enough, so only extensive aquaculture should be allowed (see subsection 2.2.5). In such a case, the value of the foreshore can be increased with around $10 \cdot 10^3$ VND/m²/y (50% of the income from intensive aquaculture).

4.3.3. Comparison

The two approaches will be compared using an example. For the example, a coastal protection strategy with a lifetime of 100 years needs to be designed. The boundary conditions have a return period of 100 years as well. The bathymetry is the mild profile with a bottom slope of 1:1500. In the first approach, a dike is designed with a lifetime of 20 years, and every 20 years a new dike is designed. In the second approach, a dike with a lifetime of 100 years is designed. Throughout its lifetime, more and more foreshore becomes available for alternative use, in this case extensive aquaculture. It is estimated that extensive aquaculture can produce an income of $10 \cdot 10^3$ VND/m²/y, this is half the income produced inside the protection of the dike.

In Figure 4.10, the construction and maintenance costs of both dike designs is given. The costs of a dike with a lifetime of 20 years are visualised by the full line, while the costs of a dike with a lifetime of 100 years are represented by the dashed line. The x-coordinate represents the location of the dike in the cross-section, the origin located at the low water line.

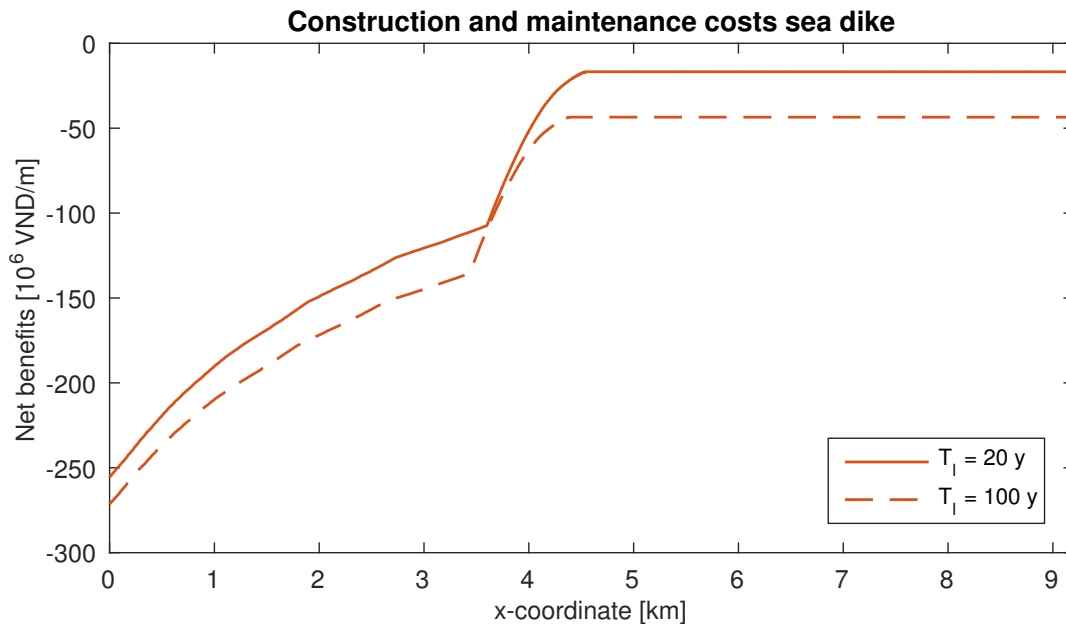


Figure 4.10: Comparison between the costs and benefits of a dike with a lifetime of 20 years and a dike with a lifetime of 100 years. The return period of the boundary conditions is in both cases 100 years. The horizontal axis, with its origin at the low water line, shows the location of the dike in the cross-section, and the vertical axis gives the net benefits for each dike location.

This graph shows that the construction and maintenance costs of both dikes are almost equal, the dike with a shorter lifetime is only a little bit cheaper, but these costs only cover the first 20 years. Therefore, it can immediately be concluded that it is cheaper to construct a dike with a long lifetime, instead of constructing five times a dike with a short lifetime. The fact that the difference is so small, indicates that a significant part of the costs consists of “initial costs”, costs that are required for any dike, independent of dike height or lifetime. Even when part of the material can be recycled for the later dikes, the total costs for building five times a dike with a lifetime of 20 years would still be significantly higher than constructing one dike with a lifetime of 100 years. Further calculations of possible use of the foreshore and behind the dike are not even necessary.

The exact location of the dike depends on the amount of land that definitely needs to be protected by a dike. Further seaward requires a higher investment, but more land behind the dike. Further shoreward requires lower investments, and results in a wider foreshore that will become available over time for alternative activities, such as extensive aquaculture.

4.3.4. Conclusion

It can be concluded that in the case of accretion, it is better to design a dike with a long lifetime, and invest in possible activities on the foreshore. The additional costs of building a dike with a longer lifetime are only minor, compared to the total investment required to construct and maintain a dike, due to the relatively small maintenance costs. Moreover, the land that can be gained every time the dike is placed further seaward, is only limited. If a coastline accretes 20 m/y, this would mean that after 20 years the dike can be placed 400 m further seaward, which is not enough to justify such a large investment. However, the foreshore will grow over time, and to prevent abuse of the mangrove forest, extensive aquaculture should be strictly organised and monitored, in order to optimise the sustainable use of the foreshore.

Finally, there is also another reason why it is better not to follow the accreting coastline by displacing the dike regularly. Coastlines generally show a very dynamic behaviour. Periods of accretion are followed by periods of erosion. By following the accreting movement, the following erosion motion is blocked, leading to erosion problems, either in the project area, or downstream.

4.4. Cost-benefit analysis in case of erosion

If a coastline is eroding, the coastal protection system will become more and more exposed over time. This may lead to reduced protection and even complete failure. Therefore, when designing a coastal protection system for an eroding coastline, this erosion has to be accounted for.

In subsection 2.3.3, four possible strategies have been identified for eroding coastlines (see also Figure 2.5). The first strategy tries to stop or slow down the erosion by using the strength of mangrove forests. In the second strategy, the erosion is accepted and the dike is placed more inland, this is called managed retreat. The last two strategies have been imagined with extreme erosion rates in mind. The third strategy applies so-called soft solutions, for example nourishments, while the fourth strategy follows the hard strategy, designing a construction that can withstand the extreme erosion and wave loads.

The four strategies will be compared for an extreme erosion rate of 60 m/y. Although this seems exaggerated, subsection 2.2.4 shows that these rates are actually observed along the east coast of the Mekong Delta. In this example, a lifetime of 50 years and a return period of 100 years are applied to a bottom slope of 1:800.

4.4.1. Mangrove reforestation

Mangrove forests can slow down erosion because the roots of the mangrove trees hold the sediment together. However, if the erosion rates are too high, the mangrove trees will lose the sediment and eventually perish. The chosen erosion rate in this example, 60 m/y, is definitely too high for mangroves to survive. Therefore, this strategy is impossible.

4.4.2. Managed retreat

In the case of managed retreat, the entire system is located further inland, such that the foreshore can erode, without the dike becoming exposed. In this case, the dike would have to be located 3 km inland (erosion rate multiplied by lifetime), compared to the same situation on a stable coastline.

This means that 3 km of foreshore is sacrificed to the sea, and the value of this land has to be included as a cost in the CBA. However, the foreshore will erode gradually, and especially in the beginning of the lifetime, it can still be used extensively, or provide ecosystem services. In such a way, the value of the land that is not protected by the dike and is therefore considered "lost land", can be earned back through alternative use and ecosystem services.

Therefore, if it is possible to retreat, this is most probably the optimal solution. However, in many cases that will not be possible, due to land use. In those cases, only the last two strategies remain.

4.4.3. Soft solution

Erosion occurs when there is a shortage in the sediment budget. Introducing more sediment in the system can mitigate the effects of the erosion. Therefore, it can be combined with a simple coastal protection system. Nevertheless, the nourishment should be repeated at regular intervals, to keep the sediment budget in balance. In this project the nourishment interval will be 5 years.

In this case, the foreshore erodes by 60 m/y. For this quick calculation, the foreshore is considered up to a depth of 10 m. This means that yearly, 600 m³ sediment per meter coastline erodes. Over 5 years, this gives a volume of 3000 m³/m. However, the nourished volume needs to be larger, in order to guarantee that the required volume ends up on the foreshore. In this case, twice the required volume will be nourished. This will cost $1.2 \cdot 10^9$ VND/m every five years. The present value of the nourishments costs over a lifetime of 50 years is $5.7 \cdot 10^9$ VND/m. Note that these costs are an order of magnitude higher than the costs for a simple sea dike on a stable coastline with the same boundary conditions. However, nourishment alone is not a coastal protection strategy, it still requires sea dikes. Therefore, the costs have to be added to the costs of the stable coastline situation.

So the costs are ten times larger than for a stable coastline, but the benefits remain the same. Protecting a severely eroding coastline by fixing the coastline with nourishments is therefore only beneficial if the value of the land behind the dike is sufficiently high. It is expected that this strategy is not yet viable in the Mekong Delta, because of the current land use.

4.4.4. Hard solution

The idea of this strategy is to construct a dike or breakwater that can withstand all erosion and increased wave load. In theory, an erosion rate of 60 m/y corresponds to a lowering of the bottom level of 7.5 cm. Although this does not seem much, over a lifetime of 50 years this already adds up to almost 4 m. Moreover, as higher waves reach the toe of the construction, a scour hole will be created due to reflection. As such, the depth in front of the structure can easily increase by more than 10 meters. This means that the foundation of the structure has to go even deeper, and scour protection has to be added. Furthermore, the outer slope of the dike has to be well protected by a revetment to withstand the increased wave load. All these measures are rather expensive, leading to high costs which can be in the range 5 to 10 times the costs of a normal dike. However, not only the construction costs are significantly higher, also the maintenance will be more expensive.

Compared to the soft solution strategy, this quick estimate indicates that for now, the hard solution may be less expensive. However, this has to be investigated in detail for each specific situation.

4.4.5. Conclusion

It can be concluded that the first two strategies (mangrove reforestation and managed retreat), or a combination of both, have significantly lower costs than the last two strategies. However, the last two strategies are possible for any erosion rate, while the first two are limited by the erosion rate.

Mangrove forests can only slow down a limited erosion rate, if the erosion continues, or if the erosion rate is too high, the mangrove forests will collapse. Managed retreat is in theory possible for any erosion rate, but there are often practical limits imposed by the current land use. It is also an unpopular strategy, if stakeholders are forced to sacrifice land. Nevertheless, the costs can be kept low.

It is difficult to estimate the costs of the last two strategies, but quick estimates indicate that they often are an order of a magnitude higher than the costs of the first two strategies. The benefits, dominated by the reduced flooding risk, are more or less constant over the four strategies. This implies that the higher costs can only be justified if the benefits also increase, which is the case if the value of the land increases. At the moment, the value of the land in the Mekong Delta is still relatively low, however, the Delta is developing rapidly, and these developments may justify higher investments. Therefore, it is recommended in case of high erosion rates in combination with rapidly developing hinterland, to design for shorter lifetimes with the first two strategies. After this lifetime, maybe the latter two strategies may have become more favourable.

5

Conclusions and recommendations

The Mekong Delta has proved to be an extremely interesting research area, full of variation, but with serious coastal protection problems. The Delta, which had been prograding over the last millennia, now suffers from coastal erosion along almost the entire coastline. Wide mangrove belts, which used to protect the coasts in a natural manner, are disappearing at alarming rates, but at the moment the awareness of their ecosystem services is growing. Although the research has focused on the Mekong Delta, it has been set up in such a general manner that the conclusions can be applied to mangrove coasts all over the world experiencing the same issues of coastal erosion and mangrove squeeze.

5.1. Conclusions

To conclude this project, it is wise to go back to the start, the goals. These are summarised in the title of this thesis: wave load and overtopping of sea dikes, as function of their location in the cross-section, for different foreshore geometries. In other words, the goal was to determine where the dike should be located in the cross-section and what the effect of the foreshore geometry is on the wave load.

The key parameter in this has proved to be the erosion parameter, identifying three crucially different situations: a stable coastline, an accreting coastline and an eroding coastline. For each of the three key situations, several protection strategies have been identified. These have been numerically modelled and the costs and benefits have been analysed in order to determine the optimal strategy for each situation.

Although the end users of the decision support tool are most interested in the optimal protection strategy, during this project also some other extremely interesting discoveries have been made. Therefore, first the conclusions on the performance and validity of the numerical model are presented. After this, the conclusions on the optimal protection strategy for each of the three key situations are summarised.

5.1.1. Numerical modelling of gently sloping mangrove coasts

Due to the complete lack of measurements and data, the numerical SWAN-SWASH model had to be analysed based on theory. Although the models perform well for simple cases, such as linear wave conditions or simple irregular wave conditions, their behaviour changes significantly if the design conditions for the Mekong Delta are modelled.

One of the causes of this divergent behaviour is the bottom slope. The bottom slopes of the Mekong Delta are so gentle (in the order of 1:1000), that they may lie outside the scope of both SWAN and SWASH. These models were not developed with this kind of slopes in mind, and have never been validated for these slopes. However, a distinction must be made between SWAN and SWASH, as SWAN uses parameterisation, which is valid only for a certain range, whereas SWASH solves the momentum and mass balance. Therefore, the application of SWAN to these gentle slopes may be incorrect, but there is no reason why SWASH should be wrong. Nevertheless, both models require measurements and laboratory tests for validation.

In order to understand all processes involved in wave transformation, the individual source terms of the energy balance have been investigated in SWAN. It was discovered that the quadruplet wave-wave interactions dominate all other source terms, whereas they should only be transferring a relatively

small amount of energy over the spectrum. All other source terms act exactly according to theory. Therefore, it has been decided to exclude the quadruplet wave-wave interactions for this research. Due to excluding the quadruplets, there will however be no energy transfer to lower frequencies, and lower energy transfer to higher frequencies (only in shallow water due to triad wave-wave interactions). As a result, the peak frequency might be slightly overestimated and the mid-frequencies may contain too much energy.

Finally, two test cases have been modelled in order to determine whether SWAN and SWASH, modified as explained above, could be used with sufficient confidence to model design storm conditions along the Mekong Delta coast. The results were encouraging enough to continue the adopted approach.

The most important conclusion of this project is therefore not the outcome of the cost-benefit analysis, but the discovery that wave transformation on extremely gentle slopes is a seriously under-researched subject which deserves further investigation.

5.1.2. Stable coastline

When the coastline is stable over time, the cost-benefit analysis is rather straightforward. It is generally more beneficial to construct the dike further inland, as the foreshore is very valuable through wave attenuation and possible ecosystem services in case a mangrove forest is present. This is also confirmed by the fact that the mildest bathymetry required the lowest construction and maintenance costs.

The cost-benefit analysis also indicated that it is wise to design for a long lifetime and return period, as the additional investments are relatively small, compared to the additional benefits.

The effect of vegetation is concentrated inside the mangrove forest, where the wave energy is strongly attenuated, leading to lower hydraulic conditions at the dike toe and therefore cheaper dikes. Further, it was concluded that mangrove reforestation, if possible, is always favourable, because the costs of mangrove reforestation are significantly lower than the ecosystem services derived from it, but mostly because the reduction in dike costs is orders of magnitude higher than the reforestation costs. This reduction in dike costs can in reality be even higher than what resulted from this cost-benefit analysis, as the costs of revetment may be excluded if there is sufficient wave damping inside the mangrove forest.

Finally, 5% to 15% of the construction costs can be saved by allowing a limited overtopping discharge. Therefore, wise use of the land just behind the dike can make a large difference in the total required budget.

The above conclusions on the effect of the different parameters on the optimal coastal protection strategy are of course also valid for accreting and eroding coastlines. However, the effect of accretion or erosion needs to be added to this mix before determining the optimal strategy.

5.1.3. Accretion

When the sediment balance is positive, the coastline accretes over time. This is favourable for the coastal protection, as the wave damping on the foreshore will increase over time, reducing the wave load and overtopping on the dike. Although it might seem attractive to follow the accreting coastline and displace the dike regularly, there are two reasons why this is not the best approach. First, the cost-benefit analysis showed that it requires only a small additional investment to build a dike for a longer lifetime, while building a completely new dike for a short lifetime is relatively expensive. Second, coastline dynamics often follow a cycle, therefore erosion may follow a period of accretion, and especially in the Mekong Delta, eroding parts serve as sediment source to other parts of the coastline. However, if a dike with a long lifetime is constructed, as the foreshore will grow over the lifetime of the dike, its value can be optimised by using it for extensive aquaculture.

5.1.4. Erosion

Erosion complicates coastal protection significantly. Several approaches are possible in case of erosion. The easiest one is just to accept the erosion, and place the dike more inland, such that even after a period of erosion it is still sufficiently protected by the remaining foreshore. This is called managed retreat. In theory, this approach is always possible, however in practice there are often limitations, for example as a result of previous land use (a city cannot be abandoned).

Another approach is to slow down the erosion using the natural strength of mangroves. However, this approach is only possible for limited erosion, both in rate and in duration. If the erosion becomes too strong, the mangrove forest will collapse, after which the effects of erosion will increase significantly.

A third approach is to stop the erosion by adding sediment to the system through nourishments, thus restoring the sediment balance. This is common practice for sandy coasts, but has never been applied to muddy coasts. For this report, it is assumed the nourishments are technically possible, and a rough estimate of the costs is made, so that the approach can be compared with the other approaches. However, the costs turned out to be a factor 10 higher. Therefore, they are only relevant in case the two previous approaches are not possible, and the value of the land to be protected is sufficiently high to justify the investment.

The last approach is to build such a strong structure that it can withstand the erosion and subsequent increased wave load. These structures require for example strong revetments, extremely deep foundations and scour protection, which are all very expensive measures. The costs of this approach lie therefore closer to the costs of the nourishment strategy.

Currently, the value of land in the Mekong Delta is relatively low, due to low value crops and limited industry. However, the Mekong Delta is developing rapidly, and the value of land will increase accordingly, eventually justifying higher investments in coastal protection. Therefore, especially in case of strong erosion, it is recommended to apply one of the first two approaches, with a small lifetime, and re-evaluate the situation after that.

5.2. Limitations

No approach is perfect, no method can include all aspects. The adopted approach in this project also shows a range of limitations and shortcomings. However, it is important to distinguish those limitations that have weighed on the process and its conclusions, as opposed to limitations that only had minor consequences. For this distinction, the objective of the project should be kept in mind: generating understanding of the effect of foreshore geometry and dike location on wave load and overtopping.

A first limitation that influenced the entire process is the fact that no variation over time has been included. An obvious example is the value of land. In such a rapidly developing region as the Mekong Delta, the value of land is expected to increase significantly over the following decades. In case of high erosion, some protection strategies are currently not viable as they are too expensive, but when the value of land increases, the reduced risk of flooding will become more important and the net costs may turn into benefits. However, if the evolution of land value were included in this analysis, one can determine the turning point when for example nourishments become viable, and choose a protection strategy that opts for managed retreat until the turning point, after which that dike location is fixed and protected by foreshore nourishments. Another limitation of the absence of variation over time is the fact that the key parameter of this project, the erosion rate, is constant and morphodynamics have been excluded from the model. As a result, only linear erosion and accretion can be modelled through analysing snapshots over time. Situations where accretion and erosion alternate, or the erosion or accretion rate vary significantly over time, may require a different protection system, which is not covered in this project. Another development over time is climate change. Sea level rise is included in the hydraulic boundary conditions, but other effects, such as more frequent or more intense storms, have been left out. Especially for longer lifetimes, climate change may have a significant effect on the boundary conditions.

Another limitation is inherent to cost-benefit analyses: it is impossible to account for all benefits resulting from a coastal protection system. Complex chain reactions, as well as continued benefits beyond the lifetime of the coastal protection measure, ensure that the real benefits may be significantly higher than estimated in this evaluation framework. A proper coastal protection can serve as an incubator for developments.

One of the strengths of the generic approach adopted in this project, is that its conclusions may be exported to other regions. However we must remain aware of the fact that some important details have been excluded and that as a result some of the conclusions may be too black and white. This must be kept in mind when applying the conclusions for other regions.

5.3. Recommendations

The recommendations can be divided into two categories, one comprising recommendations to improve this specific project and the adopted approach, and another presenting recommendations for the coastal protection of the Mekong Delta, or mangrove coasts in general.

A first recommendation specific to this project, is to collect more data, although this recommendation

also applies to mangrove coasts in general. In the Mekong Delta, there is simply a strong deficit of data, therefore measurement campaigns are urgently needed. However, some of the data that does exist, is not freely available, which is a pity and an obstruction to further development.

Another specific recommendation is to improve and validate the numerical model. Especially the wave transformation on these extremely gentle slopes (in the order of 1:1000) has never been researched, let alone measured, therefore there is no way to validate the model performance in these situations. However, flume experiments are not straightforward, as the bottom slopes are of such an order that it would require impossibly long flumes. Moreover, wind also plays an important role on these foreshores, so the extremely long flume should also be able to test with various wind strengths.

The strength of this project is that a generic approach has been developed, to compare and evaluate different coastal protection strategies. However, as the context has remained generic, it still has to be validated by applying it to specific situations. This application will not only validate, but growing experience will also increase the quality of the approach. Furthermore, this approach will become much richer if some variation over time is included.

On a more general level, there are two recommendations related to the protection of mangrove coasts worldwide.

First, the protection of mangrove coasts almost always includes restoration of mangroves at some level. Although some mangrove reforestation projects have been successful in the past, there are still many projects that do not succeed, and the exact causes for success or failure are often obscure. Further investigation into the parameters controlling the erosion process, as well as into the parameters defining the restoring process can increase the success rate of these reforestation projects.

Nourishing muddy mangrove coasts appears to be very promising, as the vulnerability of mangrove systems is often (partially) caused by a sediment deficit. Therefore, it is recommended to investigate not only the technical feasibility of this concept, but also to explore further applications. In this project, foreshore nourishment has been used to compensate erosion, but it can also be used to modify the shape of the foreshore, or even assist in mangrove reforestation projects.

Bibliography

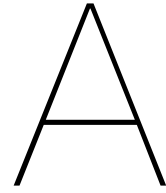
- Alagan Chella, M., Bihs, H., Myrhaug, D., and Muskulus, M. (2015). Breaking characteristics and geometric properties of spilling breakers over slopes. *Coastal Engineering*, 95:4–19.
- Albers, T. and Stolzenwald, J. (2014). Coastal Engineering Consultancy in the Ca Mau Province. Technical report, Deutsche Gesellschaft für Internationale Zusammenarbeit (GIZ).
- Anthony, E. J., Brunier, G., Besset, M., Goichot, M., Dussouillez, P., and Nguyen Van Lap (2015). Linking rapid erosion of the Mekong River delta to human activities. *Scientific Reports*, 5.
- Battjes, J. A. and Janssen, J. P. F. M. (1978). Energy Loss and Set-Up Due To Breaking of Random Waves. *Proceedings of 16th Conference on Coastal Engineering, ASCE*, 1:569–587.
- Beckley, B. D., Lemoine, F. G., Luthcke, S. B., Ray, R. D., and Zelensky, N. P. (2007). A reassessment of global and regional mean sea level trends from TOPEX and Jason-1 altimetry based on revised reference frame and orbits. *Geophysical Research Letters*, 34(14):L14608.
- Berg, H., Ohman, M. C., Troeng, S., and Linden, O. (1998). Environmental Economics of Coral Reef Destruction in Sri Lanka. *Ambio*, 27(8):627–624.
- Binh, C. T., Phillips, M. J., and Demaine, H. (1997). Integrated shrimp-mangrove farming systems in the Mekong delta of Vietnam. *Aquaculture Research*, 28:599–610.
- Bosboom, J. and Stive, M. J. F. (2015). *Coastal Dynamics I*. Delft Academic Press, Delft, 0.5 edition.
- Bretschneider, C. L. (1966). Wave generation by wind, deep and shallow water. *Estuary and coastline hydrodynamics*, pages 133–196.
- Breugem, W. A. and Holthuijsen, L. H. (2007). Generalized shallow water wave growth from Lake George. *Journal of Waterway, Port, Coastal, and Ocean Engineering*, 133(3):173–182.
- Burger, B. (2005). *Wave attenuation in mangrove forests: Numerical modelling of wave attenuation by implementation of a physical description of vegetation in SWAN*. Master thesis, Delft University of Technology.
- CIRIA, CUR, and CETMEF (2007). *The Rock Manual. The use of rock in hydraulic engineering*. C683, CIRIA, London.
- Clough, B., Phan Van Hoang, Huynh Huu To, and Luu Trieu Phong (2016). Mangrove Rehabilitation in the Mekong Delta in the period 2008-2014. Good Practices and Lessons Learned. Technical report, GIZ, Ho Chi Minh City, Vietnam.
- Consortium Royal HaskoningDHV, WUR, Deltares, Rebel (2013). Mekong Delta Plan. Long-term vision and strategy for a safe, prosperous and sustainable delta. Technical report, Netherlands Advisory Team for the Mekong Delta Plan, Amersfoort, the Netherlands.
- Dalrymple, R. A., Kirby, J. T., and Hwang, P. A. (1984). Wave diffraction due to areas of energy dissipation. *Journal of Waterway, Port, Coastal, and Ocean Engineering*, 110(1):67–79.
- DEMIS Mapserver (2015). Map showing the Mekong River and tributaries.
- Divoky, D., Le Méhauté, B., and Lin, A. (1970). Breaking waves on gentle slopes. *Journal of Geophysical Research*, 75(9).
- Do Duc Dung, Bui Ngoc, Nghiem Dinh Thanh, and Nguyen Thien Cam (2013). Reviewing the sea dyke system of Ca Mau province. Technical report, Southern Institute for Water Resources Planning (SIWRP), Ho Chi Minh City, Vietnam.

- Einsele, G. (2000). *Sedimentary Basins: Evolution, Facies, and Sediment Budget*. Springer Science & Business Media.
- Fiselier, J. L. (1990). Living off the tides. Strategies for the integration of conservation and sustainable resource utilization along mangrove coasts. Technical report, Environmental Database on Wetland Interventions.
- Gedan, K. B., Kirwan, M. L., Wolanski, E., Barbier, E. B., and Silliman, B. R. (2011). The present and future role of coastal wetland vegetation in protecting shorelines: answering recent challenges to the paradigm. *Climatic Change*, 106(1):7–29.
- GIZ (2015). Shoreline changes from 1904 till 2015 in the Mekong Delta.
- Guannel, G., Ruggiero, P., Faries, J., Arkema, K., Pinsky, M., Gelfenbaum, G., Guerry, A., and Kim, C.-K. (2015). Integrated modeling framework to quantify the coastal protection services supplied by vegetation. *Journal of Geophysical Research: Oceans*, 120(1):324–345.
- Harihar, S. (2015). *Design of mangrove rehabilitation projects on tropical coasts*. Msc thesis, Delft University of Technology.
- Hasselmann, S., Hasselmann, K., Allender, J. H., and Barnett, T. P. (1985). Computations and Parameterizations of the Nonlinear Energy Transfer in a Gravity-Wave Spectrum. Part II: Parameterizations of the Nonlinear Energy Transfer for Application in Wave Models. *Journal of Physical Oceanography*, 15(11):1378–1392.
- Hillen, M. M. (2008). *Safety Standards project. Risk analysis for new sea dike design guidelines in Vietnam*. Msc thesis, Delft University of Technology.
- Hillen, M. M., Jonkman, S. N., Kanning, W., Kok, M., Geldenhuys, M. A., and Stive, M. J. F. (2010). Coastal defence cost estimates: Case study of the Netherlands, New Orleans and Vietnam. Technical Report April, Delft University of Technology.
- Hoang Van Huan and Nguyen Huu Nhan (2006). Results on study about wave field of Dong Nai-Saigon estuaries and suggestion of sea bank and river mouths protection methods. In *Vietnam-Japan Estuary Workshop*, pages 140–150, Hanoi, Vietnam.
- Hoi An Erosion Consortium (2015). Appendix 2: Portfolio of beach nourishments in the Netherlands.
- Holthuijsen, L. H. (2007). *Waves in Oceanic and Coastal Waters*. Cambridge University Press.
- Kuenzer, C., Guo, H., Huth, J., Leinenkugel, P., Li, X., and Dech, S. (2013). Flood mapping and flood dynamics of the mekong delta: ENVISAT-ASAR-WSM based time series analyses. *Remote Sensing*, 5(2):687–715.
- Le Anh Tuan, Chu Thai Hoanh, Miller, F., and Bach Tan Sinh (2007). Chapter 1 : Flood and Salinity Management in the Mekong Delta, Vietnam. In *Challenges to sustainable development in the Mekong delta: Regional and national policy issues and research needs*, pages 15–68. Stockholm Environment Institute.
- Lewis, R. R. (2001). Mangrove Restoration - Costs and Benefits of Successful Ecological Restoration. In *Proceedings of the Mangrove Valuation Workshop*, Stockholm, Sweden. Beijer International Institute of Ecological Economics.
- Linham, M. M., Green, C. H., and Nicholls, R. J. (2010). Costs of adaptation to the effects of climate change in the world's large port cities. Technical report, AVOID programme (AV/WS2/D1/R14).
- Linham, M. M. and Nicholls, R. J. (2010). *Technologies for Climate Change Adaptation - Coastal Erosion and Flooding*. UNEP Risø Centre on Energy, Climate and Sustainable Development, Roskilde, Denmark.
- Lu, X. X. and Siew, R. Y. (2005). Water discharge and sediment flux changes in the Lower Mekong River. *Hydrology and Earth System Sciences Discussions*, 2(6):2287–2325.

- Mai Van Cong (2010). *Probabilistic Design of Coastal Flood Defences in Vietnam*. Dissertation, Delft University of Technology.
- Mai Van Cong, van Gelder, P. H. A. J. M., Vrijling, J. K., and Mai, T. C. (2008). Risk Analysis of Coastal Flood Defences- a Vietnam Case. In *4th International Symposium on Flood Defence: Managing Flood Risk, Reliability and Vulnerability*, pages 93–1 – 93–8.
- Mcivor, A., Möller, I., Spencer, T., and Spalding, M. (2012a). Reduction of Wind and Swell Waves by Mangroves. Technical report, UK and Cambridge Coastal Research Unit, Department of Geography, University of Cambridge.
- Mcivor, A., Spencer, T., and Möller, I. (2012b). Storm Surge Reduction by Mangroves. Technical report, UK and Cambridge Coastal Research Unit, Department of Geography, University of Cambridge.
- Mcivor, A., Spencer, T., and Möller, I. (2013). The response of mangrove soil surface elevation to sea level rise. Technical Report 3, UK and Cambridge Coastal Research Unit, Department of Geography, University of Cambridge.
- Mekong River Commission (MRC) (2010). *State of the basin report 2010*. O.S. Printing House, Vientiane, Lao PDR.
- Milliman, J. D. and Farnsworth, K. L. (2011). *River discharge to the coastal ocean: a global synthesis*. Cambridge University Press.
- Milliman, J. D. and Syvitski, J. P. M. (1992). Geomorphic/tectonic control of sediment discharge to the ocean: the importance of small mountainous rivers. *Journal of Geology*, pages 525–544.
- Ministry of Natural Resources and Environment (MONRE) (2008). National Target Program to respond to climate change. Technical Report 60, MONRE, Hanoi, Vietnam.
- Narayan, S. (2009). *The Effectiveness of Mangroves in Attenuating Cyclone- induced Waves*. Master thesis, Delft University of Technology.
- National Oceanic and Atmospheric Administration (2008). Mangrove forests. <http://www.fermentas.com/techinfo/nucleicacids/maplambda.htm>.
- National Oceanic and Atmospheric Administration (2014). Data provided by Royal HaskoningDHV through personal communication.
- Nguyen M Quang (2000). Mekong delta floods in the past and present.
- Nguyen Tan Dung (2007). National strategy for natural disaster prevention, response and mitigation to 2020.
- Nguyen Thi Kim Cuc, Suzuki, T., de Ruyter van Steveninck, E. D., and Hai, H. (2015). Modelling the impacts of mangrove vegetation structure on wave dissipation in Ben Tre Province, Vietnam, under different climate change scenarios. *Journal of Coastal Research*, 31(2):340–347.
- Nowacki, D. J., Ogston, A. S., Nittrouer, C. A., Fricke, A. T., and Van Pham Dang Tri (2015). Sediment dynamics in the lower Mekong River: Transition from tidal river to estuary. *Journal of Geophysical Research: Oceans*, 120(9):6363–6383.
- Ojendal, J. (2000). *Sharing the Good. Models of Managing Water Resources in the Lower Mekong River Basin*. Gotenborg University.
- Othman, M. A. (1994). Value of mangroves in coastal protection. *Hydrobiologia*, 285:277–282.
- Oxfam (2008). Viet Nam: The development of national health insurance. Technical report, Oxfam, Hanoi, Vietnam.
- Oxmann, J. F., Pham, Q. H., Schwendenmann, L., Stellman, J. M., and Lara, R. J. (2010). Mangrove reforestation in Vietnam: the effect of sediment physicochemical properties on nutrient cycling. *Plant and Soil*, 326(1-2):225–241.

- Phan Khanh Linh, Van Thiel De Vries, J. S. M., and Stive, M. J. F. (2015). Coastal Mangrove Squeeze in the Mekong Delta. *Journal of Coastal Research*, 31(2):233–243.
- Renaud, F. G. and Kuenzer, C. (2012). *The Mekong Delta System*. Springer Environmental Science and Engineering. Springer Netherlands, Dordrecht.
- Salem, M. E. and Mercer, D. E. (2012). The economic value of mangroves: A meta-analysis. *Sustainability*, 4(3):359–383.
- Sathirathai, S. and Barbier, E. B. (2001). Valuing mangrove conservation in Southern Thailand. *Contemporary Economic Policy*, 19(2):109–122.
- Schiereck, G. J. and Verhagen, H. J. (2012). *Introduction to bed, bank and shore protection*. VSSD, Delft, 2 edition.
- Spalding, M., Mcivor, A., Tonneijck, F., Tol, S., and van Eijk, P. (2014). Mangroves for coastal defence. Guidelines for coastal managers & policy makers. Technical report, Wetlands International and The Nature Conservancy.
- Ta Thi Kim Oanh, Nguyen Van Lap, Tateishi, M., Kobayashi, I., Tanabe, S., and Saito, Y. (2002). Holocene delta evolution and sediment discharge of the Mekong River, southern Vietnam. *Quaternary Science Reviews*, 21(16-17):1807–1819.
- The SWAN team (2009). SWAN user manual.
- The SWAN team (2015). SWAN scientific and technical documentation.
- The SWASH team (2015). SWASH user manual.
- Tolhurst, T. J. and Chapman, M. G. (2005). Spatial and temporal variation in the sediment properties of an intertidal mangrove forest: implications for sampling. *Journal of Experimental Marine Biology and Ecology*, 317(2):213–222.
- Tran Quang Hoai, Nguyen Binh Thin, and Dinh Vu Thanh (2012). Technical guidelines on sea dike design. Technical report, Ministry of Agriculture and Rural Development (MARD), Hanoi, Vietnam.
- Tran Viet Lien, Nguyen Dang Bich, and Nguyen Vo Thong (2004). On the wind pressure zone map of the Vietnam territory. In *Proceeding of Workshop on Regional Harmonization of Wind Loading and Wind environmental Specifications in Asia-Pacific Economies (APEC-WW)*, pages 1–7. Tokyo Polytechnic University.
- van Gent, M. R. A. (2001). Wave runup on dikes with shallow foreshores. *Journal of Waterway, Port, Coastal, and Ocean Engineering*, 127(5):254–262.
- Verhagen, H. J. and Tran Thi Loi (2012). The use of mangroves in coastal protection. In *8th International Conference on Coastal and Port Engineering in Developing Countries*. COPEDEC.
- Vo Thanh Danh (2012). Adaptation to sea level rise in the Vietnamese Mekong River Delta: Should a sea dike be built? Technical Report 13, School of Economic and Business Administration, Can Tho University, Can Tho, Vietnam.
- Vo Thanh Danh and Huynh Viet Khai (2014). Using a Risk Cost-Benefit Analysis for a Sea Dike to Adapt to the Sea Level in the Vietnamese Mekong River Delta. *Climate*, 2(2):78–102.
- World Bank Group (2016). Real interest rate. <http://data.worldbank.org/indicator/FR.INR.RINR>. Accessed on 19 May 2016.
- World Wildlife Fund (2004). Seven from Mountain to Sea: Asia Pacific River Basin Big Wins.
- Xue, Z., He, R., Liu, J., and Warner, J. C. (2012). Modeling transport and deposition of the Mekong River sediment. *Continental Shelf Research*, 37:66–78.
- Xue, Z., Liu, J. P., DeMaster, D., Nguyen Lap Van, and Ta Thi Kim Oanh (2010). Late Holocene Evolution of the Mekong Subaqueous Delta, Southern Vietnam. *Marine Geology*, 269(1-2):46–60.

Young, I. R. and Verhagen, L. A. (1996). The growth of fetch limited waves in water of finite depth. Part 1. Total energy and peak frequency. *Coastal Engineering*, 29(1-2):47–78.



Appendix: Boundary conditions

In section 2.4 the boundary conditions necessary to numerically model every scenario have been defined. For the hydraulic boundary conditions (wave characteristics and water levels, corresponding to various return periods), some more calculations and research were required. This is presented in this appendix. First, the wave characteristics are derived based on three data sources (section A.1), then the individual components of the design water level are determined and combined into one design water level for each return period (section A.2).

A.1. Wave conditions

A.1.1. Available data

In contrast to the Netherlands, wave and water level data are not easily available in Vietnam. This can be explained by two reasons: first, there have not been many measurement campaigns, let alone long term measurement stations, and second, the measured data are not always available. The data are often owned by institutes who will only sell their data to a limited group of users.

Determining design conditions with large return periods is therefore very difficult. For this project, three data sources have been used. The first source contains wind pressure zone maps, providing wind speeds related to return periods used for construction norms (Tran Viet Lien et al., 2004). These wind speeds can be translated into corresponding wave heights. The second source contains the only measured waves, from a wave station in Bach Ho, just north of the Mekong Delta, over the last 20 years (Hoang Van Huan and Nguyen Huu Nhan, 2006). The third data source is the NOAA wave model (National Oceanic and Atmospheric Administration, 2014).

Wind pressure zones

Although the available wave measurements are limited, there is a database with wind information, which was used for the Vietnamese code of practice for wind loads on structures (Tran Viet Lien et al., 2004). There are four climate stations relevant for the sea dikes along the Mekong Delta: Rach Gia (capital of the Kien Giang province), Soc Trang (capital of the Soc Trang province), Ca Mau (capital of the Ca Mau province) and the Con Dao islands off the eastern Mekong Delta coast. Especially this last station is very useful, since it gives the wind for an offshore location, and is thus suitable for wave generation computations. Table A.1 gives the mean wind speed (in m/s) over 10 minutes, related to different return periods, for the four climate stations mentioned above, based on Tran Viet Lien et al. (2004).

Climate station	Return period [years]			
	10	20	50	100
Rach Gia	21.0	24.0	26.0	28.0
Soc Trang	18.6	20.6	21.9	23.2
Ca Mau	19.7	22.5	24.3	26.2
Con Dao	25.7	30.1	33.0	35.8

Table A.1: Wind speed (in m/s) averaged over 10 minutes for different return periods

These wind speeds represent the maximum values (averaged maximum over 10 minutes) that will occur on average once in the duration of the return period. However, it takes more than 10 minutes to generate storm waves or storm surges. Therefore, the assumption is made of a representative design storm with a duration of 6 hours during which the wind speed is 75% of the maximum value found in Table A.1.

Further, the wind speeds at Con Dao have been extrapolated to estimate the wind speed corresponding to all return periods defined in subsection 2.4.1 (10, 20, 25, 40, 50, 100, 200, 250 and 500 years). This is done by fitting a logarithmic function through the data. The fitted function is given in Equation A.1, the result is given in the first two columns of Table A.3.

$$u = 7.2866 \cdot \log(T_r) + 12.4325 \quad (\text{A.1})$$

Where

u	wind speed	[m/s]
T_r	return period	[y]

Translate wind speeds to wave characteristics

To estimate the wave characteristics of the waves generated by the design wind speed, the approach of Young and Verhagen (1996) is followed, modified by Breugem and Holthuijsen (2007). This approach is totally dimensionless, therefore, a couple of dimensionless parameters first needs to be introduced. Note that dimensionless parameters are indicated with a tilde.

$$\tilde{H} = \frac{g \cdot H}{u^2} \quad (\text{A.2})$$

$$\tilde{T} = \frac{g \cdot T}{u} \quad (\text{A.3})$$

$$\tilde{F} = \frac{g \cdot F}{u^2} \quad (\text{A.4})$$

$$\tilde{h} = \frac{g \cdot h}{u^2} \quad (\text{A.5})$$

Where

\tilde{H}	dimensionless wave height	[-]
g	gravitational acceleration (9.81 m/s ²)	[m/s ²]
H	wave height	[m]
u	wind speed	[m/s]
\tilde{T}	dimensionless wave period	[-]
T	wave period	[s]
\tilde{F}	dimensionless fetch	[-]
F	fetch	[m]
\tilde{h}	dimensionless water depth	[-]
h	water depth	[m]

The growth curves of the significant wave height and peak wave period, for all water depths, as given by Young and Verhagen (1996) and Breugem and Holthuijsen (2007), are given in Equation A.6 and Equation A.7.

$$\tilde{H} = \tilde{H}_{\infty} \cdot \left[\tanh(k_3 \cdot \tilde{h}^{m_3}) \cdot \tanh\left(\frac{k_1 \cdot \tilde{F}^{m_1}}{\tanh(k_3 \cdot \tilde{h}^{m_3})}\right) \right]^p \quad (\text{A.6})$$

$$\tilde{T} = \tilde{T}_{\infty} \cdot \left[\tanh(k_4 \cdot \tilde{h}^{m_4}) \cdot \tanh\left(\frac{k_2 \cdot \tilde{F}^{m_2}}{\tanh(k_4 \cdot \tilde{h}^{m_4})}\right) \right]^q \quad (\text{A.7})$$

Where

\tilde{H}_{∞}	dimensionless wave height for fully developed sea state in deep water	[-]
\tilde{T}_{∞}	dimensionless wave period for fully developed sea state in deep water	[-]

The values of the coefficients used in Equation A.6 and Equation A.7 are given in Table A.2.

Significant wave height		Peak wave period	
Coefficient	Value	Coefficient	Value
\tilde{H}_{∞}	0.24	\tilde{T}_{∞}	7.69
k_1	$4.41 \cdot 10^{-4}$	k_2	$2.77 \cdot 10^{-7}$
k_3	0.343	k_4	0.10
m_1	0.79	m_2	1.45
m_3	1.14	m_4	2.01
p	0.572	q	0.187

Table A.2: Coefficients for the Young and Verhagen formulae, modified by Breugem and Holthuijsen (2007)

Finally, the wave characteristics at the offshore boundary of the SWAN model can be computed, for a water depth of 65 m and a fetch of 250 km. For the wind speeds corresponding to the different return periods, the significant wave height and peak wave period are given in Table A.3.

Return period [y]	Wind speed [m/s]	Wave height [m]	Wave period [s]
10	19.7	5.3	9.8
20	21.9	6.0	10.2
25	22.6	6.1	10.4
40	24.1	6.6	10.7
50	24.8	6.7	10.8
100	27.0	7.3	11.2
200	29.2	7.9	11.6
250	29.9	8.1	11.7
500	32.1	8.6	12.1

Table A.3: Estimated significant wave height and peak wave period based on wind speed for different return periods.

Wave station at Bach Ho

Hoang Van Huan and Nguyen Huu Nhan (2006) present the results of wave measurements at Bach Ho between 1986 and 2006. However, for longer return periods, they refer to data of Vietsopetro, an oil platform in the neighbourhood.

The wave station lies at a depth of 50 m, so the effect of the bed can be ignored. The wave direction of the highest waves is northeast. Table A.4 gives an overview of the wave height and wave period with their corresponding return periods, which vary between 1 and 100 years.

Return period [y]	Wave height [m]	Wave period [s]
1	3.5	8.1
10	4.5	8.7
25	5.5	9.2
50	6.4	9.5
100	7.2	9.7

Table A.4: Wave height and wave period for different return periods at Bach Ho wave station, based on Hoang Van Huan and Nguyen Huu Nhan (2006).

Again, these data need to be extrapolated to all return periods under consideration. For this, a logarithmic function is fitted to the data. Equation A.8 gives the fitted function for the wave height, Equation A.9 for the wave period.

$$H_s = 1.8355 \cdot \log(T_r) + 3.1818 \quad (\text{A.8})$$

$$T_p = 0.8250 \cdot \log(T_r) + 8.0340 \quad (\text{A.9})$$

The extrapolated wave data, calculated with equations A.8 and A.9 are given in Table A.5.

Where

H_s	significant wave height	[m]
T_p	peak wave period	[s]
T_r	return period	[y]

Return period [y]	Wave height [m]	Wave period [s]
10	5.0	8.9
20	5.6	9.1
25	5.7	9.2
40	6.1	9.4
50	6.3	9.4
100	6.9	9.7
200	7.4	9.9
250	7.6	10.0
500	8.1	10.3

Table A.5: Extrapolated wave height and wave period for different return periods at Bach Ho wave station, based on Hoang Van Huan and Nguyen Huu Nhan (2006).

NOAA wave model

The NOAA wave model is based on measurements for the period 1979 - 2014. However, the domain of the model is large, and there are not necessarily measurements near the Mekong Delta. Previous projects of Royal HaskoningDHV in Vietnam have shown that NOAA data may underestimate the wave heights by up to 25% (Royal HaskoningDHV, personal communication, April 2016). This can be corrected if satellite altimeter data is available. Royal HaskoningDHV has provided revised data for two locations, both slightly north of the Mekong Delta.

The data do not provide the relation between wave height and period. However, the largest wave encountered during a period of 25 years can be assumed to have a return period of about 25 years. This highest wave has a wave height of more than 5 m, which is in fair agreement with the other two sources. Unfortunately, the longest wave period of 16 s is absolutely not close to the other two sources (but the exact relation between wave heights and wave periods is unclear).

The NOAA model also provides wind data, therefore it can be used to compare with the wind data of Tran Viet Lien et al. (2004). The strongest wind recorded during 25 years is larger than 20 m/s. Tran Viet Lien et al. (2004) gives a wind speed of 22.6 m/s for a return period of 25 years, which is in fair agreement.

A.1.2. Design wave characteristics

In summary, the design wave characteristics will be based on three sources: wind data for Con Dao (Tran Viet Lien et al., 2004), wave data from a wave station in Bach Ho (Hoang Van Huan and Nguyen Huu Nhan, 2006) and wave data from the NOAA wave model (National Oceanic and Atmospheric Administration, 2014).

The three sources agreed relatively well on the wave height, but the NOAA wave model diverged with respect to the wave period. To come up with the design wave conditions, a logarithmic function will be fitted through the data provided by the three sources. This is visualised in Figure A.1. The resulting wave characteristics are given in Table A.6. Note that for the calculation of the design wave period, the NOAA data are left out.

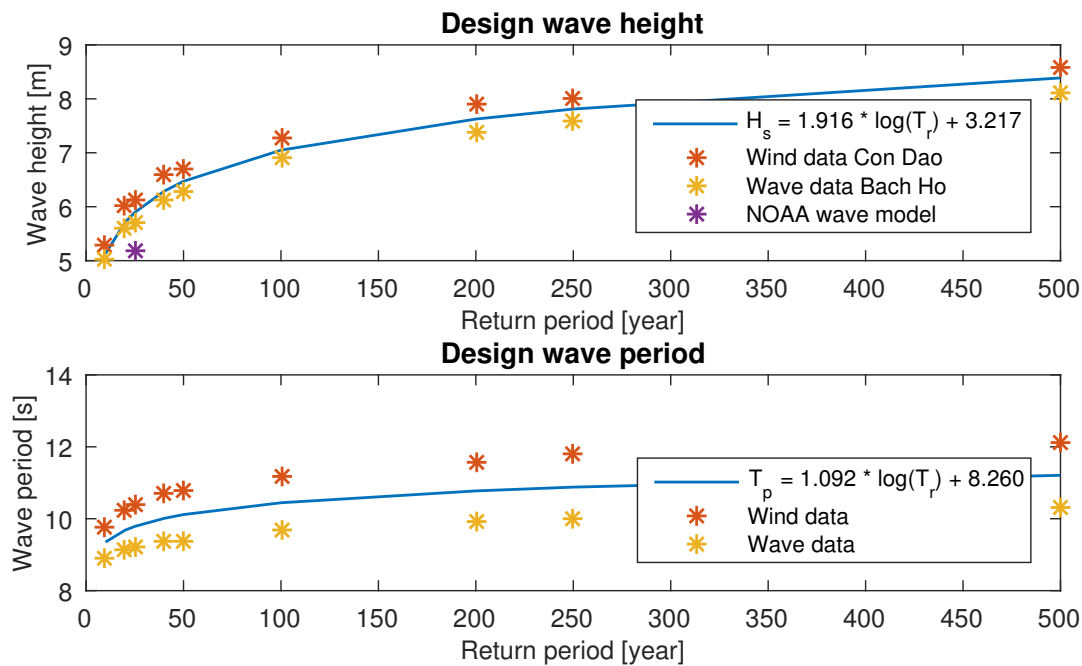


Figure A.1: Design wave conditions, fitted to available data.

Return period [y]	Wind speed [m/s]	Wave height [m]	Wave period [s]
10	19.7	5.1	9.4
20	21.9	5.7	9.7
25	22.6	5.9	9.8
40	24.1	6.3	10.0
50	24.8	6.5	10.1
100	27.0	7.0	10.4
200	29.2	7.6	10.8
250	29.9	7.8	10.9
500	32.1	8.4	11.2

Table A.6: Design wave conditions

A.2. Water level

Extreme water levels are a combination of a high (spring) tide and a storm surge. This storm surge can be composed of four components: wind set-up, wave set-up, a barometric effect and the effect of the shape of the land. Finally, the future water levels are also influenced by relative sea level rise.

A.2.1. Tides

There is a distinct difference between the tidal regimes along the East Sea coast and the West Sea coast (Do Duc Dung et al., 2013).

Along the East Sea coastline, the tidal regime is semi-diurnal with some daily inequality. The amplitude is largest along the coast of Bac Lieu, while the daily inequality increases when approaching the southern tip of Ca Mau. Each month there are two spring tide periods. The tidal amplitude varies between 2.5 and 3.5 m (Do Duc Dung et al., 2013; Albers and Stolzenwald, 2014; Xue et al., 2010).

The West Sea coast experiences a mixed tidal regime, more diurnal than semi-diurnal. Even though at most places there are two high and two low tides each day, the daily inequality is significant. The tidal amplitude is smaller and varies between 0.7 and 1.0 m (Do Duc Dung et al., 2013; Albers and Stolzenwald, 2014). Each month there is one spring tide period, around full moon.

Since the east coast of the Mekong Delta is twice as long as the west coast, the tidal characteristics will be chosen representative of the East Sea tides, with an amplitude of 3 m. For the design water level, the tidal component equals half of the tidal amplitude, so 1.5 m.

A.2.2. Wind set-up

Wind blowing over the water surface causes a shear stress. Where a (shallow) water body is enclosed, for example by a coastline, this results in a slope of the water surface. For a simple 1D situation, as described in the Rock Manual (CIRIA et al., 2007), the slope of the water surface can be expressed by Equation A.10.

$$\frac{\partial \eta}{\partial x} = \frac{1}{\rho_w \cdot g \cdot d} \cdot \tau_w \quad (\text{A.10})$$

Where

d	actual water depth, $d = h + \eta$	[m]
h	still water depth	[m]
η	set-up	[m]
ρ_w	density of water (1030 kg/m ³)	[kg/m ³]
τ_w	wind shear stress, see Equation A.11	[Pa]

$$\tau_w = \rho_a \cdot C_D \cdot u^2 \quad (\text{A.11})$$

Where

ρ_a	density of air (1.21 kg/m ³)	[kg/m ³]
C_D	drag coefficient (varies between $0.8 \cdot 10^{-3}$ and $3.0 \cdot 10^{-3}$)	[-]
u	wind speed	[m/s]

For a closed lake with a horizontal bottom, the water level set-up can be approximated by Equation A.12.

$$\Delta h = \frac{1}{2} \cdot \kappa \cdot \frac{u^2}{g \cdot h} \cdot F \quad (\text{A.12})$$

Where

Δh	water level set-up due to wind friction	[m]
κ	$= C_D \cdot \frac{\rho_a}{\rho_w}$	[-]
F	fetch, in this case equal to the length of the lake	[m]

For an open sea, however, it is best to use Equation A.13, which was derived by Bretschneider (1966).

$$\Delta h = \sqrt{2 \cdot \kappa \cdot \frac{u^2}{g} \cdot F + h^2} - h \quad (\text{A.13})$$

These formulae are developed for a horizontal bottom, while in reality the bottom slopes up towards the coast. To account for this, the cross-shore transect is divided in a couple of segments, and for each segment the individual set-up is calculated, starting at the offshore end, and adding the set-up to the water depth of the neighbouring segment before computing the set-up in that segment. This is illustrated in Figure A.2.

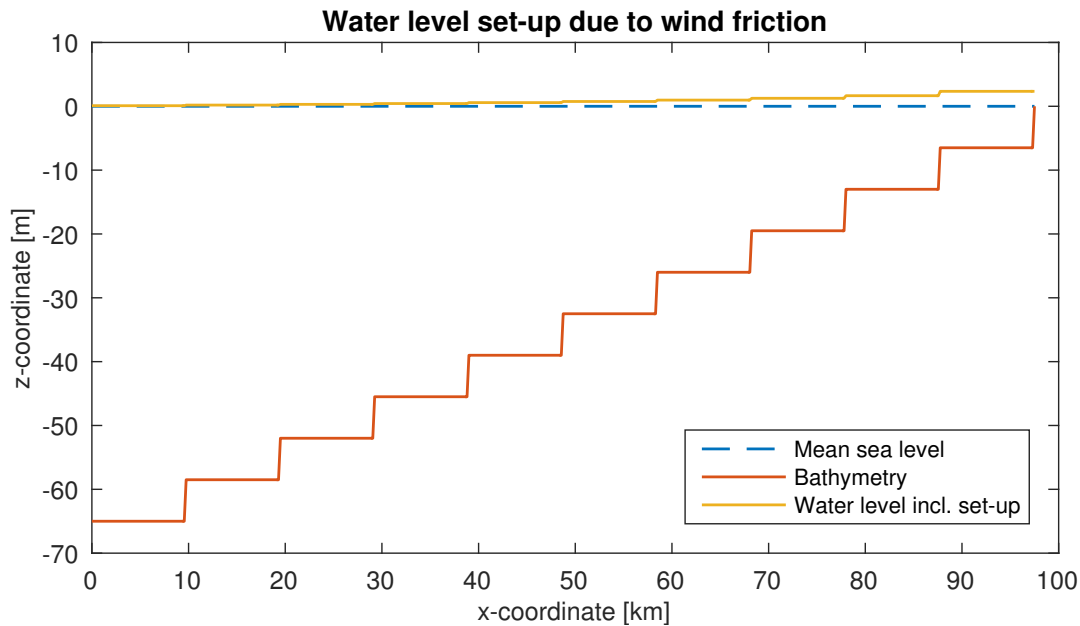


Figure A.2: Water level set-up generated by wind friction, computed for different segments in cross-shore transect

Following this approach, the set-up can be estimated for the wind speeds related to different return periods at the Con Dao climate station (Tran Viet Lien et al., 2004). Since the bottom slope plays a significant role in the wind set-up, creating a higher set-up for milder bottom slopes, the wind set-up will be different for each of the three representative bathymetric profiles (defined in subsection 2.4.2). The resulting wind set-up for the different return periods and bathymetries can be found in Table A.7..

Bathymetry	Mild	Mudflat	Steep
Return period [y]			
10	0.6	0.5	0.3
20	0.7	0.6	0.4
25	0.8	0.6	0.4
40	0.9	0.7	0.5
50	0.9	0.7	0.5
100	1.1	0.8	0.6
200	1.2	1.0	0.7
250	1.3	1.0	0.7
500	1.4	1.1	0.8

Table A.7: Estimated water level set-up due to wind friction for different return periods and bathymetric profiles.

A.2.3. Other components storm surge

Local low barometric pressures cause a rise in water level. Especially in regions where cyclones occur, this water level rise can be significant. In general, a pressure drop of 1 hPa in open water corresponds

to a rise in water level of 1 cm. However, there is little data available on the occurrence and strength of cyclones in the Mekong Delta.

Therefore, a lumped set-up of 0.5 m has been chosen to represent barometric set-up and wave set-up. In the generic approach, land effects are ignored (they can be included later in specific case studies).

A.2.4. Relative sea level rise

The absolute sea level rise is estimated to be around 3 mm/year (Beckley et al., 2007). However, to determine the design water level, it is the relative sea level rise that needs to be accounted for. The Mekong Delta experiences strong subsidence rates, which results in a higher relative sea level rise. Anthony et al. estimated the subsidence along the coastline of the Mekong Delta around 15 mm/year (Anthony et al., 2015).

For design purposes, not the measured absolute sea level rise should be used, but the sea level rise prescribed by the governmental standards. The Vietnamese design guidelines require a sea level rise of 6 mm/y to be taken into account (Tran Quang Hoai et al., 2012).

Finally, the relative sea level rise can be determined by adding the prescribed absolute sea level rise to the subsidence rate. This gives a rate of 21 mm/y.

A.2.5. Design water level

Finally, all the components can be added to determine the design water level. Since the wind set-up depends on the bathymetry and return period, and the sea level rise on the lifetime, each combination of bathymetry, return period and lifetime will have its own design water level. This is summarised in Table A.8.

Bathymetry		Mild	Mudflat	Steep
Lifetime [y]	Return period [y]			
20	10	3.0	2.9	2.8
	20	3.2	3.0	2.8
	40	3.3	3.1	2.9
	100	3.5	3.3	3.0
50	25	3.8	3.7	3.5
	50	4.0	3.8	3.6
	100	4.1	3.9	3.7
	250	4.3	4.1	3.8
100	50	5.0	4.8	4.6
	100	5.2	4.9	4.7
	200	5.3	5.1	4.8
	500	5.5	5.2	4.9

Table A.8: Estimated design water levels (in m above MSL) for different combinations of lifetime, return period and bathymetry.

B

Appendix: Input files SWAN and SWASH

In this appendix an example is given of input files for SWAN and SWASH that have been used to model the various scenarios.

B.1. Input file SWAN

```

$ _____
$          START-UP
$ _____
$ (*) Start-up commands
PROJECT 'BC_c_l_y' '1'
SET LEVEL = 3.7
SET MAXERR = 2
MODE STAT ONED
$ _____
$          MODEL DESCRIPTION
$ _____
$ (*) Computational grid
CGRID REG 0. 0. 0. 52000. 0. 520 0 SEC -30. 30. 360 0.001 1. 100
$ (*) Input fields
INPGRID BOT REG 0. 0. 0. 1 0 52000. 0.
READINP BOT 1. 'Bathy_swn_c.bot' 1 0 FREE
WIND 27.0 0.
$ (*) Initial and boundary conditions
BOU SIDE W CCW CON PAR 7.0 10.4 0. 800.
$ (*) Physics
OFF QUAD
TRIAD
BREAK
FRIC
SETUP
$ _____
$          OUTPUT
$ _____
$ (*) Output locations
POIN 'SWS' 28000. 0.
POIN 'SWN' 0. 0.
POIN 'S10' 44000. 0.
POIN 'S20' 36000. 0.
CURVE 'DOM' 0. 0. 520 52000. 0.
CURVE 'ENR' 0. 0. 20 52000. 0.
$ (*) Write or plot output quantities
SPEC 'SWS' SPEC1D 'Spc_sws_c_l_y.spc'
SPEC 'SWN' SPEC1D 'Spc_swn_c_l_y.spc'
SPEC 'S10' SPEC1D 'Spc_s10_c_l_y.spc'
SPEC 'S20' SPEC1D 'Spc_s20_c_l_y.spc'
TABLE 'DOM' NOHEAD 'BC_c_l_y.tbl' XP HSIG BOTLEV
TABLE 'ENR' NOHEAD 'BC_c_l_y_enr.tbl' XP GENERAT GENWIND REDIST ...
REDQUAD REDTRIAD DISSIP DISBOT DISSURF DISWCAP
$ _____
$          LOCK-UP
$ _____
$ (*) Lock-up input file
COMP
STOP

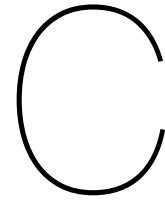
```

B.2. Input file SWASH

```

$ _____
$          START-UP
$ _____
$ (*) Start-up commands
PROJ '1_c_l_y_3' '1'
SET LEVEL = 2.9
MODE NONST ONED
$ _____
$          MODEL DESCRIPTION
$ _____
$ (*) Computational grid
CGRID REG 0. 0. 0. 32000. 0. 6400 0
VERT 2
$ (*) Input fields
INP BOT REG 0. 0. 0. 1 0 32000. 0.
READ BOT 1. 'Bathy_sws_c.bot' 1 0 FREE
INP NPLA REG 0. 0. 0. 640 0 50. 0.
READ NPLA 1. 'Vege_c.veg' 1 0 FREE
$ (*) Initial and boundary conditions
INIT ZERO
BOU SIDE W COW BTYP WEAK SMOO 10 SEC CON SPECF 'Spc_sws_up_c_l_y.spc' ...
CYCLE 60. MIN
$ (*) Physics
FRIC
BRE
VEGE 0.5 0.02 1000 0.25 6. 0.3 17 0.25 2. 0.5 1000 0.25
$ (*) Numerics
NONHYD
DISCRET UPW MOM
DISCRET CORR MUS
TIMEI METH EXPL 0.1 0.5
$ _____
$          OUTPUT
$ _____
$ (*) Output locations
$ (*) Write or plot output quantities
QUANT HSIG DUR 60 MIN
BLOCK 'COMPGRID' NOHEAD '1_c_l_y_3.mat' LAY 3 XP HSIG BOTLEV
$ _____
$          LOCK-UP
$ _____
$ (*) Lock-up input file
COMP 000000.000 0.02 S 012000.000
STOP

```

Appendix: Evaluation framework

In section 2.6 the evaluation framework has been set up, and an overview of the estimated values of all components of the cost-benefit analysis has been given in Table 2.5. In this appendix, these estimates will be supported by more detailed calculations and literature references. In section C.1 the costs and benefits related to the construction and maintenance of protection measures will be discussed, while the costs and benefits related to the value of land will be presented in section C.2.

C.1. Construction and maintenance

In this section the estimated construction and maintenance costs, as given in Table 2.5, are explained in greater detail and supported by references to literature. First, the hydraulic conditions that have been computed by the model are translated into dike dimensions. Then, the costs of a dike, as function of its dimensions are given. Next, the costs related to construction and maintenance of mangrove forests (reforestation) are discussed. To conclude, the costs related to the construction and maintenance of hard solutions (such as super strong concrete breakwaters) and soft solutions (such as nourishment) are estimated.

C.1.1. From hydraulic conditions to dike dimensions

The combined SWAN-SWASH model computes the hydraulic conditions at the toe of the dike. In the next paragraphs, these hydraulic conditions are translated to dike dimensions. The idea is not to make a detailed dike design, but a design based on the standard cross-section, the only purpose of which is being able to estimate the construction and maintenance costs.

According to the Vietnamese technical guidelines (Tran Quang Hoai et al., 2012), the main failure mechanisms of sea dikes and revetments in Vietnam are a too high wave overtopping discharge, dike slope sliding, toe erosion, failure of the dike body and protection layers, dike settlement, failure of structures on dikes, failure at transitions and erosion of coastal natural dikes and dunes. Not all of these failure mechanisms can be accounted for in this project, due to limitations imposed by the followed approach. For example, failure at transitions cannot be included due to the pure 1D approach, in which only one cross-section is modelled and investigated. For the same reason, structures on dikes are excluded as well. Also, natural dikes and dunes are not present in the Mekong Delta.

Further, as the dike design is limited in detail, some failure mechanisms are only included through simplifications and assumptions. For example, toe erosion will only be included through a simple consideration whether toe protection is needed or not, the toe protection will not be designed in detail. Similarly, only the need for a slope protection is considered, but this protection is not designed in detail. This approach will require some assumptions, which will be elaborated in the following paragraphs.

For the dike design, Schiereck and Verhagen (2012) and Tran Quang Hoai et al. (2012) are followed. In general, the dike crest level is determined based on both direct elements, through the design water level, and indirect elements, through wave run-up and allowable overtopping. The waves also determine the need for a revetment and toe protection. Mangroves also influence the dike design indirectly, through attenuation of wave energy. If the mangrove forest is wide enough, it can make a revetment unnecessary. Through wave attenuation, also the wave run-up will reduce, resulting in a lower required

crest level. The effect of mangroves on the design water level is neglected.

The design dike crest level consists of three components: the design water level, a certain freeboard above this design water level and a safety height increment, see Equation C.1.

$$h_{design} = z_w + R_{cp} + z_s \quad (C.1)$$

Where

h_{design}	design dike crest level	[m]
z_w	design water level	[m]
R_{cp}	freeboard	[m]
z_s	safety height increment	[m]

This design crest level is the level of the dike crest when the dike body has settled. In other words, the dike will be constructed with a crest level which is the design crest level plus the estimated settlement, see Equation C.2.

$$h_{D,con} = h_{design} + S_{tot} \quad (C.2)$$

Where

$h_{D,con}$	dike height upon construction	[m]
S	settlement	[m]

The design water level depends on the lifetime of the dike, the return period of the normative conditions and the bathymetry of the foreshore. It contains a tidal component, wind set-up, relative sea level rise and a component lumping all other aspects. This is elaborated in 2.4.4.

If the dike were to be constructed at the design water level, every single wave would overtop the dike. Therefore a certain freeboard is required. Depending on the height of the freeboard, no overtopping or some overtopping will occur. If no overtopping is allowed, for example because the land use behind the dike is intolerant to salt (rice fields), the freeboard is significantly higher than when some overtopping is allowed, leading to higher costs. However, if some overtopping is allowed, the inner slope of the dike has to be protected in order to avoid failure through slope sliding.

In case no overtopping is allowed, the freeboard equals the wave run-up. The wave run-up can be calculated with Equation C.3. This formula can be extended with reduction factors for obliquely incident waves, the presence of a berm and the effect of roughness elements on the slope. It is assumed that the waves arrive perpendicular to the coast (1D approach), the dike does not have a berm (simple design) and the slope is smooth. In other words, the calculations are conservative, and it is recommended to optimise the final design. However, for a rough design this is most efficient.

$$R_{up} = \begin{cases} 1.75 \cdot \xi_0 \cdot H_s & \text{if } 0.5 < \xi_0 < 1.8 \\ \left(4.3 - \frac{1.6}{\sqrt{\xi_0}}\right) \cdot H_s & \text{if } 1.8 < \xi_0 < 10 \end{cases} \quad (C.3)$$

Where

R_{up}	wave run-up	[m]
ξ_0	breaker parameter	[-]
H_s	design wave height at the toe of the dike	[m]

The breaker parameter ξ_0 is defined in Equation C.4 as the ratio of the dike slope α over the wave steepness s_0 . The wave steepness is defined in Equation C.5.

$$\xi_0 = \frac{\tan \alpha}{\sqrt{s_0}} \quad (C.4)$$

Where

α	dike slope	[-]
s_0	wave steepness	[-]

$$s_0 = \frac{2\pi \cdot H_s}{g \cdot T_{m-1,0,p}^2} \quad (C.5)$$

Where

$T_{m-1,0,p}$	spectral wave period $T_{m-1,0,p} = T_p/1.1$	[-]
---------------	--	-----

If a certain overtopping discharge is allowed, the required crest height can be calculated with Equation C.6. Again, any possible reduction factor is neglected for a conservative design.

$$R_{cp} = \begin{cases} -\frac{1}{4.3} \cdot H_s \cdot \xi_0 \cdot \ln\left(\frac{q\sqrt{\tan\alpha}}{0.067\sqrt{g \cdot H_s^3}}\right) & \text{if } \xi_0 \leq 2 \\ -\frac{1}{2.3} \cdot H_s \cdot \ln\left(\frac{5q}{\sqrt{g \cdot H_s^3}}\right) & \text{if } 2 < \xi_0 \leq 7 \\ -H_s \cdot (0.33 + 0.022\xi_0) \cdot \ln\left(\frac{q}{0.21\sqrt{g \cdot H_s^3}}\right) & \text{if } \xi_0 > 7 \end{cases} \quad (C.6)$$

Where

R_{cp}	freeboard corresponding to allowable overtopping	[m]
q	allowable overtopping discharge	[m ³ /s/m]

To illustrate the effect of allowing a certain amount of overtopping on the required freeboard, an example is calculated. In the example, a wave height at the toe of the dike of $H_s = 2$ m and a peak wave period of $T_p = 10$ s is used. If no overtopping is allowed, the required freeboard is $R_{up} = 7.0$ m. If an overtopping discharge of $q = 1$ l/s/m is allowed, the required freeboard is $R_{cp} = 6.5$ m. For an overtopping discharge of $q = 10$ l/s/m, the required freeboard becomes $R_{cp} = 4.5$ m, however, for such overtopping, the inner slope has to be well protected.

So far, the design water level and required freeboard have been treated. The only remaining component determining the design crest level in Equation C.1 is the safety height increment. The Vietnamese technical standards prescribe a safety height increment depending on the class of the dike, varying between 0.5 m and 0.3 m (Tran Quang Hoai et al., 2012). For the Mekong Delta, a standard safety height increment of 0.5 m is chosen. This is the maximum increment, leading again to a conservative design.

In order to guarantee the dike crest level, the dike must be constructed at a higher level, allowing for the dike to settle. The settlement consists of two components, an initial settlement which occurs immediately after the loading of the soil, and a consolidating settlement due to external loads. The initial settlement can be calculated with Equation C.7.

$$S_i = \zeta \cdot P \cdot \frac{B(1 - \mu^2)}{E} \quad (C.7)$$

Where

S_i	initial settlement	[m]
ζ	influence factor	[-]
P	uniform pressure on the dike foundation	[kPa]
B	short side dimensions of the dike foundation	[m]
μ	Poisson's ratio of the soil (for saturated soil $\mu = 0.5$)	[-]
E	Elastic modulus of foundation soil	[kPa]

The influence factor for plastic foundation soil for a very long dike, averaged over the foundation area is $\zeta = 3.7$. The elastic modulus of the foundation soil is determined by an undrained tri-axial shearing test or a mono-axial compression test. For the Mekong Delta a value of $E = 8 \cdot 10^3$ kPa is assumed. The pressure P on the dike foundation can be written as a function of the dike height h , see Equation C.8.

$$\begin{aligned} P &= \frac{A \cdot \rho \cdot g}{B} \\ &= \frac{h \cdot (3h + 3) \cdot \rho \cdot g}{6h + 3} \\ &= \frac{\rho \cdot g \cdot h \cdot (h + 1)}{2h + 1} \end{aligned} \quad (\text{C.8})$$

Where

A	area of the dike foundation	[m ²]
ρ	density of the dike material	[kg/m ³]
B	short side of the dike foundation	[m]
h	dike height	[m]

Combining equations C.7 and C.8, the initial settlement can be expressed as a function of the dike height, which is given in Equation C.9.

$$S_i = \frac{\zeta \cdot \rho \cdot g \cdot h \cdot (3h + 3) \cdot (1 - \mu^2)}{E} \quad (\text{C.9})$$

Since there is no detailed information available on the soil properties, it is assumed that the consolidation settlement is equal to the initial settlement. Therefore, the total settlement is twice the initial settlement. The dike crest has to be constructed at a level equal to the sum of the design crest level and the total settlement, see Equation C.2.

C.1.2. Construction and maintenance costs of dikes

The construction costs of the dike are in the first place a function of the dike height. For other important parameters determining the construction costs, such as labour costs, sand and clay costs, fixed rates have been applied. Note that especially labour costs are hard to determine, since there is little information available in Vietnam, and part of the labour is done for free as part of social service. Therefore, estimates made by Hillen (2008), based on budgets of sea dike upgrading projects of the Asian Development Bank, will be used.

Following the approach of Hillen (2008), the construction costs consist of four components: costs of the dike body, costs of land use, costs of a berm (if necessary) and costs of the revetment. These four components will be analysed below, and expressed as a function of the dike height, in order to come to the final expression for the dike construction costs as function of the dike height (as given in Table 2.5). The cross-section of the dike is designed following the Vietnamese dike design standards (Tran Quang Hoai et al., 2012) and is visualised in Figure C.1 (Hillen, 2008).

The dike body consists of a sand body, covered by a clay layer with a thickness of 0.5 m. Hillen (2008) estimated the total costs of the sand (including transport and labour costs) at 150 000 VND/m³. Following a similar reasoning, the total costs of the clay are 250 000 VND/m³. Since all calculations are expressed per meter dike width, the volume of the sand body and clay layer are represented by the surface area in the cross-section as shown in Figure C.1. The surface area of the sand body is calculated in Equation C.10, the surface area of the clay layer in Equation C.11. Multiplying these surface

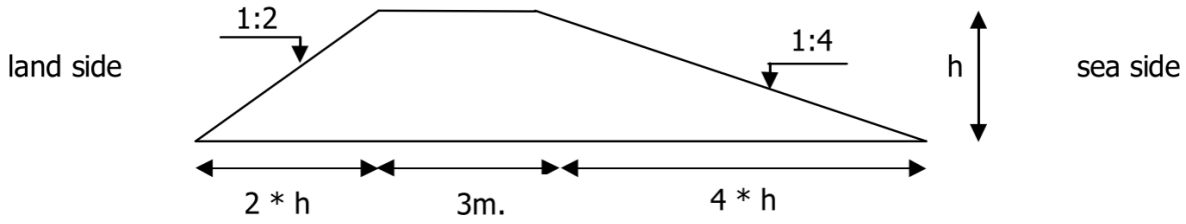


Figure C.1: Standard dike cross-section according to the Vietnamese design guidelines (Tran Quang Hoai et al., 2012). Figure taken from Hillen (2008).

areas with their corresponding costs per volume, yields an expression for the costs of the dike body, given in Equation C.12.

$$\begin{aligned} A_{SB} &= \frac{1}{2} \cdot h_D \cdot (2h_D + 3 + 4h_D + 3) \\ &= h_D \cdot (3h_D + 3) \end{aligned} \quad (C.10)$$

Where

A_{SB}	cross-sectional area sand body	[m ²]
h_D	dike height	[m]

$$A_{CL} = 0.5 \cdot \left(3 + \sqrt{5h_D^2} + \sqrt{17h_D^2} \right) \quad (C.11)$$

Where

A_{CL}	cross-sectional area clay layer	[m ²]
----------	---------------------------------	-------------------

$$\begin{aligned} C_{DB} &= C_S \cdot A_{SB} + C_C \cdot A_{CL} \\ &= 0.15 \cdot h_D \cdot (3h_D + 3) + 0.5 \cdot 0.25 \cdot \left(3 + \sqrt{5h_D^2} + \sqrt{17h_D^2} \right) \\ &= 0.45 \cdot h_D^2 + 0.45 \cdot h_D + 0.125 \cdot \left(\sqrt{5h_D^2} + \sqrt{17h_D^2} \right) + 0.375 \end{aligned} \quad (C.12)$$

Where

C_{DB}	total costs of the dike body	[10 ⁶ VND/m]
C_S	costs of sand per cubic meter	[10 ⁶ VND/m ³]
C_C	costs of clay per cubic meter	[10 ⁶ VND/m ³]

Estimating the costs related to land use and property rights is very difficult, since some land is already owned by the government, while other land is still private property. Hillen (2008) has decided to double the costs of the sand body, in order to account for the costs of land use. This is summarised in Equation C.13.

$$C_{LU} = 0.45 \cdot h_D \cdot (h_D + 1) \quad (C.13)$$

Where

C_{LU}	costs of land use and property rights	[10 ⁶ VND/m]
----------	---------------------------------------	-------------------------

The design guidelines also include the design of a berm (Tran Quang Hoai et al., 2012), however, it is

not specified when a berm should be included. For simplicity, berms will not be included in this dike design. Of course, during the detailed design phase, they can be added.

Finally, the costs of the revetment have to be estimated. This includes protection of both the inner and outer slope, as well as protection of the dike crest and toe. In case of extreme erosion, a strong toe protection is needed, which can double the costs of the revetment. For normal situations, the costs of the revetment are approximated by Equation C.14 (Hillen, 2008).

$$C_R = 5 \cdot h_D \quad (C.14)$$

Where

$$C_R \quad \text{costs of the revetment} \quad [10^6 \text{ VND/m}]$$

The total construction costs of the dike are given in Equation C.15 and are a summation of Equations C.12, C.13 and C.14.

$$\begin{aligned} I_D &= C_{DB} + C_{LU} + C_R \\ &= \left[0.45 \cdot h_D^2 + 0.45 \cdot h_D + 0.125 \cdot \left(\sqrt{5h_D^2} + \sqrt{17h_D^2} \right) + 0.375 \right] + [0.45 \cdot h_D \cdot (h_D + 1)] + [5 \cdot h_D] \\ &= 0.9 \cdot h_D^2 + 5.9 \cdot h_D + 0.375 + 0.125 \cdot \left(\sqrt{5h_D^2} + \sqrt{17h_D^2} \right). \end{aligned} \quad (C.15)$$

To get an impression of the construction costs, these costs are computed for some dike heights varying between 2 and 10 m high in Table C.1.

Dike height m	Dike body 10 ⁶ VND/m	Land use 10 ⁶ VND/m	Revetment 10 ⁶ VND/m	Total costs	
				10 ⁶ VND/m	10 ³ USD/m
2	4.86	2.70	10.00	17.36	0.87
4	12.55	9.00	20.00	41.55	2.08
6	24.04	18.90	30.00	78.70	3.94
8	39.13	32.40	40.00	118.54	5.93
10	57.82	49.50	50.00	165.57	8.28

Table C.1: Cost components and total dike construction costs for various dike heights.

Note that the revetment costs represent a significant part of the total construction costs, up to 60% for the lowest dikes. A mangrove belt in front of the dike can sufficiently dampen the waves to render a revetment unnecessary. In those cases, the construction costs of the dike can be significantly lower. However, in the case the dike is built before the mangrove belt is sufficiently restored, a revetment is still required. For this project, it is assumed that the mangroves need to be restored, and therefore the revetment will always be necessary.

Maintenance of sea dikes in Vietnam is a difficult concept. The only maintenance that occurs is repair of damage. Most of the dikes are earth dikes without revetment and therefore very fragile. Hillen (2008) mentions that for the two northern provinces in his case study, the maintenance costs vary every year, because MARD, the Ministry of Agriculture and Rural Development, has a changing budget that is distributed over the provincial dike departments. Therefore, the average of $260 \cdot 10^3$ VND/m/y currently spent on dike maintenance is insufficient. Especially since planned dike maintenance is not yet accepted in common practice, a large budget should be provided.

Vo Thanh Danh (2012) gives the sea dike maintenance costs in the Mekong Delta for the period 2005 - 2009. During these five years $1.792.943 \cdot 10^6$ VND was spent. The current sea dike system in the Mekong Delta has a length of 620 km, this means that on average $580 \cdot 10^3$ VND/m/y has been spent. This is almost twice the amount spent in the north of Vietnam (Hillen, 2008). Mai Van Cong et al. (2008) makes a rough estimate of the maintenance costs at 20 - 40 USD/m/y, which is about $0.4 - 0.8 \cdot 10^6$ VND/m/y. Assuming that this is closer to a sufficient maintenance budget, the maintenance costs for sea dikes in this cost-benefit analysis will be set at $1 \cdot 10^6$ VND/m/y.

C.1.3. Mangrove reforestation

Lewis (2001) explains that there are various categories of mangrove reforestation projects. In some cases, only the hydrologic situation is restored (and nature does the rest), while in other situations hydrologic restoration is complemented by mangrove planting (to speed up the process). The costs of the first type of mangrove restoration are estimated at 20 000 USD/km² (400 VND/m²), which is much cheaper than the second type, which averages a cost of 70 000 USD/km² (1400 VND/m²).

Clough et al. (2016) summarises the outcomes and lessons learned from mangrove rehabilitation activities supported by GIZ in the Mekong Delta between 2008 and 2014. It gives a clear overview of the techniques, as well as the costs. These costs are composed of three components: site preparation, seedling costs and planting costs. On average, the mangrove reforestation projects of GIZ in the Mekong Delta have cost 1527 VND/m². This is in agreement with the costs mentioned by Lewis (2001) for hydrologic restoration and mangrove planting. For the cost-benefit analysis, the mangrove rehabilitation costs are set at 1500 VND/m².

Mangrove reforestation projects are actually using and enhancing natural processes, by catching sediment and creating quiet areas where mangroves can grow. Eventually, these mangrove plants will become strong enough to withstand the natural influences without help of artificial measures. Therefore, maintenance will reduce throughout a mangrove rehabilitation project, until it no longer is required. Based on the experience of GIZ (source: personal communication with GIZ), it is assumed that maintenance will be needed for the first 10 years of the mangrove reforestation project. The major part of the maintenance costs is labour costs. On average, the first two years, 27 man-days are required per km², the three subsequent years, about 25 man-days are spent. It is assumed that the maintenance costs will reduce further over the last 5 years. This is summarised in Table C.2.

Years after construction	Maintenance costs	
	VND/m ²	10 ⁻³ USD/m ²
1	540	27
2	540	27
3	500	25
4	500	25
5	500	25
6	450	22.5
7	400	20
8	350	17.5
9	300	15
10	250	12.5

Table C.2: Maintenance costs mangrove reforestation

One must realise that in current practice mangrove reforestation projects regularly fail. Therefore, the real costs often lie higher than what is estimated here. However, for this project it is assumed that the mangrove reforestation techniques have been optimised and the mangrove forest can be restored successfully.

C.1.4. Hard solutions

In Cà Mau several concrete breakwaters have been built, an example is shown in Figure C.2. These structures have been designed without much knowledge of design conditions or the effectiveness of the structure. However, they actually act as some kind of permanent sediment fences. Five years after the first concrete breakwaters were built, a tentative conclusion can be drawn that they are effective in reducing wave energy and stopping further erosion of the coast. However, they also block all sediment transport, so at a regular distance (every 100 m) the rock filling has been removed to allow sediment to enter the protected area behind the breakwater. The construction costs of these breakwaters are 2000 USD/m (personal communication with representative of local dike department, May 2016). No maintenance has been executed so far, however it is to be expected that in the future maintenance will be required. Furthermore, it is unknown which boundary conditions it can survive, but from observation it is expected that the first big storm will cause significant damage.

Due to the lack of information on these concrete breakwaters, and the expectation that they will lose their



Figure C.2: Concrete breakwater along west coast of Cà Mau (photo taken by author during field trip in May 2016). In the third compartment from bottom right, the rock filling has been removed to allow for sediment transport.

function during the design conditions, an educated guess is required to determine the construction and maintenance costs of such a strong structure that it can withstand both erosion and extremely strong wave conditions. As a starting point, the costs of a normal sea dike are used. However, the extremely strong structures in this category require additional toe protection and adequate protection of the inner slope (in case of a dike), or a strong foundation and adequate reinforcements (in case of a concrete breakwater for example). These additional investments are rather expensive. Therefore, it is assumed that the total costs of such a structure are twice the costs of a regular sea dike. This assumption also holds for the maintenance costs (as monitoring and repair will be more complex as well).

C.1.5. Soft solutions

There is no experience with nourishing fine sediment coasts such as the coasts of the Mekong Delta. To make an estimate of the costs, only information on sandy nourishments is available. Combining these costs with reasonable assumptions on the differences between nourishing with fine sediment and with sand, an estimate can be made of the initial nourishments costs. Nourishment is a repetitive process, therefore maintenance is crucial. To assess the costs of maintenance, it should be estimated how fast the nourished sediment leaves the nourishment location. Since there is no data available, an educated guess has to be made.

Costs of nourishment projects can vary over a very wide range. Linham et al. (2010); Linham and Nicholls (2010) investigated the costs of beach nourishments, and came to the conclusion that costs usually vary between 3 USD/m³ and 15 USD/m³ at 2009 price levels, when dredge sites are available locally. The costs depend most strongly on the transport distance of the sediment. In this case, this distance is expected to be relatively large, due to the gently sloping foreshore. The larger the project size, the lower the unit price, therefore a nourishment strategy is expected to be viable only for relatively large projects.

Further, as the dredging industry in Vietnam is not yet very large, the costs for equipment will be larger. On the other hand, as the depth at the nourishment site is relatively shallow, only small equipment can be used and this is available in the area. This small equipment is more sensitive to weather conditions, and can therefore only be used during calm periods. Combined with relatively large tidal ranges, the duration of the project will be relatively long, increasing the price. Further, there is no experience with

beach nourishments, so knowledge and experience will have to be imported.

There are also some differences between sandy nourishments and muddy nourishments. Fine sediment causes significantly less equipment wear and tear, lowering an important cost aspect. On the other hand, the losses will be larger for fine sediment, as it needs calmer conditions and more time to settle. It is assumed that the advantages and disadvantages of muddy nourishments cancel each other and the prices of sandy nourishments can be used for the cost estimation.

Taking into account all aspects mentioned in this section, a unit price of 20 USD/m³ will be assumed for the cost estimates of the nourishment scenario. Further, it is assumed that the nourishment has to be repeated every 5 years. The costs for maintenance also include monitoring.

C.2. Value of land

In this section, all costs and benefits related to the value of land are discussed. An overview of the costs and benefits has been given in Table 2.5.

C.2.1. Flooding risk

The damage that can be caused to the hinterland by flooding, depends largely on how that hinterland is used. The damage to a city or industry will be much higher than to agricultural land. In the case of agricultural land, the damage is approximately equal to the value of the lost crops. According to Hillen (2008), the damage to industry can be estimated at 50% of the yearly output of that industry. The damage caused to houses in the Mekong Delta lies lower, since these houses are relatively simple, and the inhabitants are used to regular flooding and rebuilding after storms. However, it should be kept in mind that due to future development, the damage will increase.

In the coastal regions of the Mekong Delta, most land is used for agriculture and aquaculture. Hillen (2008) estimated the damage to agri- and aquaculture due to flooding between 3 and 4.5 billion VND/km² per year. However, it is unclear how much damage has been prevented by coastal protection. Vo Thanh Danh (2012) estimates the damage to flooding for the entire Mekong Delta at almost 1.5% of the GDP, which boils down to a lower value of the damage than the values mentioned by Hillen (2008). However, since the estimates of Vo Thanh Danh (2012) are based on historical data, and the Mekong Delta is undergoing rapid development, the current damage costs will already be higher and the future damage costs even more. Therefore, the average damage due to flooding, or the value of land, is estimated at 20 billion VND/km² per year.

For the cost-benefit analysis, it is not the pure damage, but the avoided damage that will be accounted for. This avoided damage is the benefit provided by coastal protection, since the probability of flooding is reduced. In other words, it is the reduced flooding risk that will be used to find the optimal protection strategy through balancing the costs and benefits. This flooding risk is equal to the probability of flooding times the damage upon flooding. The reduced flooding risk is therefore equal to decrease in flooding probability times the flooding damage.

C.2.2. Ecosystem services

An aspect that has been traditionally overlooked in cost-benefit analyses, because it is so difficult to be expressed in terms of money, is the value generated by ecosystems, such as mangrove forests. By the economic valuation of ecosystem services, it has become possible to include these services in economic considerations. Much research has been done in valuating ecosystem services, however Salem and Mercer (2012) were the first to provide a synthesis of ecosystem services literature, solely focussing on mangrove forests. The different estimates of the value of mangrove ecosystem services vary extremely, from 7000 - 375 000 USD/km²/y estimated by Berg et al. (1998) in Sri Lanka, up to 2.7 - 3.5 million USD/km²/y in Thailand (Sathirathai and Barbier, 2001). Therefore, Salem and Mercer (2012) have calculated the mean value of all values in literature. The mean total economic value provided by mangrove forests is estimated at 2 866 200 USD/km²/y, however, the distribution is very skewed, with a much lower median value. In this cost-benefit analysis, the benefit provided by mangrove ecosystem services is set at 2.5 million USD/km²/y, which is 50.000 VND/m²/y.

A significant part of the remaining mangrove forests in the Mekong Delta is deteriorated. To account for this, the density of the mangrove forest is varied in the model simulations. Three situations will be compared: spare density, average density and dense density. It is assumed that a mangrove forest with lower density will provide fewer ecosystem services. Therefore, the ecosystem services will also be

scaled to the density: 100% for the dense forest, 50% for the average forest and 25% for the sparsely wooded forest. This is respectively 12.500 VND/m²/y, 25.000 VND/m²/y and 50.000 VND/m²/y.

C.2.3. Land loss

This parameter is used to account for the loss that results from not using all land behind the low water line, but instead placing the dike more inland. The loss is equal to the profit that could have been generated on that surface, by agriculture, aquaculture or industry. It is estimated at 20 billion VND/km², the value of land, or the flooding damage, as was assessed in the previous paragraph.

C.2.4. Land conversion

The land between the low water line and the dike is considered to be “given back to the sea”. However, this does not mean that it has no value. It has significant indirect value through reducing wave energy in front of the dike, but it can also have direct value, for example through ecosystem services if it is colonised by mangrove vegetation. In such a case, the value of ecosystem services as given in the previous paragraph can be used. Other possible ways to generate value are for example fishing, or aquaculture. In those cases, the value of the converted land can be considered equal to the income gained from those activities.